L&T Infra Engineering

L&T Infrastructure Engineering Ltd.

Client: **National Center for Coastal Research**
Chennai

Project: Model Studies for Kalpasar Dam	**Project No.:** C1221503	
Title: Draft Inundation Study Report	**Document No.:** RP002	**Rev.:** 0

File path:
L:\PORTS\2022\C1221503 - MODEL - STUDY - KALPASAR\Working\Reports\RP002-Draft-Inundation-Report

Notes:

1.

Revision Details:

0	31/03/2023	First Submission			ASA		PRJ	
Rev.	**Date**	**Details**	**Init.**	**Sign.**	**Init.**	**Sign.**	**Init.**	**Sign.**
			Prepared		**Checked**		**Approved**	

TABLE OF CONTENTS

LIST OF FIGURES

LIST OF TABLES

LIST OF ENCLOSURES

1 Introduction

The Kalpasar department, Government of Gujarat, proposes to construct World's largest fresh water reservoir in sea at Gulf of Khambhat region, Gujarat. This project comprises of construction of a Dyke, 60Km in length, to store surface water resources in the gulf. In the reservoir, the discharge from Dhadhar, Mahi, Sabarmati and other Saurashtra rivers will be stored. The stored water can be used for irrigation, water supply and other industrial requirements.

National Centre for Coastal Research (NCCR) appointed L&T Infrastructure Engineering Limited (L&T IEL) to carry out model studies to assess the impact of Dyke on Gulf of Khambhat. L&T IEL will carry out mathematical model studies to assess the impact of Dyke on hydrodynamics & morpho-dynamics in Gulf of Khambhat.

The detailed scope of the work is as follows,

- Study of inundation of regions to the north of the dyke due to flooding in rivers such as Mahi, Sabarmati, Dhadhar and make a comparative analysis pre and post dyke construction
- Study of the morphology in the reservoir owing to the ingress of sediments from Rivers Mahi, Sabarmati, Dhadhar etc.
- Study of morphological changes in the regions south of the dyke pre and post dyke construction

2 Objective and scope of the report

The objective of this report is to present the calibration of the 2D Hydrodynamics model and assessment of changes in water levels at downstream and upstream of the dyke, post its construction.

The following have been identified as the scope of this report: -

- Calibration & Validation of the hydrodynamics model by comparing the modelled tide and current with observed data.
- To assess the effect of proposed dyke on water levels downstream of the dyke by studying the changes in hydrodynamics.
- To assess the effect of proposed dyke on water levels upstream of the dyke by studying river hydraulics and reservoir outflow.

3 Methodology

3.1 Data Analysis

The data such as bathymetry, topography, etc., received from NCCR and various other sources like GEBCO 2022, SRTM were analysed and compiled. The details of data sources and various analyses performed on these data to achieve quality control and to prepare these data to be used in various models are presented in Section 4.

3.2 Hydrodynamic model calibration

TELEMAC-2D numerical tool was used to simulate the hydrodynamic conditions for the chosen domain. The offshore boundary condition is prescribed using tidal constituents provided by the OSU (Oregon State University) database.

Calibration of a numerical model is a process of tuning the model to give results comparable with actual site observations during a sufficient period of time. A proper calibration of any numerical model is necessary for ensuring the authenticity of the model. The measured tide and currents at several locations, provided by NCCR, were used for calibrating and validating the hydrodynamic model. The model setup and calibration process are provided in Section 5.

3.3 Inundation study

Coastal flooding is caused by extreme sea levels driven by combined effect tide, storm surges and mean sea level. For demarking the extent of flooding, an accurate representation of bathymetry and topography features are required. The resolution of data provided (approximately 1Km) was not adequate and data from secondary sources (GEBCO 2022 Grid and SRTM data; on a 15 arc-second interval grid) were considered for the model studies. With this limitation, demarking the inundation extent may lead to imprecise inundation patterns. Hence extreme levels are estimated for different locations by analysing the magnitude of tides, storm surges and sea level rise. The various cases simulated to estimate downstream and upstream water levels and their results are discussed in Section 6 and Section 7.

3.3.1 Effects of the dyke on water levels downstream

Construction of Kalpasar Dyke is expected to make changes in the hydrodynamics of the Gulf which can cause changes in the high and low water levels and sedimentation patterns in the Gulf. In order to study this impact, the calibrated HD model was used to simulate various scenarios with and without the proposed dyke in place. The maximum water level will mainly be affected by three major phenomena, namely, tide, storm surges and sea level rise. The various cases simulated and their results are discussed in Section 6.

3.3.2 Effects of the dyke on water levels upstream

On upstream of the dyke, water levels are expected to rise as the dyke impounds huge quantity of water. The extent of the water level change depends on the water level and storage maintained at the reservoir among other factors. Along with the water levels, sedimentation patterns upstream of the dyke will also be affected as the reservoir traps sediments. In order to study this impact, the calibrated HD model was used to simulate various scenarios. The intensity and duration of flood in the rivers along with the outflow of the reservoir will drive the upstream water levels. The various cases simulated and their results are discussed in Section 0.

4 Inputs for the study

Compilation of all the data used for the study and the analysis carried out on each of the data used for the model study are presented in this section.

4.1 Project site environment

The Gulf of Khambhat is located in the North-West India between Kathiawar Peninsula and Central and South Gujarat. The funnel shaped gulf, as presented in Figure 4-1, has a width of 80 km at its mouth in the Arabian Sea, indents northward and narrows down to 25 km approx. at its head near Sabarmati and Mahi River mouths. The major river basins like Sabarmati, Mahi, Dhadhar and Narmada discharges water into the gulf along with other small river basins.

Figure 4-1 Project Location

The tides in gulf are majorly of semi-diurnal type and amplify as they propagate form south to north. The geometry of the gulf along with other factors has resulted in distinct tidal hydrodynamics with large tidal ranges, and currents magnitudes. The tidal range within the gulf is the largest along the Indian coast and reaches well above 10 m (observed at Athelai and Dahej). The currents in the gulf are predominantly tide induced amassing speeds about 3.5 m/s. Tidal propagation is also affected by other factors such as friction, bathymetry, morphology of the channel etc.

The large tidal range and current magnitude results in highly dynamic morphology and bottom behaviour. Bathymetry varies from 5 m to 30 m across the study area. The gulf also possesses mud flats which offer significant friction to the tide propagation. Mahi and Sabarmati river basins contain extensive intertidal mud and sand flats. The sediment inflow to the gulf is governed by tidal currents as well as river flows. The particle size analysis results show that D50 of non-cohesive sediment ranges between 0.1 to 0.6 mm and that of cohesive sediment ranges between 0.005 to 0.056 mm.

The study area experiences irregular rainfall frequency, duration, and intensity. The Monsoon period (June to September) brings an average rainfall about 800mm. Salinity ranges from 33 to 37 (PSU) across the study area. However, due to the impact of freshwater flux, a low salinity of 30-31 (PSU) can occur at the river mouths during Monsoon.

The wave heights close to the proposed dyke usually range from 0.5 m to 1.5 m. On an average, one cyclone per year occurs in Arabian Sea and only four cyclones have passed in close proximity to Gulf of Khambhat from 1945 to 2022. However the frequency of intense storms over Arabian Sea has increased in recent years. During May 2021, Tauktae, an Extremely Severe Cyclonic Storm made its landfall near the gulf with wind speeds close to 200 kmph.

4.2 Bathymetry and Topography

Bathymetric data is the primary information which is required for any kind of coastal development projects. Any unrealistic variations in the bathymetry will result in unrealistic values in the output. Therefore, the input for the bathymetry should be of good quality and should come from a reliable and verified source.

Many models in this study are expected to cover a large area. However, bathymetry from a single source may not be available to cover the entire region. Therefore, bathymetry from several sources must be acquired and combined, enabling all the models to use the same bathymetry and therefore cancelling out errors due to inconsistent bathymetry.

The surveyed bathymetry data with respect to MSL was provided by NCCR. The spacing of survey bathymetry is approximately 1Km. The bathymetry data received is presented in Figure 4-2 and Figure 4-3.

Secondary information on bathymetry was taken from GEBCO 2022 Grid (General Bathymetric Chart of the Oceans). GEBCO 2022 Grid is a global terrain model for ocean and land, providing elevation data in meters, on a 15 arc-second interval grid. The GEBCO grid has been built from data from a number of sources, including regional and global grids and hundreds of individual surveys made available through international and national databases such as the IHO Data Center for Digital Bathymetry (IHO-DCDB).

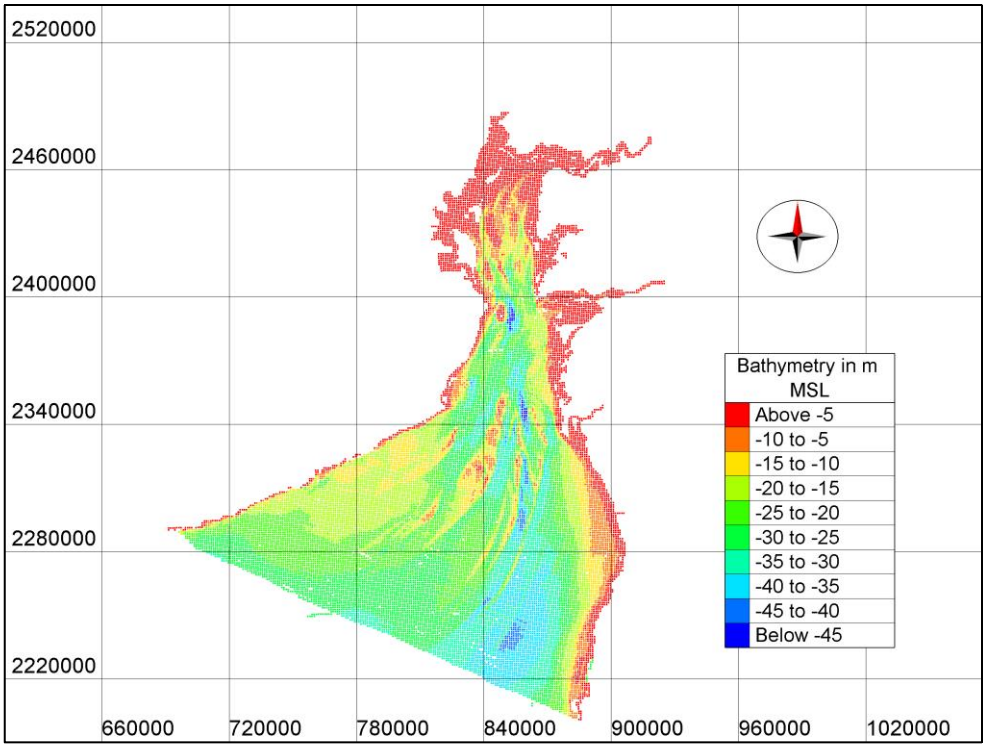

Figure 4-2 Surveyed Bathymetry used for the Model Study

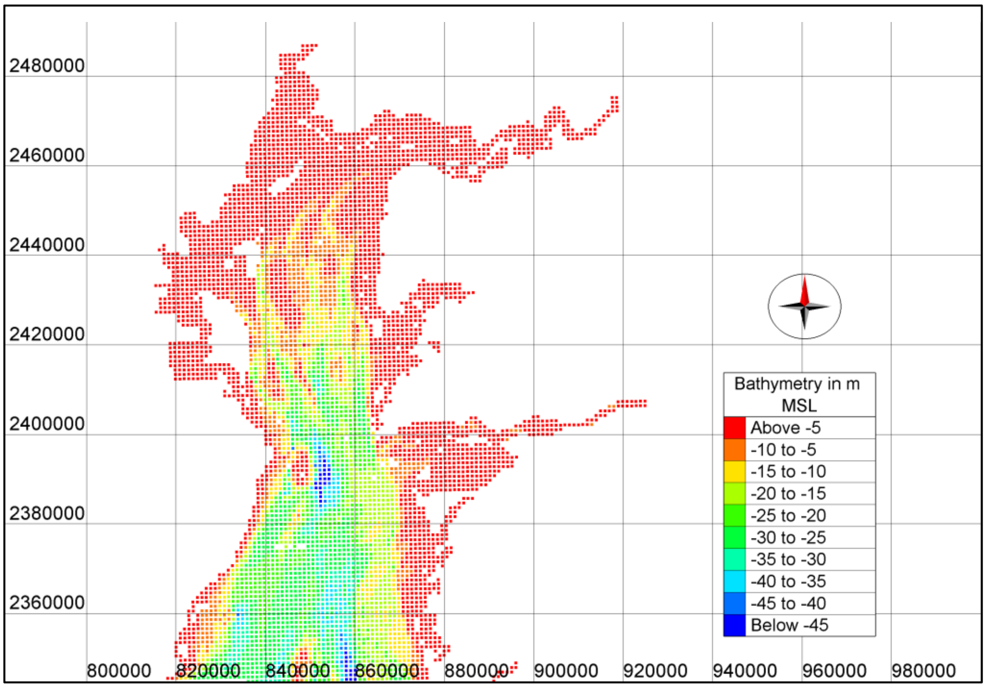

Figure 4-3 Surveyed Bathymetry used for the Model Study (Close-up view)

The combined bathymetry used in the models is presented in Figure 4-4. The topography data provided was not sufficient for studying inundation patterns upstream of the dyke. Hence secondary data such as GEBCO 2022 and SRTM data were used. The secondary data may not be as accurate as measured data. Some irregularities in bathymetry are evident in the region where surveyed bathymetry is interpolated with GEBCO 2022.

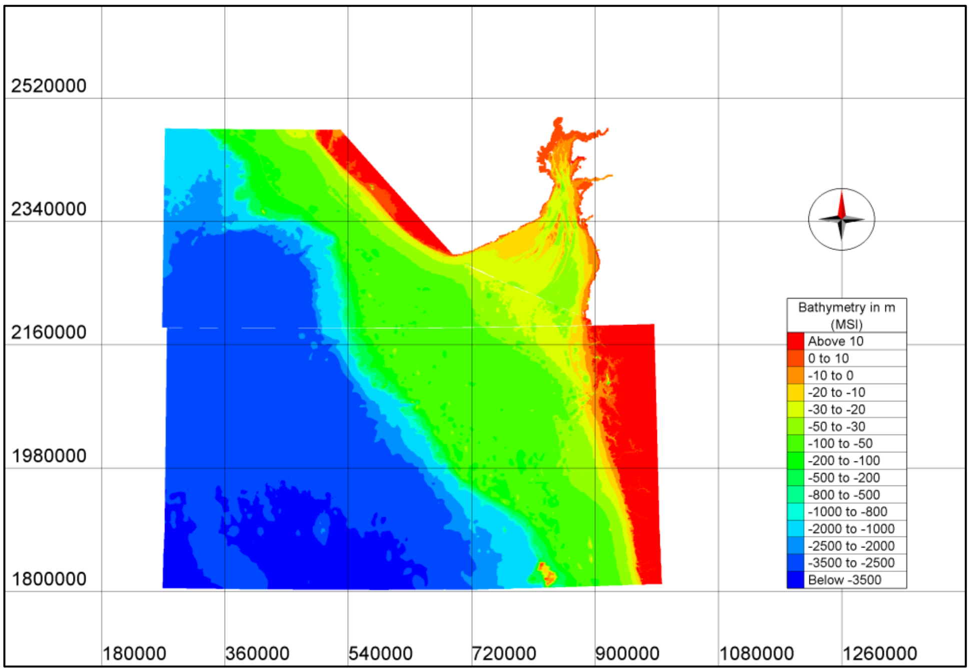

Figure 4-4 Combined Bathymetry considered for the Model Study

4.3 Tide

Tide levels were measured at 23 locations, as presented in Figure 4-5, using Acoustic Tidal Gauge (ATG). The period of observation and tidal ranges are presented in Table 4-1. From measured tide, it is noticed that on the western bank the maximum tide level amplify from 1.2 m at Diu to 5.8 m at

Bhavnagar. Similarly on the eastern bank, the maximum tide level amplifies from 3.0 m at Vandhavan to 3.9 m at Daman and 5.6 m at Dahej.

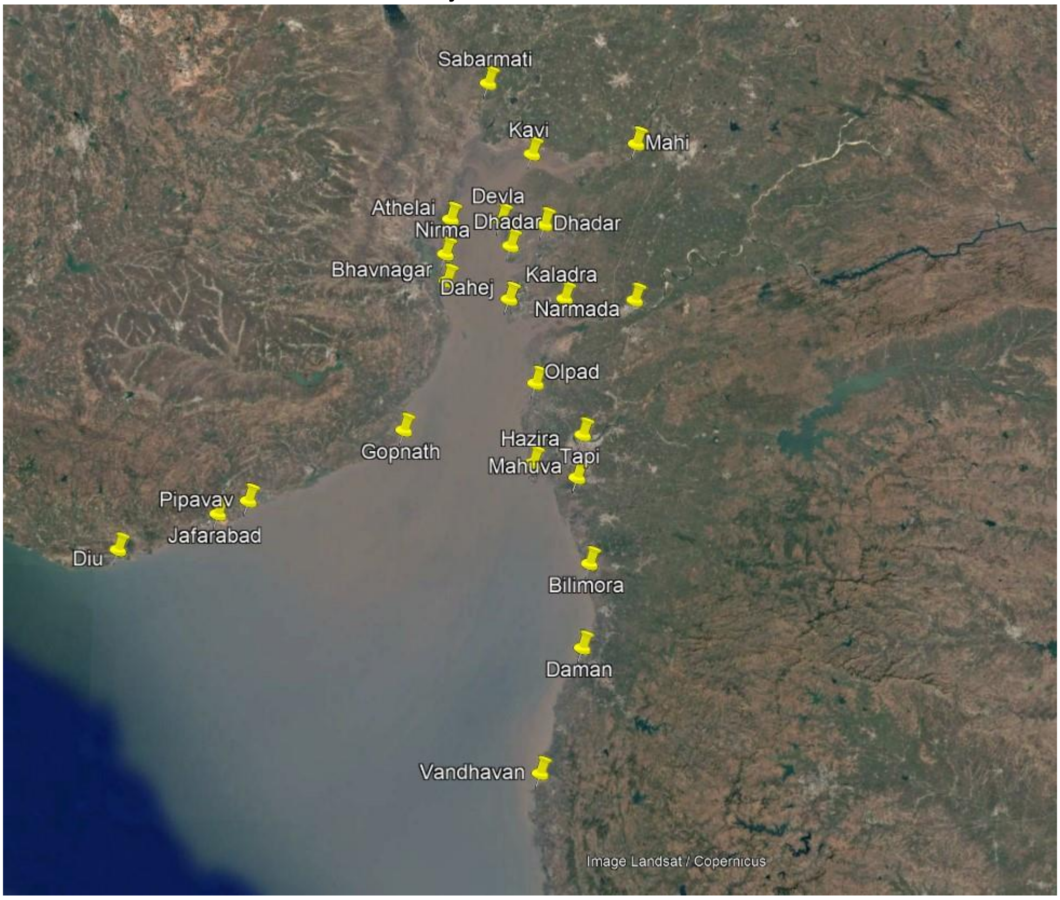

Figure 4-5 Locations at which water levels are measured

Table 4-1 Tide observation period and Tidal ranges

Location	Longitude	Latitude	Start date	End Date	Maximum Tide level (m)	Minimum Tide level (m)
Tapi River	72.815	21.193	10-12-2012	23-06-2014	10.21	-1.21
Narmada River	73.006	21.691	23-01-2013	17-01-2014	11.31	0.84
Dhadhar	72.643	21.960	30-12-2012	11-04-2013	5.95	-0.46
Sabarmathi	72.405	22.475	13-12-2012	22-03-2013	1.97	-0.43
Athelai	72.272	21.971	10-04-2012	01-06-2012	5.93	-6.60
Bhavnagar	72.265	21.744	01-04-2012	31-03-2013	5.83	-0.35
Billimora	72.853	20.722	18-04-2012	17-12-2012	3.92	-4.31
Dhadhar	72.512	21.879	24-04-2012	13-12-2012	5.75	-6.43
Dahej	72.512	21.683	01-04-2012	31-03-2013	5.55	-5.49
Daman	72.832	20.412	18-04-2012	17-12-2012	3.85	-3.70
Devla	72.472	21.971	05-04-2012	24-12-2012	6.03	-7.21

Location	Longitude	Latitude	Start date	End Date	Maximum Tide level (m)	Minimum Tide level (m)
Diu	70.995	20.719	01-04-2012	31-03-2013	1.18	-1.94
Gobnath	72.112	21.193	01-05-2012	13-12-2012	3.36	-3.97
Hataab	72.623	21.086	16-04-2012	12-12-2012	4.97	-5.19
Hazira	72.623	21.086	01-04-2012	29-03-2013	4.03	-4.83
Jafarabad	71.388	20.864	14-04-2012	30-03-2013	2.06	-2.17
Kalathra	72.730	21.690	14-05-2012	31-03-2013	8.41	1.11
Kavi	72.587	22.218	25-09-2012	31-03-2013	7.47	0.16
Mahi	72.998	22.264	01-04-2012	31-03-2013	12.22	2.09
Mahuva	72.796	21.036	17-04-2012	14-12-2012	3.27	-2.92
Nirma	72.256	21.843	01-04-2012	31-03-2013	5.81	-6.10
Olpad	72.625	21.378	01-04-2012	31-03-2013	4.78	-4.98
Pipavav	71.507	20.916	01-04-2012	31-03-2013	2.41	-2.31
Vandhavan	72.679	19.947	19-04-2012	15-12-2012	3.02	-3.25

The observed water levels at four locations namely Bhavnagar, Kavi, Dahej and Daman are presented in Figure 4-6 to Figure 4-9. It shall be noted that the observed low water levels are getting truncated in Bhavnagar and Kavi. This is due to shallow water depth at observed locations. Similar tendency is observed at Tapi, Dhadhar, Sabarmati and Narmada river.

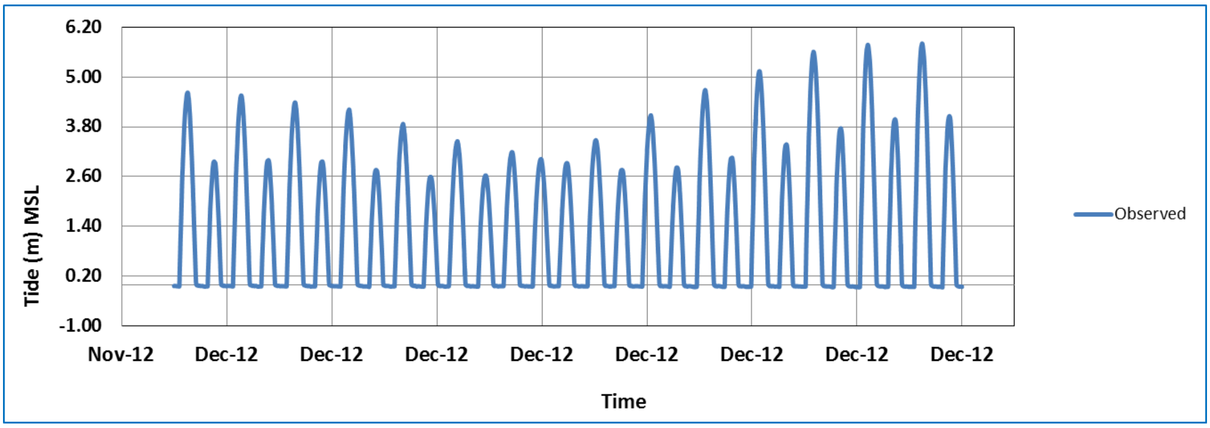

Figure 4-6 Observed water levels at Bhavnagar

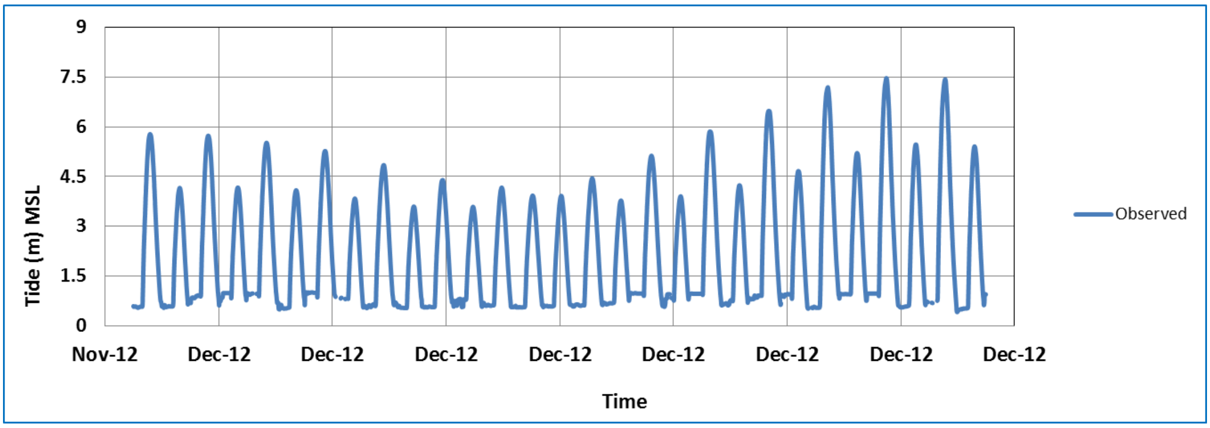

Figure 4-7Observed water levels at Kavi

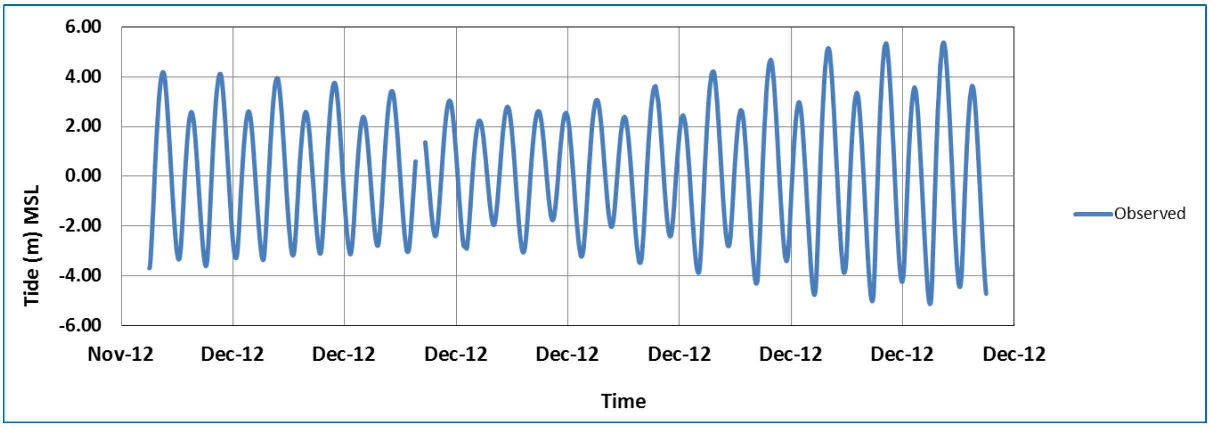

Figure 4-8 Observed water levels at Dahej

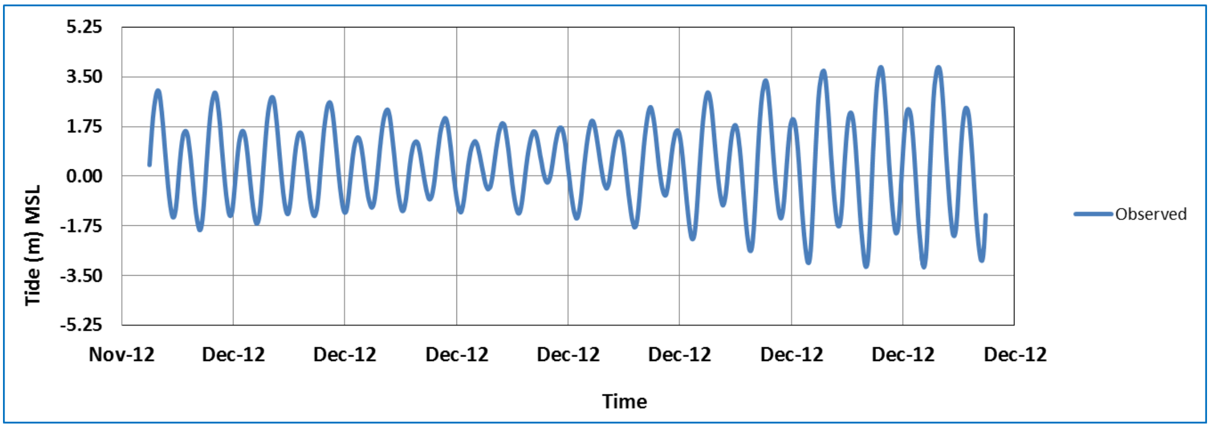

Figure 4-9 Observed water levels at Daman

4.3.1 Harmonic Analysis

The harmonic Constituents study was carried out with observed tide at Dahej. The amplitude and phase lag of 60 harmonic constituents at Dahej are presented in Table 4-2. Tide levels at the project location were predicted for 20 years using the harmonic constituents obtained from the analysis of observed data. The comparison between predicted tide and observed tide is presented in Figure 4-10. The maximum tide levels were observed during January 2018. Therefore simulations were carried out during this period to obtain maximum water level.

Table 4-2 Amplitude and Phase lag of Harmonic constituents at Dahej

Number of constituents	Name of constituents	Amplitude of constituents	Phase lag of constituents
1	Z0	0.2524	0
2	SSA	0.0436	254.88
3	MSM	0.0219	345.83
4	MM	0.0182	259.49
5	MSF	0.0071	112.13
6	MF	0.0008	353.16
7	ALP1	0.0043	125.26
8	2Q1	0.0086	48.03
9	SIG1	0.0218	116.17
10	Q1	0.061	86.29
11	RHO1	0.0157	11.85
12	O1	0.2858	76.86
13	TAU1	0.0297	137.24
14	BET1	0.0108	340.17
15	NO1	0.0406	169.25
16	CHI1	0.0101	348.38
17	P1	0.216	92.61
18	K1	0.6437	89.64
19	PHI1	0.0083	32.5
20	THE1	0.0071	63.14
21	J1	0.0359	146.74
22	SO1	0.0443	261.4
23	OO1	0.0329	154.58
24	UPS1	0.0053	145.94
25	OQ2	0.0248	30.51
26	EPS2	0.0477	267.07
27	2N2	0.1401	55.26
28	MU2	0.0912	322.87
29	N2	0.6943	103.7
30	NU2	0.1737	112.69
31	M2	3.0576	128.38
32	MKS2	0.0144	193.54

Number of constituents	Name of constituents	Amplitude of constituents	Phase lag of constituents
33	LDA2	0.0564	142.78
34	L2	0.1406	144.03
35	S2	0.9719	168.76
36	K2	0.2743	167.94
37	MSN2	0.0325	8.14
38	ETA2	0.0106	75.1
39	MO3	0.0431	25.33
40	M3	0.0275	288.29
41	SO3	0.0328	58.38
42	MK3	0.0548	75.91
43	SK3	0.0284	121.65
44	MN4	0.0864	97.64
45	M4	0.1824	118.89
46	SN4	0.0244	154.43
47	MS4	0.125	165.07
48	MK4	0.0397	162.39
49	S4	0.0208	213.56
50	SK4	0.0117	227.35
51	2MK5	0.0249	44.75
52	2SK5	0.0008	206.1
53	2MN6	0.0385	63.82
54	M6	0.0564	83.29
55	2MS6	0.0629	128.88
56	2MK6	0.0182	122.84
57	2SM6	0.0182	172.4
58	MSK6	0.0114	185.21
59	3MK7	0.0071	31.46
60	M8	0.0111	85.83

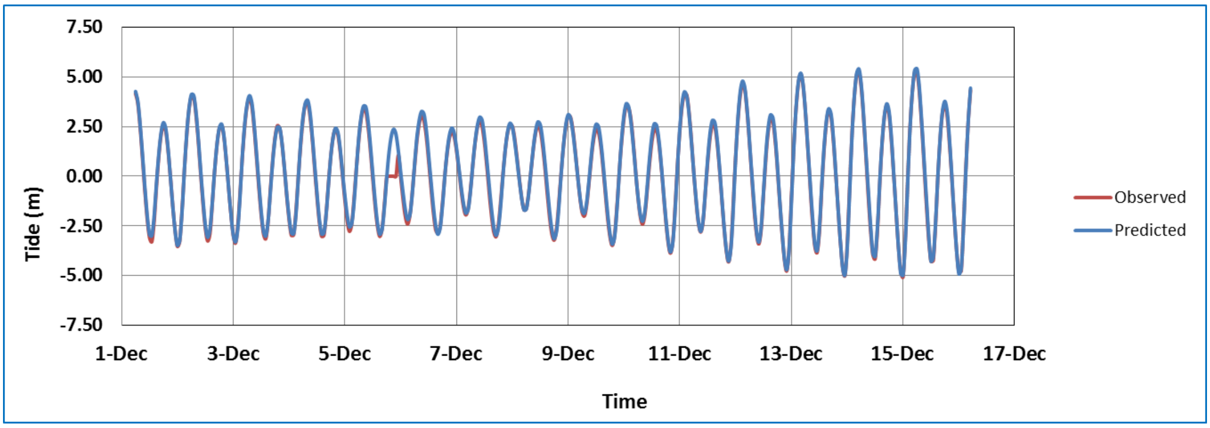

Figure 4-10 Comparison between observed tide and predicted tide at Dahej

4.4 Current

Currents were measured at 5 locations using Acoustic Doppler Current Profile (ADCP). The locations of current measurement are presented in Figure 4-11 and the observed Current velocities are presented from Figure 4-12 to Figure 4-27. Some anomalous values of current velocities are noticed in the observed data which may be an observation error. The period of observation of currents are presented in Table 4-3.

Figure 4-11 Locations at which currents are measured

Table 4-3 Period of observation of Currents

Location	Longitude	Latitude	Start date	End Date
Dam Corridor(Season1)	72.715	20.706	02-02-2013	15-02-2013
Dam Corridor(Season2)	20.706	20.706	06-04-2013	20-04-2013
MC Diu	71.878	20.278	31-03-2012	13-04-2012
MC-Diu	71.878	20.278	27-06-2012	11-07-2012
Mid – Channel –TSS5	72.311	20.767	22-01-2013	08-02-2013
Mid – Channel – TSS8	72.354	21.485	13-01-2013	27-01-2013
Mid – Channel – TSS8	72.354	21.485	02-04-2013	16-04-2013
Narmada	72.519	21.489	23-02-2013	28-02-2013

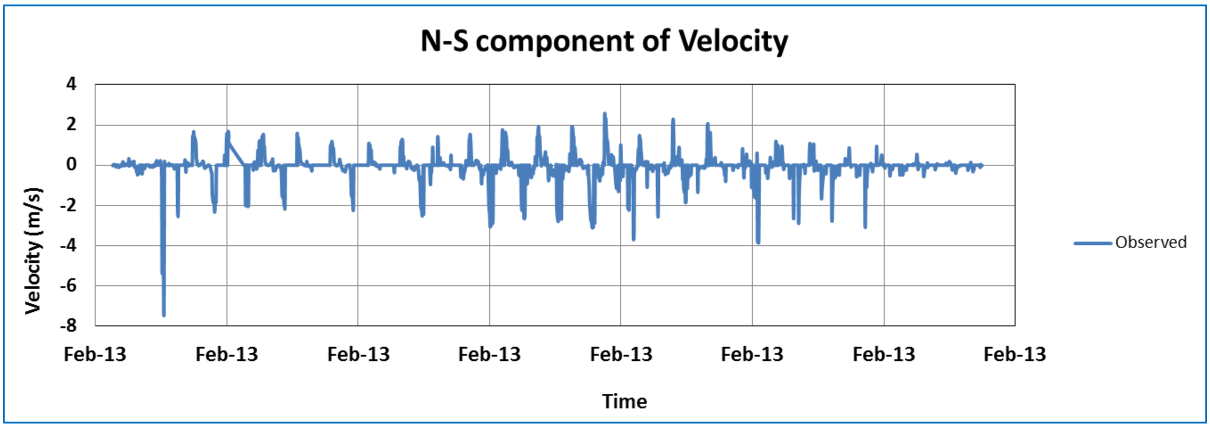

Figure 4-12 N-S component of current velocity at Dam-corridor-01 (season 1)

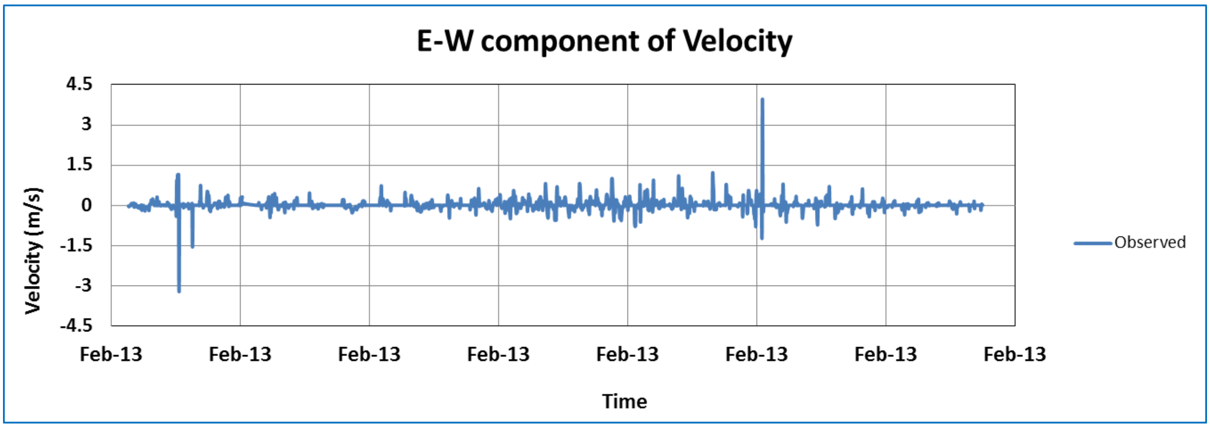

Figure 4-13 E-W component of current velocity at Dam-corridor-01 (season 1)

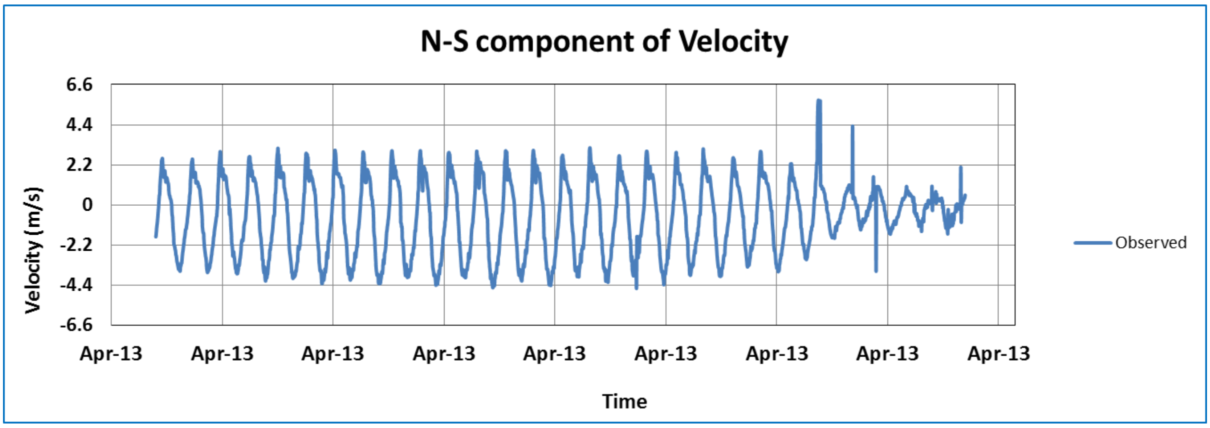

Figure 4-14 N-S component of current velocity at Dam-corridor-01 (season 2)

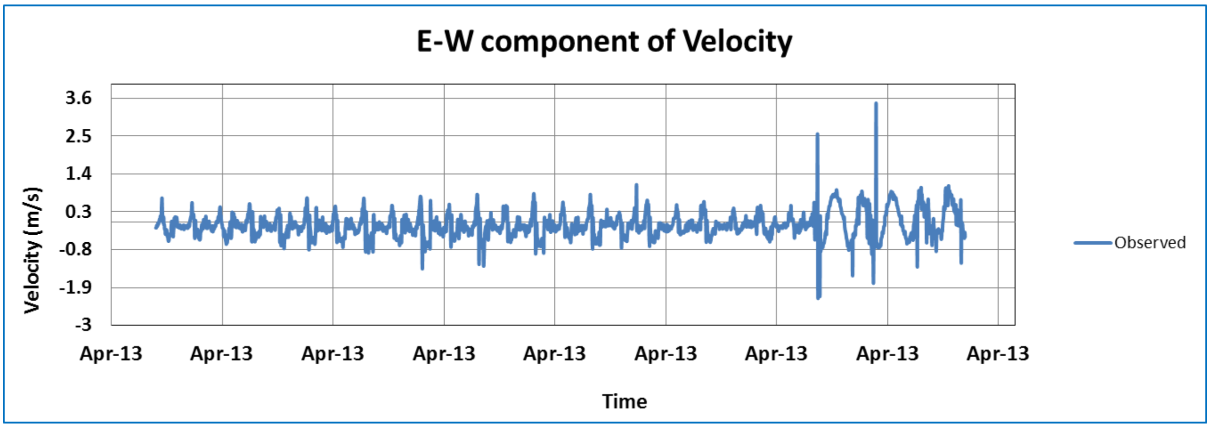

Figure 4-15 E-W component of current velocity at Dam-corridor-01 (season 2)

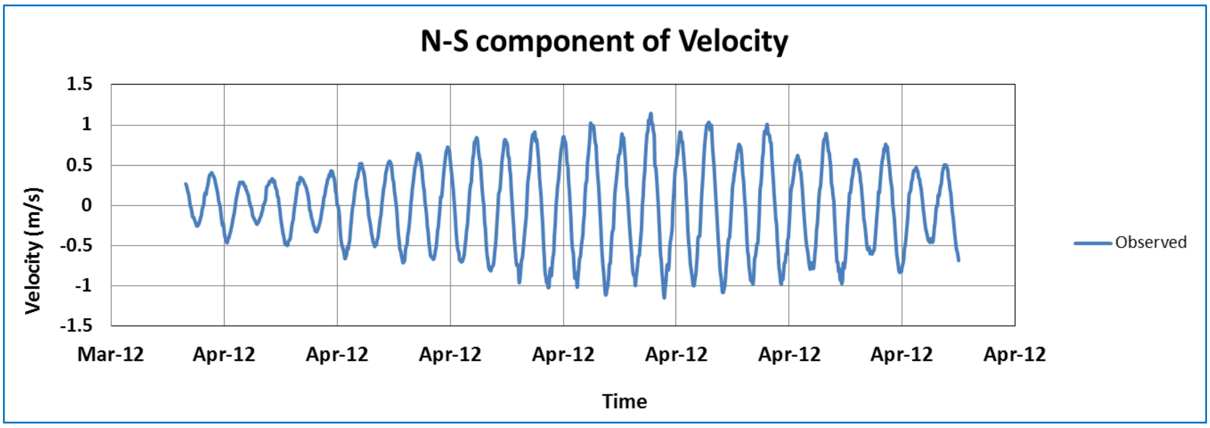

Figure 4-16 N-S component of current velocity at MC-Diu (season 1)

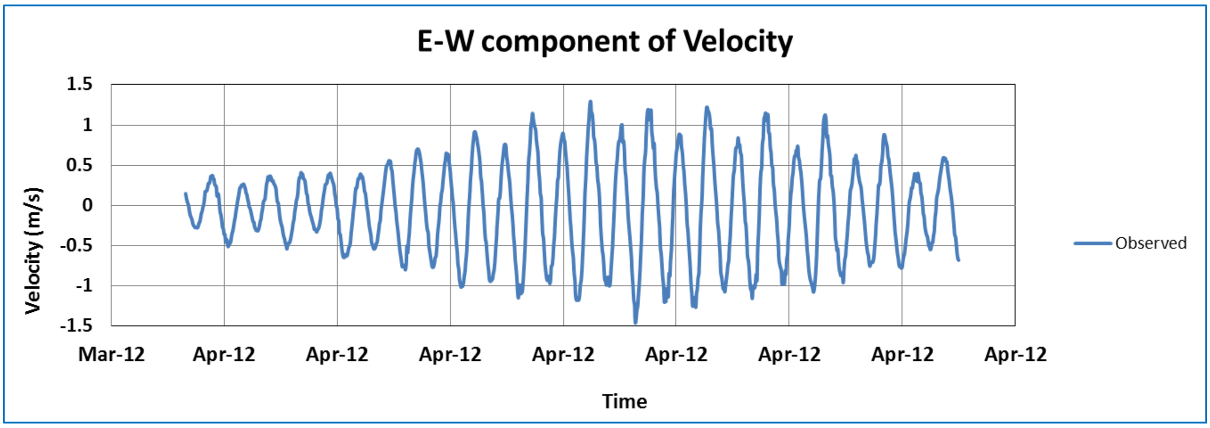

Figure 4-17 E-W component of current velocity at MC-Diu (season 1)

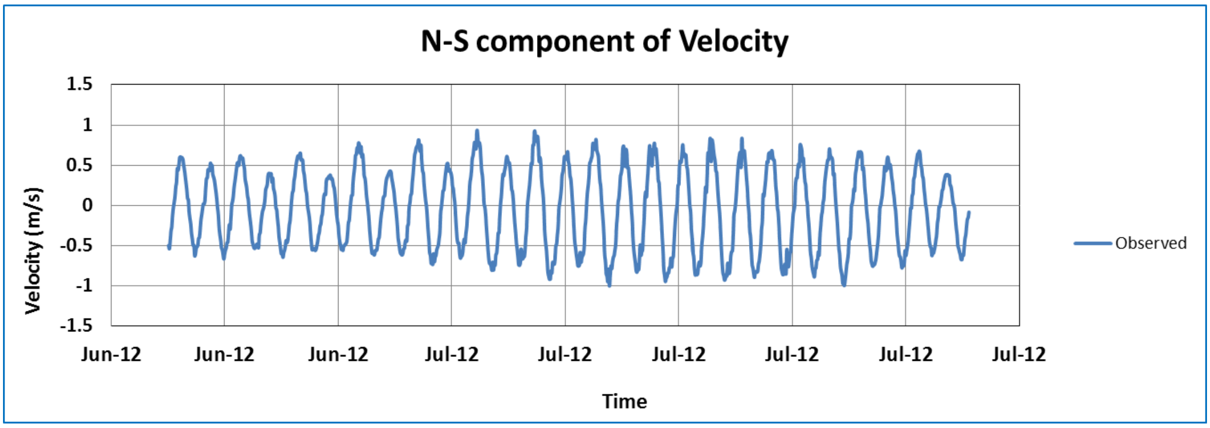

Figure 4-18 N-S component of current velocity at MC-Diu (season 2)

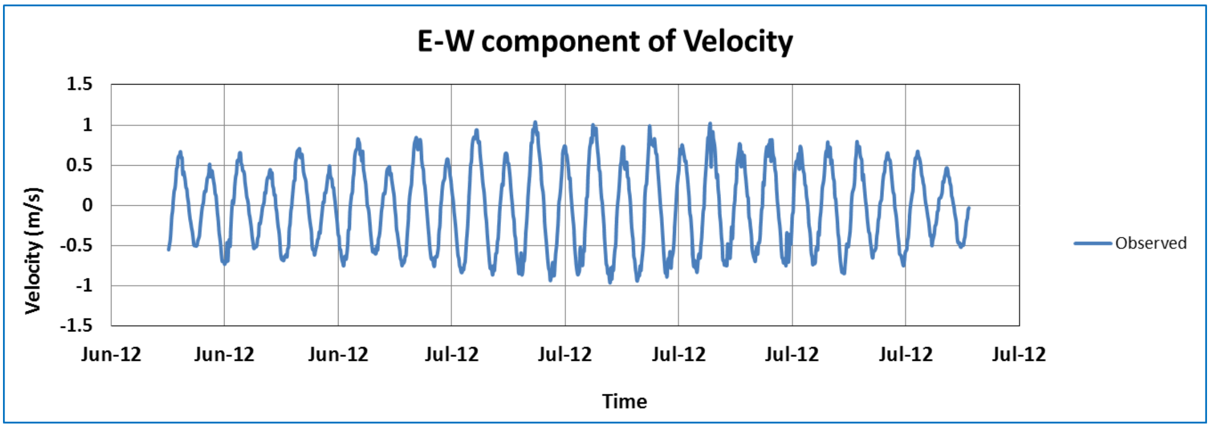

Figure 4-19 E-W component of current velocity at MC-Diu (season 2)

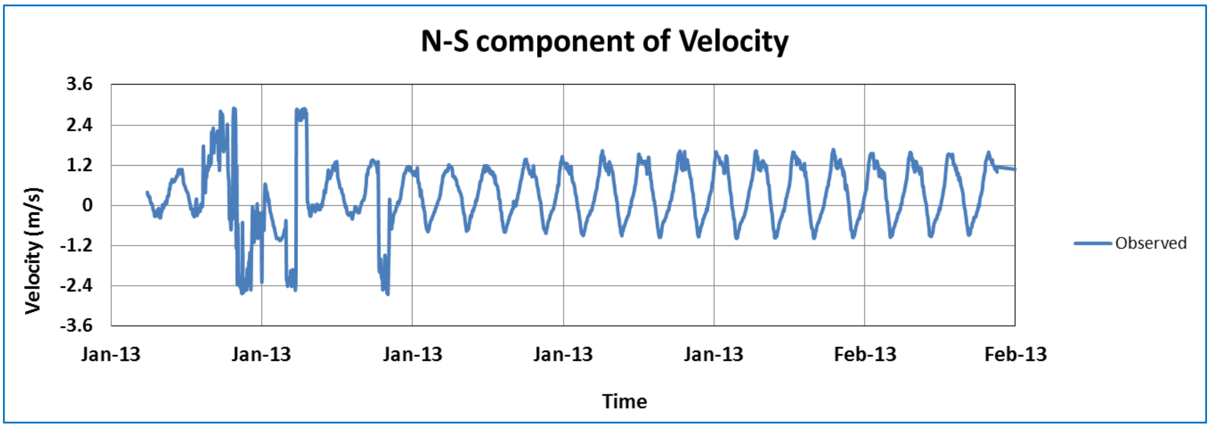

Figure 4-20 N-S component of current velocity at Mid – Channel – TSS5

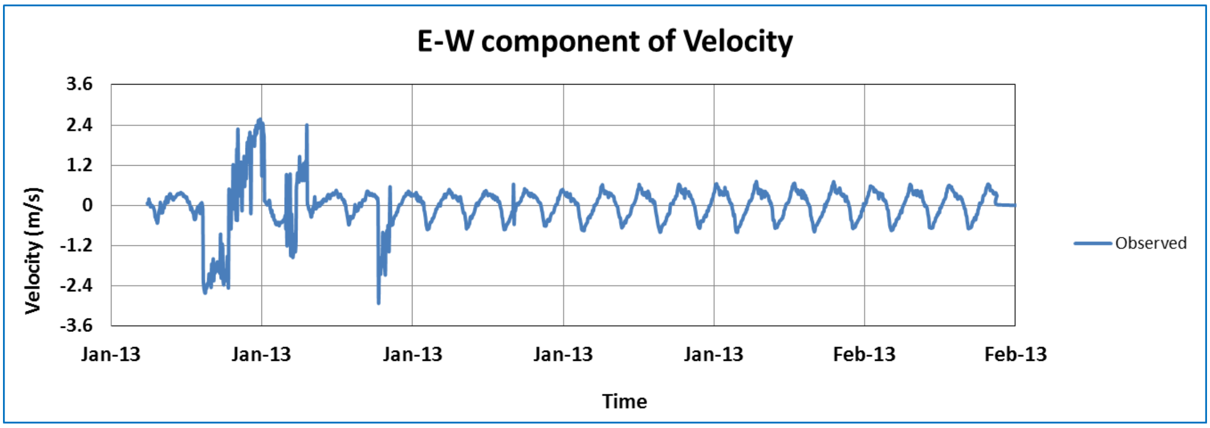

Figure 4-21 E-W component of current velocity at Mid – Channel – TSS5

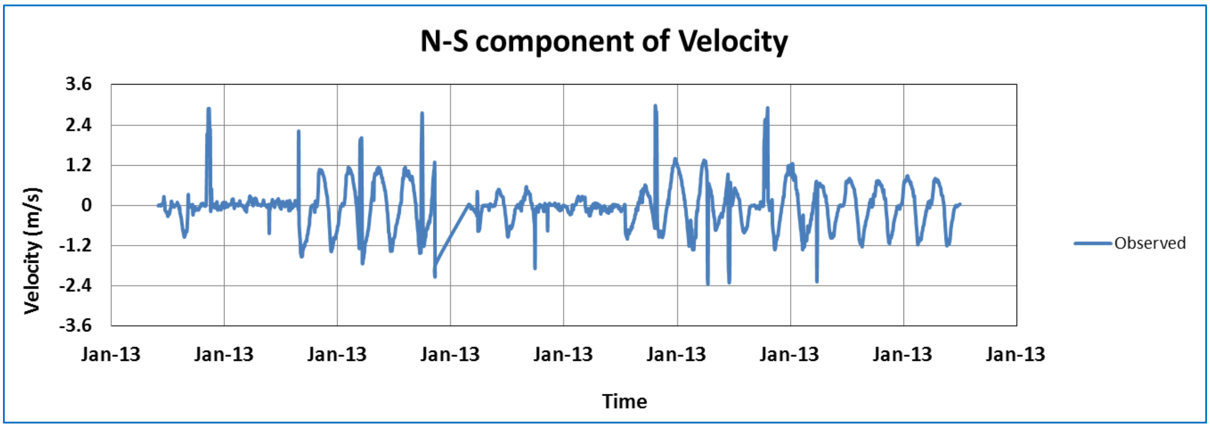

Figure 4-22 N-S component of current velocity at Mid – Channel – TSS8 (Season 1)

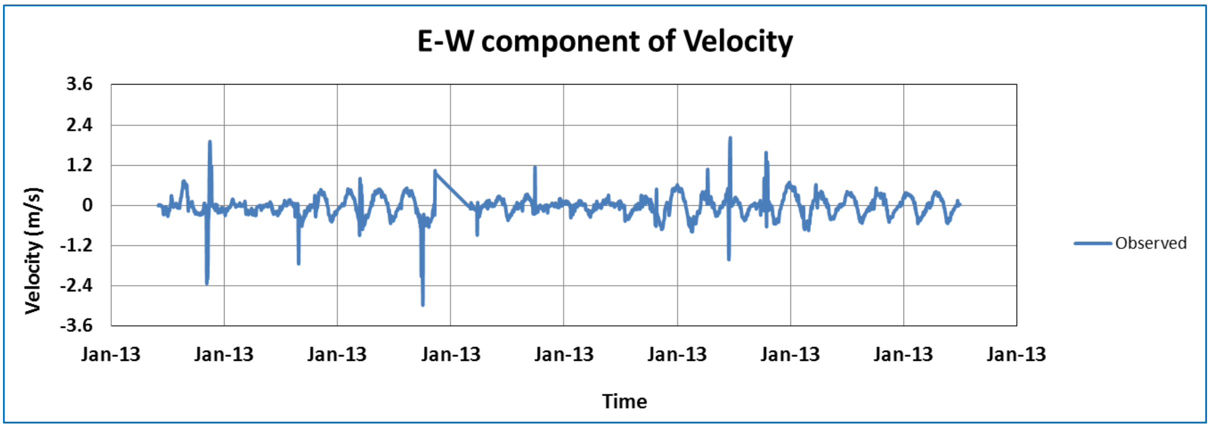

Figure 4-23 E-W component of current velocity at Mid – Channel – TSS8 (Season 1)

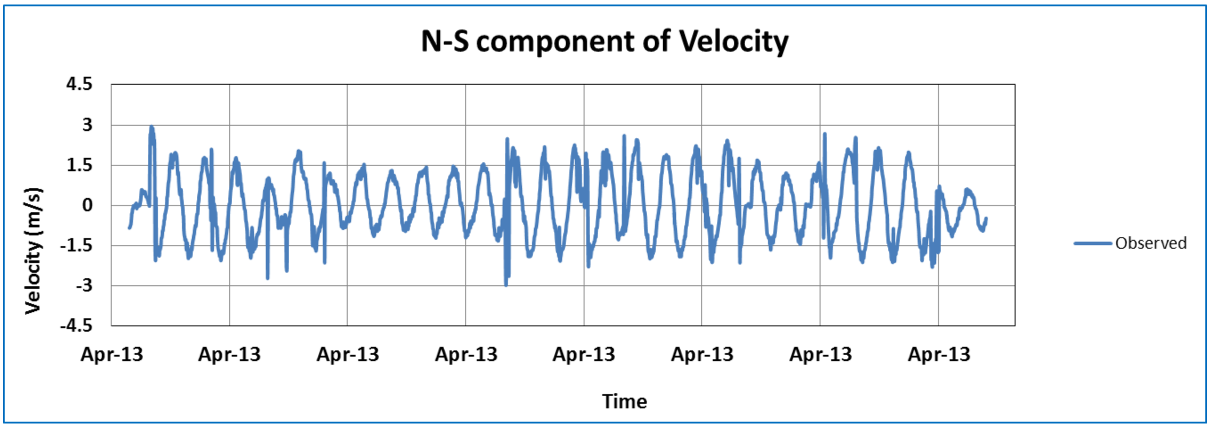

Figure 4-24 N-S component of current velocity at Mid – Channel – TSS8 (Season 2)

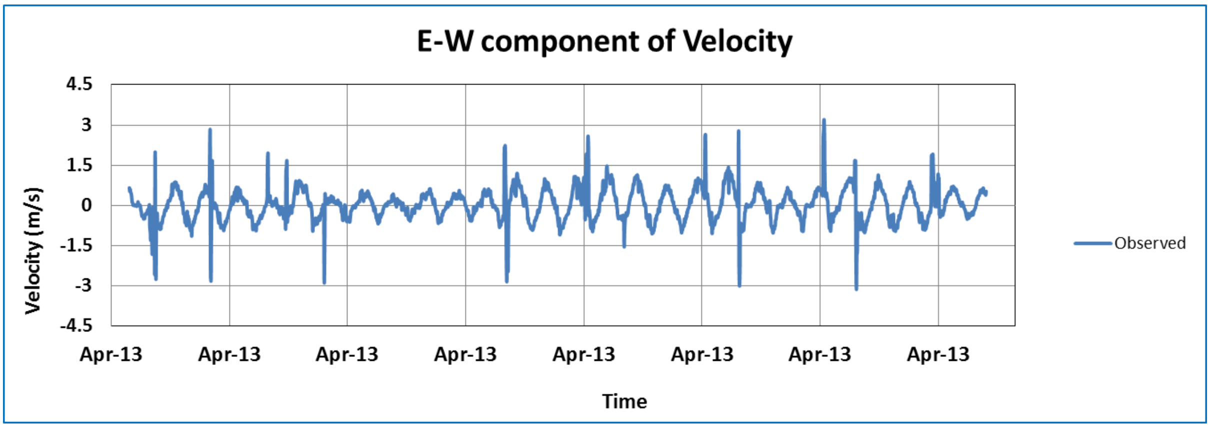

Figure 4-25 E-W component of current velocity at Mid – Channel – TSS8 (Season 2)

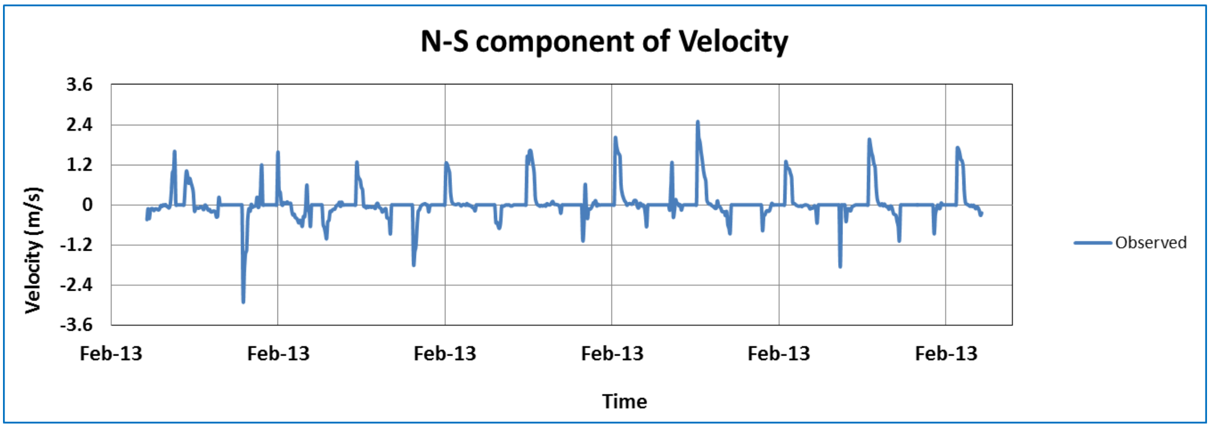

Figure 4-26 N-S component of current velocity at Narmada

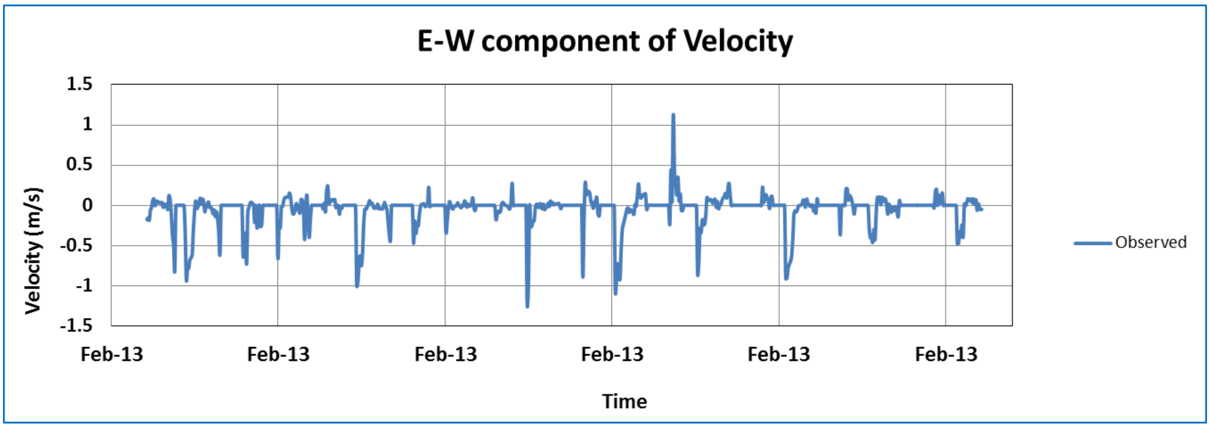

Figure 4-27 E-W component of current velocity at Narmada

4.5 River Discharge

The major river basins like Sabarmati, Mahi, Dhadhar and Narmada discharges water into the gulf along with other small river basins. The average annual discharge rates are provided below.

- Sabarmati – 120 m^3/s
- Mahi – 383 m^3/s
- Narmada – 1,447 m^3/s

The monthly average discharge[1] for the period 1901 t0 2006 is provided in Table 4-4.

Table 4-4 Monthly average discharge

Error! Not a valid link.

When flood events in the rivers discharging into Kalpasar reservoir coincide with high tide levels, reservoir outflow is impeded which in turn increases the upstream water level. Intensity and duration of flood in the rivers are significant inputs to study upstream water levels.

IIT Roorkee and National Institute of Hydrology have carried out the hydrology studies for the rivers discharging into Gulf of Khambhat. The Probable Maximum Flood for Dhadhar, Mahi and Sabarmati river basins estimated by IIT Roorkee, presented in Figure 4-28, is used for studying upstream water levels.

[1] Techno-economic Feasibility Report Phase-I of Gulf of Khambhat Development Project (KGDP)

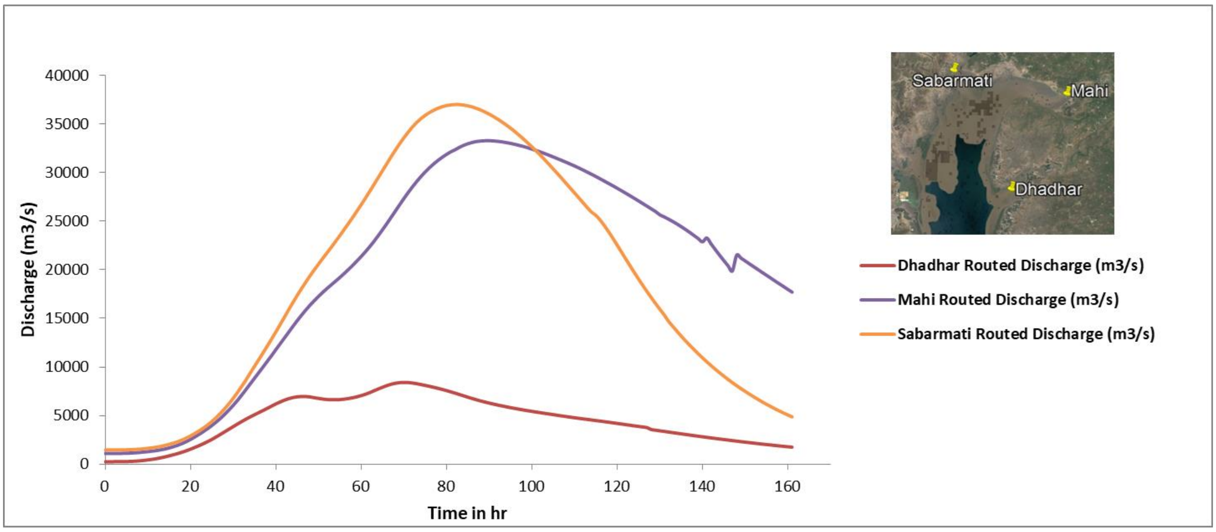

Figure 4-28 PMF for Dadhar, Mahi and Sabarmati

4.6 Sediment data

Sediment samples were collected in 205 locations along the Gulf of Khambhat as shown in Figure 4-29. Sieve analysis was carried out for sediment sizes greater than 0.075 whereas hydrometer analysis was carried out for sediment sizes less than 0.075. The results from the analyses are tabulated below in Table 4-5 Results from sieve analysis and
Table 4-6.

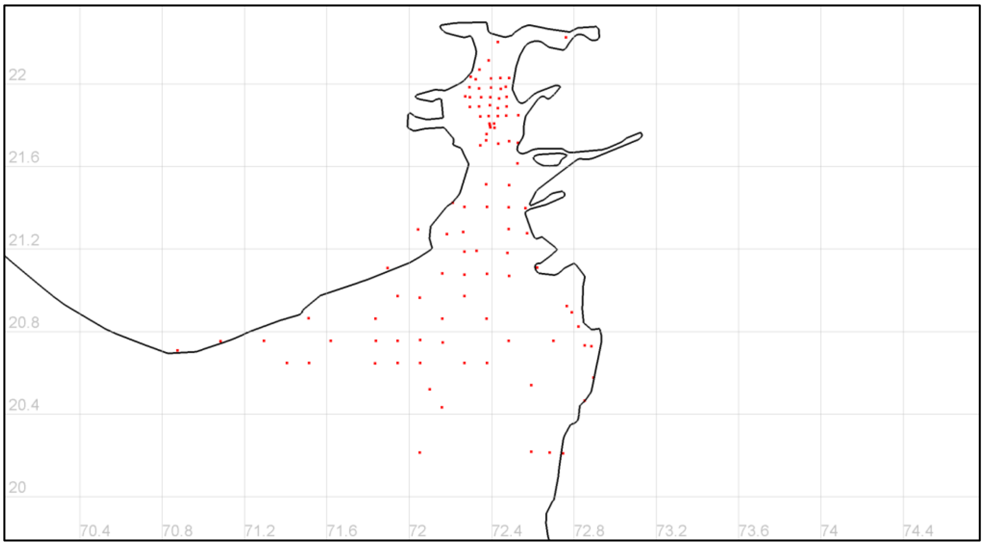

Figure 4-29 Sediment Sample Location

Table 4-5 Results from sieve analysis

Sl.No	Sample No	Location		Specific Gravity , G	% of Soil Fraction						Soil Type	Co-efficient			IS Classification (IS: 1498)
		Latitude	Longitude		Fine Grained Soil		Coarse Grained Soil					Cu	Cc	D50	
					Clay, %	Silt, %	Fine sand, %	Medium sand, %	Coarse sand, %	Fine Gravel, %					
					< 0.002 mm	0.002 - 0.075 mm	0.075 - 0.425mm	0.425 – 2 mm	2 - 4.75 mm	4.75 – 20 mm					
1	8	20˚45.3384'	71˚17.7192'	2.47	3.26	12.91	21.23	40.7	18.43	3.48	Silty Sand	48.16	2.37	0.72	SM
2	10	20˚38.8488'	71˚24.3192'	2.75	2.42	10.43	54.48	13.15	9.55	9.98	Silty Sand	7.12	0.76	0.193	SM
3	14	20˚38.8842'	71˚30.7692'	2.62	11.03		36.48	35	15.45	2.05	Medium to fine sand	18.16	1.37	0.412	SP-SM
4	16	20˚51.8892'	71˚30.6762'	2.83	0.18		23.1	53.1	12.7	10.93	Fine to medium sand	3.59	0.84	0.69	SP
5	20	20˚45.384'	71˚37.0782'	2.76	1.8		86.15	8.8	2.98	0.28	Fine sand	2.03	0.91	0.138	SP
6	32	20˚38.7'	71˚50.0082'	2.82	0.95		81.8	11.44	1.67	4.15	Fine sand	1.83	0.97	0.288	SP
7	33	20˚45.3216'	71˚50.1924'	2.86	1.53		96.68	1.25	0.53	0.03	Fine sand	1.59	0.97	0.142	SP
8	34	20˚51.8328'	71˚50.0976'	2.87	3.7		95.58	0.68	0.05	0	Fine sand	1.47	0.95	0.11	SP
9	40	20˚45.369'	71˚56.6676'	2.83	0.43		95.38	2.75	0.93	0.53	Fine sand	1.9	1.15	0.299	SP
10	42	20˚58.32'	71˚56.6148'	2.56	2.9		94.43	2.1	0.58	0	Fine sand	2.41	1.03	0.192	SP
11	44	20˚12.8304'	72˚3.0654'	2.75	1.66		86.78	10.01	1.45	0.1	Fine sand	1.76	0.93	0.232	SP
12	48	20˚38.8794'	72˚3.1716'	2.77	4.85		94.55	0.6	0	0	Fine sand	1.45	1.01	0.114	SP

13	49	20˚45.5352'	72˚3.1806'	2.78	0.85		50.75	17.03	5	26.38	Gravelly Fine sand	2.3	0,87	0.416	SP
14	51	20˚57.8544'	72˚3.0846'	2.84	3.88		94.78	1.25	0.1	0	Fine sand	1.41	0.96	0.107	SP
15	55	20˚25.9248'	72˚9.561'	2.83	6.44		91.23	2.23	0.1	0	Fine sand	1.47	0.97	0.108	SP-SM
16	58	20˚44.814'	72˚9.7728'	2.6	3.34		95.72	0.94	0	0	Fine sand	1.58	1.1	0.149	SP
17	61	21˚4.9584'	72˚9.651'	2.77	0.73		86.88	4.65	0.85	6.9	Fine sand	1.67	1.09	0.29	SP
18	63	21˚16.3872'	72˚10.9788'	2.72	4.43		92.03	3.08	0.48	0	Fine sand	2.24	1.17	0.3	SP
19	135	22˚12.300'	72˚25.800'	2.83	0.2		97.53	2.1	0.08	0.1	Fine sand	2.11	1.17	0.258	SP
20	65	21˚56.4282'	72˚16.2498'	2.84	2.03		95.3	2.63	0.05	0	Fine sand	2.75	1.25	0.237	SP
21	72	20˚38.8788'	72˚16.0674'	2.58	5.48		39.18	39.53	13.58	2.25	Fine to medium sand	11.43	1.28	0.551	SP-SM
22	75	20˚58.341'	72˚16.0668'	2.79	2.9		96.85	0.18	0.08	0	Fine sand	1.45	0.97	0.116	SP
23	76	21˚4.6404'	72˚16.002'	2.72	1.28		79.9	16.65	1.85	0.33	Medium to fine sand	2.05	1.03	0.298	SP
24	77	21˚11.2698'	72˚16.0914'	2.72	4.95		84.7	8.55	1.8	0	Fine sand	2.02	0.91	0.141	SP
25	78	21˚16.9416'	72˚15.7362'	2.75	10.38		85.43	3.65	0.55	0	Fine sand	1.62	0.94	0.109	SP-SM
26	79	21˚24.2226'	72˚16.0344'	2.68	3.36	15.79	40.18	15.05	10.73	14.9	Silty Sand	27.2	0.89	0.336	SM
27	92	21˚56.149'	72˚21.021'	2.75	0.45		98.23	1.33	0	0	Fine sand	1.23	1.05	0.19	SP
28	84	21˚53.3616'	72˚17.67'	2.75	3.53		95.28	1.15	0.05	0	Fine sand	2.29	1.19	0.222	SP
29	85	21˚56.1708'	72˚17.6808'	2.86	0.68		98.45	0.83	0.05	0	Fine sand	1.82	1.13	0.246	SP
30	86	21˚59.0256'	72˚17.6094'	2.84	5.73		93.15	1.13	0	0	Fine sand	1.45	0.95	0.107	SP-SM
31	87	22˚2.1576'	72˚17.8932'	2.72	5.43		93.75	0.83	0	0	Fine sand	2.15	0.98	0.157	SP-SM
32	120	22˚1.655'	72˚23.829'	2.71	4.82		94.25	0.93	0	0	Fine sand	3.05	1.29	0.274	SP
33	90	21˚50.5746'	72˚20.7372'	2.77	5.85		91.03	2.8	0.33	0	Fine sand	2.5	1.08	0.179	SP-SM
34	91	21˚53.5494'	72˚20.313'	2.85	8.1		91.45	0.45	0	0	Fine sand	1.39	0.96	0.099	SP-SM
35	93	21˚58.760'	72˚20.342'	2.96	4.17		94.66	1.16	0	0	Fine sand	1.62	1.09	0.143	SP
36	94	22˚1.4556'	72˚19.3668'	2.77	7.08		92.3	0.63	0	0	Fine sand	1.74	1.09	0.134	SP-SM

37	95	22°4.205'	72°20.412'	2.77	11.06		87.6	1.03	0.32	0	Fine sand	2.65	1.03	0.153	SP-SM
38	104	20°38.8932'	72°22.6218'	2.83	3.23		93.5	0.83	0	0	Fine sand	1.47	0.95	0.112	SP
39	105	21°45.4134'	72°22.5618'	2.8	1.28		94.28	4.03	0.23	0.2	Fine sand	1.83	1.1	0.259	SP
40	106	20°51.8634'	72°22.5624'	2.82	1.28		96.71	1.91	0.11	0	Fine sand	1.52	1.1	0.179	SP
41	108	21°4.842’	72°22.6134'	2.74	0.73		82.8	16.23	0.13	0.13	Medium to fine sand	1.55	1.03	0.325	SP
42	109	21°11.5278'	72°19.6374'	2.84	3.9		94.8	1.15	0.15	0	Fine sand	1.55	1.05	0.134	SP
43	110	21°17.733'	72°2.5864'	2.8	2.18		85.03	12.1	0.68	0.03	Fine sand	1.53	1.01	0.307	SP
44	111	21°24.2562'	72°22.608'	2.83	9.63		78.48	10.2	1.7	0	Fine sand	3.32	1.27	0.262	SP-SM
45	39	20°38.895’	71°56.6466'	2.4	0		11.22	86.44	1.4	0.94	Medium sand	1.26	0.98	0.497	SP
46	112	21°30.8874'	72°22.4586'	2.86	0.33		97.7	1.78	0.2	0	Fine sand	1.71	1.07	0.229	SP
47	114	21°43.6866'	72°22.4088’	2.78	1.03		96.38	2.3	0.3	0	Fine sand	2.1	1.18	0.317	SP
48	119	21°58.927'	72°23.830'	2.79	3.53		94.23	1.28	0.96	0	Fine sand	2.13	1.19	0.315	SP
49	116	21°50.6364'	72°23.1792'	2.83	11.03		88.33	0.65	0	0	Fine sand	2.07	1.14	0.137	SP-SM
50	141	22°1.756'	72°29.136'	2.79	4.25		91.33	3.99	0.43	0	Fine sand	1.6	1.11	0.1843	SP
51	126	21°50.6238'	72°25.8354'	2.77	10.13		65.1	13	8.83	2.95	Medium to Fine sand	5.46	0.87	0.173	SP-SM
52	127	21°53.001'	72°25.7736'	2.83	8.26		90.57	0.91	0.26	0	Fine sand	1.71	1.01	0.123	SP-SM
53	128	21°55.8306'	72°26.2356'	2.73	0.98		95.05	3.93	0.05	0	Fine sand	2.2	1.2	0.312	SP
54	129	21°58.6392’	72°26.64'	2.74	6.98		88.9	3.93	0.2	0	Fine sand	2.58	1.19	0.22	SP-SM
55	130	22°1.812'	72°26.592'	2.74	0.74		93.75	5.52	0	0	Fine sand	1.63	0.98	0.216	SP
56	137	21°50.7306'	72°28.287'	2.89	11.45		87.83	0.68	0.05	0	Fine sand	2.39	1.22	0.153	SP-SM
57	138	21°53.4408'	72°28.3158'	2.7	11.98		86.58	1.15	0.3	0	Fine sand	1.48	0.95	0.1	SP-SM
58	139	21°56.2554'	72°28.3068'	2.8	1.28		92.65	6.08	0	0	Fine sand	1.94	1.16	0.332	SP
59	140	21°59.1864'	72°28.1412’	2.79	0	13.5	79.2	5.03	0.08	0	Silty Fine Sand	4.58	1.38	0.194	SM
60	153	20°45.3636'	72°29.0202'	2.84	0.4		96.95	2.18	0.05	0.43	Fine sand	1.75	1.1	0.258	SP

61	156	21˚4.1538'	72˚29.1612'	2.74	0.2		66.2	28.53	2.43	2.65	Medium to Fine sand	1.58	0.97	0.369	SP
62	157	21˚10.9356'	72˚28.6098'	2.73	0.48		89.78	8.93	0.7	0.13	Fine sand	1.38	0.96	0.284	SP
63	158	21˚17.8326'	72˚29.0466'	2.71	0.88		74.33	23.18	1.5	0.13	Medium to Fine sand	1.58	1	0.339	SP
64	159	21˚24.2064'	72˚29.0154'	2.45	1.53		88.18	8.6	1.28	0.43	Fine sand	1.57	1.05	0.311	SP
65	160	21˚30.6834'	72˚29.0754'	2.86	10.6		85.08	3.8	0.53	0	Fine sand	1.68	0.95	0.31	SP-SM
66	59	20˚51.837'	72˚9.6156'	2.76	7.03		71.35	14.07	5.58	1.97	Medium to Fine sand	2.71	0.87	0.133	SP-SM
67	162	21˚43.4226'	72˚29.0718'	2.6	4.7		57.05	29.6	8.65	0	Medium to Fine sand	5.19	0.82	0.3	SP
68	164	21˚50.977'	72˚31.781'	2.81	4.32		92.25	3.07	0.35	0	Fine sand	1.7	1.13	0.175	SP
69	185	21˚16.5372'	72˚34.2996'	2.51	1		41.13	55.53	1.63	0.73	Fine to medium sand	1.65	1.1	0.442	SP
70	186	21˚23.8608'	72˚33.8442'	2.72	3.63		83.88	8.6	2.25	1.65	Fine sand	2.41	1.13	0.272	SP
71	188	21˚36.9798'	72˚31.512'	2.73	3.2		6.25	62.18	8.68	19.7	GravellyMedium sand	4.43	0.82	0.842	SP
72	198	20˚45.306'	72˚41.988'	2.68	5.13	35	17.33	18.08	11.98	12.5	Silty Sand	42.9	0.62	0.179	SM
73	203	22˚13.537'	72˚45.601'	2.73	4.75		93.38	1.63	0.25	0	Fine sand	1.84	1.15	0.167	SP
74	S17	21˚6.646'	72˚37.200'	2.8	0.38		52.71	44.17	1.2	1.53	Medium to fine sand	3.41	1.31	0.392	SP
75	122	22˚6.900'	72˚23.100'	2.8	7.85		90.7	1.24	0.21	0	Fine sand	1.76	1.09	0.132	SP-SM
76	S 27	20˚27.944'	72˚51.102'	2.88	3.34		95.65	0.96	0.06	0	Fine sand	1.56	1.08	0.144	SP
77	S29	20˚12.554'	72˚44.776'	2.66	4.03		59.27	33.88	1.99	0.83	Medium to fine sand	1.96	0.95	0.358	SP
78	132	20˚31.270'	72˚5.913'	2.78	3.37		95.63	1	0	0	Fine sand	1.6	1.1	0.15	SP
79	X7	21˚42.122'	72˚20.760'	2.57	2.48		95.33	1.94	0.25	0	Fine sand	1.67	1.12	0.344	SP
80	X6	21˚42.653'	72˚25.897'	2.74	6.42		88.86	4.34	0.2	0.18	Fine sand	2.04	1.07	0.201	SP-SM

81	X5	21˚47.362'	72˚24.900'	2.68	4.94	92.65	2.31	0.1	0	Fine sand	2.1	1.11	0.198	SP
82	X4	21˚48.486'	72˚24.736'	2.69	3.93	94.26	1.48	0.33	0	Fine sand	1.6	1.11	0.349	SP
83	X3	21˚47.405'	72˚23.656'	2.73	3.82	92.55	3.16	0.48	0	Fine sand	1.91	1.16	0.33	SP
84	X2	21˚48.012'	72˚23.459'	2.69	1.09	77.48	21.13	0.15	0.15	Medium to fine sand	1.95	1.13	0.333	SP
85	X1	21˚48.459’	72˚23.354'	2.66	2.5	95.31	1.92	0.27	0	Fine sand	1.67	1.12	0.344	SP
86	117	21˚53.858’	72˚23.512'	2.9	1.35	97.64	1	0	0	Fine sand	1.46	1.09	0.18	SP
87	118	21˚56.215'	72˚23.666'	2.68	0.5	20.95	77.77	0.19	0.59	Fine to medium sand	1.61	1.11	0.513	SP
88	S 25	20˚34.651'	72˚53.710’	2.65	1.34	70.34	27.57	0.64	0.11	Medium to fine sand	2.47	0.89	0.234	SP
89	S 23	20˚43.975'	72˚51.158'	2.96	0.51	56.73	42.69	0.07	0	Medium to fine sand	4.5	1.39	0.356	SP
90	S 24	20˚43.788'	72˚53.079'	2.83	1.66	95.73	2.61	0	0	Fine sand	1.61	1.11	0.185	SP
91	S21	20˚49.436'	72˚49.280'	2.81	0.63	72.71	24.8	0.69	1.16	Medium to fine sand	2.27	0.92	0.237	SP
92	S 20	20˚53.602’	72˚47.360'	2.78	2.4	97.5	0.09	0	0	Fine sand	2.3	1.02	0.145	SP
93	S 19	20˚55.419'	72˚45.843'	2.71	1.37	3.12	89.52	3.54	2.45	Medium sand	1.72	1.12	0.807	SP
94	S 30	20˚45.221'	71˚4.952'	2.79	1.18	89.57	9.25	0	0	Fine sand	1.74	0.93	0.169	SP
95	S 5	21˚6.552'	71˚53.711'	2.61	7.08	90.92	2	0	0	Fine sand	1.99	1.15	0.158	SP-SM
96	S 7	21˚25.495’	72˚12.749'	2.95	4.3	95.54	0.16	0	0	Fine sand	1.71	1.13	0.156	SP
97	S 14	21˚42.914'	72˚31.643'	2.82	0.53	97.37	2.1	0	0	Fine sand	1.33	0.98	0.178	SP
98	S1	20˚42.5239'	70˚52.5128’	2.68	0.05	80.38	19.57	0	0	Medium to fine sand	1.78	0.92	0.22	SP
99	178	20˚32.418’	72˚35.532’	2.72	0.22	10.19	20.01	21.3	48.24	Gravelly sand			0.377	SP
100	175	20˚13.0146’	72˚35.5152’	2.65	0.34	1.59	36.84	25.4	35.79	Shell	4.92	0.82	2.89	SP
101	193	20˚12.8532’	72˚40.8498’	2.64	0.18	0.91	45.1	32.3	21.51	Gravelly sand	2.78	0.88	2.22	SP
102	183	21˚3.8184’	72˚35.5062’	2.69	Length= 130mm ; Breadth=25mm					Coarse gravel	Gravel			

103	113	21˚37.2924’	72˚22.896'		Length= 80mm ; Breadth=60mm	Coarse gravel	Gravel
104	154	20˚51.7062’	72˚29.0574'	2.72	Stone weight = 320.55g		Cobble

Table 4-6 Results from Hydrometer analysis

Sl. No.	Sample No.	Location		Specific Gravity, G	% of Soil Fraction							IS Classification (IS: 1498)
		Latitude	Longitude		Clay, %	Silt, %			Co-efficients			
					< 0.002 mm	0.002 - 0.075 mm	Liquid limit	Plasticity Index	Cu	Cc	D_{50}	
105	S 28	20˚25.097'	72˚49.605'	2.23	49	51	68.02	44.14	18.3	0.05	0.002	CH
106	S32	21˚17.894'	72˚6.414'	2.5	17	83	42.38	19.64	193.19	0.16	0.045	CI
107	S 26	20˚31.806'	72˚52.860'	2.52	14	86	58.46	30.07	5.53	0.21	0.004	CH
108	S 18	21˚1.170’	72˚43.558'	2.83	15	85	26.71	14.6	124	3.31	0.063	CL
109	S 15	21˚31.781’	72˚43.266’	2.57	21	79	45.92	17.72	32.6	2.16	0.014	CI
110	S16	21˚19.566’	72˚37.260’	2.66	29.5	70.5	28.21	14.35	156.1	3.03	0.01	CL
111	1	20˚38.892’	70˚58.1952’	2.53	9	91	51.36	29.41	44.02	2.33	0.014	CH
112	2	20˚38.889'	71˚4.8444'	2.76	5	95	43.78	18.96	6.95	1.58	0.038	CI
113	4	20˚38.8668'	71˚11.3058'	2.76	3	97	41.53	20.06	7.15	1.47	0.045	CI
114	5	20˚45.378'	71˚11.2518'	2.53	23	77	63.2	34.29	76.87	2.66	0.012	CH
115	6	20˚32.4024'	71˚17.8164'	2.7	12	88	33.6	15.53	457	28.5	0.036	CL
116	7	20˚11.7534'	71˚17.7942'	2.46	22	78	70.11	37.63	150.56	3.11	0.018	CH
117	9	20˚32.388'	71˚24.276'	2.64	11	89	66.96	36.33	20.11	1.86	0.025	CH
118	11	20˚45.3846'	71˚24.1794'	2.53	21	79	66.69	29.53	136.58	3.02	0.017	MH
119	12	20˚25.9176'	71˚30.7188'	2.77	8	92	27.16	5.73	19.22	1.95	0.032	CL-ML

120	13	20˚32.4132'	71˚30.78'	2.66	13	87	32.12	12.06	25.25	2.07	0.028	CL
121	15	20˚45.363'	71˚30.6888'	2.51	15	85	51.58	31.41	59.72	3.22	0.019	CH
122	17	20˚25.9296'	71˚37.1826'	2.76	13	87	29.16	10.79	52.13	2.22	0.023	CL
123	18	20˚32.3574'	71˚37.2228'	2.56	11	89	32.37	11.94	40.29	3.25	0.03	CL
124	19	20˚38.8944'	71˚37.2078'	2.98	15	85	49.69	27.99	24.93	1.59	0.018	CI
125	21	20˚51.9702'	71˚37.6626'	2.68	1	99	32.31		2.743	1.2	0.054	ML
126	22	20˚19.4472'	71˚43.6818'	2.47	35	65	80.12	52.59	72.65	0.9	0.004	CH
127	23	20˚25.9446'	71˚43.6728'	2.64	21	79	65.83	34.86	65.49	2.41	0.014	CH
128	24	20˚32.406'	71˚43.719'	2.77	6	94	29.41	8.78	13.82	1.89	0.034	CL
129	25	20˚38.9154'	71˚43.7802'	2.72	17	83	49	26.3	57.61	2.32	0.017	CI
130	26	20˚45.4668'	71˚43.9194'	2.75	10	90	26.48	9.88	13.46	1.08	0.018	CL
131	27	20˚51.8388'	71˚43.7088'	2.54	21	79	76.1	44.65	73.06	2.14	0.014	CH
132	29	20˚19.4556'	71˚50.2512'	2.52	32	68	67.64	33.82	32.27	0.39	0.005	MH
133	30	20˚25.95'	71˚50.1576'	2.54	29	71	61.72	32.82	106.45	2.83	0.01	CH
134	31	20˚32.7042'	71˚50.1798'	2.49	26	74	73.43	43.03	120.87	2.6	0.009	CH
135	35	20˚58.3434'	71˚50.0598'	2.64	6	94	37.37	18.39	11.2	1.61	0.038	CI
136	36	20˚19.428'	71˚56.6304'	2.21	44	56	82.29	36.78	50.8	0.39	0.002	MH
137	37	20˚25.8972'	71˚56.6292'	2.51	29	71	65.42	31.93	119.7	2.06	0.008	MH
138	38	20˚32.394'	71˚56.6358'	2.58	22	78	55.63	28.72	24.72	1.15	0.011	CH
139	179	20˚38.994'	72˚35.2968'	2.52	18	82	50.13	21.73	36.85	1.61	0.017	MH
140	41	20˚51.8394'	71˚56.6034'	2.34	14	86	75.57	19.23	7.55	0.052	0.007	MH
141	43	21˚4.7748'	71˚56.5692'	2.77	26	74	78.07	46.46	85.55	2.07	0.011	CH
142	45	20˚19.467'	72˚3.1098'	2.52	32	68	50.64	21.28	58.64	0.33	0.006	MH
143	46	20˚25.9296'	72˚3.1176'	2.6	34	66	82.19	43.27	51.2	0.86	0.004	MH
144	47	20˚34.0218'	72˚3.1308'	2.75	26	74	68.33	41.42	113.5	2.67	0.008	CH
145	50	19˚57.876'	72˚3.1692'	2.72	35	65	28.75	10.68	431.6	2.21	0.006	CL

146	52	21˚4.7826'	72˚3.1296'	2.72	1	99	26.3		2.73	0.96	0.036	ML
147	53	20˚12.9012'	72˚9.6078'	2.5	29	71	49.58	23.77	45.85	1.27	0.006	CI
148	54	20˚19.6362'	72˚9.5832'	2.84	21	79	58.34	31.08	31	0.99	0.01	CH
149	56	20˚32.4132'	72˚9.5994'	2.37	46	54	46.18	14.01	19.47	0.68	0.001	MI
150	57	20˚38.8698'	72˚9.6078'	2.88	7	93	52.2	25.72	15.34	2.14	0.032	CH
151	60	20˚58.3254'	72˚9.6054'	2.57	30	70	68.25	43.97	309.9	2.42	0.008	CH
152	67	20˚6.3822'	72˚15.9738'	2.32	39	61	79.07	39.1	41.1	0.89	0.002	MH
153	68	20˚12.9102'	72˚16.1538'	2.84	15	85	61.22	28.88	28.72	2.03	0.015	MH
154	69	20˚19.4442'	72˚16.1784'	2.57	25	75	71.18	37.78	77.72	2.47	0.009	MH
155	70	20˚25.938'	72˚16.1136'	2.62	32	68	84.19	44.42	30.39	0.35	0.006	MH
156	73	20˚45.348'	72˚16.0884'	2.48	30	70	62.67	27.81	75.43	1.95	0.006	MH
157	74	20˚51.8922'	72˚16.6272'	2.77	7	93	23.88		45.21	4.02	0.031	ML
158	80	21˚30.3816'	72˚16.9518'	2.66	12	88	41.74	17.54	239.6	48.53	0.027	CI
159	81	21˚43.5792'	72˚17.2236'	2.64	22	78	59.92	37.9	60.14	2.31	0.01	CH
160	99	20˚6.498'	72˚22.572'	2.56	35	65	72.59	26.36	11.7	0.61	0.002	MH
161	100	20˚12.954'	72˚22.536'	2.33	53	47	85.96	52.12	31.9	0.62	0.001	CH
162	101	20˚19.419'	72˚22.554’	2.33	35	65	78.44	43.66	25.2	1.24	0.0021	CH
163	102	20˚25.887'	72˚22.4982'	2.74	30	70	73.3	39.44	34.1	1.22	0.004	CH
164	103	20˚32.424'	72˚22.5714'	2.66	30	70	66.49	40.46	41.3	0.7	0.005	CH
165	107	20˚58.3344'	72˚22.6314'	2.32	4	96	38.22	18.75	5.83	1.41	0.031	CI
166	146	19˚59.9898'	72˚29.0448'	2.52	40	60	83.18	45.79	45.6	0.24	0.002	MH
167	147	20˚6.2682'	72˚28.9806'	2.33	56	44	72.88	32.1	152.2	11.3	0.001	MH
168	148	20˚12.9552'	72˚30.3186'	2.47	40	60	72.12	36.94	40.8	0.88	0.002	MH
169	149	20˚19.4274'	72˚29.0118'	2.32	50	50	76.91	36.86	33.2	0.27	0.001	MH
170	150	20˚25.9326'	72˚29.0154'	2.39	47	53	82.75	38.92	20.1	0.21	0.001	MH
171	151	20˚25.9326'	72˚29.0154'	2.67	29	71	71.04	39.87	27.3	0.84	0.004	CH

172	152	20˚38.8974’	72˚28.9752'	2.51	26	74	70.6	36.38	97.3	2.73	0.009	MH
173	155	20˚58.1952'	72˚28.9656'	2.51	32	68	74.44	39.68	379.2	3.06	0.007	CH
174	173	19˚59.9922'	72˚35.5296'	2.51	30	70	91.68	53.01	9.47	0.27	0.003	CH
175	176	20˚19.4694'	72˚35.5038'	2.47	44	56	71.04	33.43	32.5	0.39	0.002	MH
176	177	20˚26.1342'	72˚35.5728'	2.21	44	56	86.31	47.69	22.6	0.62	0.002	MH
177	181	20˚51.8304'	72˚35.538’	2.52	21	79	64.43	33.99	10.5	0.7	0.01	CH
178	182	20˚58.2936'	72˚35.6178'	2.6	12	88	53.15	28.39	30.1	3.58	0.016	CH
179	184	21˚11.466'	72˚33.7404'	2.58	12	88	37.73	18.73	44.2	3.78	0.017	CI
180	187	21˚30.807'	72˚33.8424'	2.63	15	85	28.22	10.92	328	31.4	0.029	CL
181	191	20˚0.0996’	72˚38.4606'	2.35	52	48	102.98	63.33	17.8	0.47	0.001	CH
182	192	20˚6.2754'	72˚39.6852'	2.41	34	66	73.04	37.85	29.4	1.29	0.003	MH
183	174	20˚6.4758’	72˚35.505'	2.4	30	70	65.2	33.79	18.9	1.16	0.005	MH
184	195	20˚25.917'	72˚41.997'	2.58	34	66	86.1	54.22	39.9	1.61	0.003	CH
185	204	20˚25.581'	72˚47.9736'	2.43	34	66	86.57	41.59	5.25	0.43	0.002	MH
186	207	20˚45.3696'	72˚44.9934'	2.34	15	85	43.77	20.87	18.9	2.78	0.02	CI
187	S 4	20˚58.813'	71˚37.027'	2.68	22.5	77.5	27.03	8.9	140.9	2.75	0.015	CL
188	S 6	21˚13.743’	72˚5.457'	2.46	18	82	50	26.68	32.1	2.11	0.013	MH
189	S 8	21˚41.460'	72˚16.740'	2.47	18.5	81.5	53.1	26.87	98.1	0.06	0.06	CH
190	S 9	21˚59.393'	72˚12.676'	2.61	14	86	37.43	16.5	18.2	2.67	0.018	CI
191	S 11	22˚17.183'	72˚36.467'	2.68	4	96	33.86		3.6	0.96	0.038	MI
192	S 12	22˚110.262'	72˚33.613’	2.56	9	91	35.36	15.83	7.55	1.56	0.02	CI
193	S 13 A	21˚54.630'	72˚32.085'	2.55	12	88	38.49	18.69	36.6	5.78	0.02	CI
194	71	20˚32.3772'	72˚16.086'	2.57	22	78	69.58	32.91	71.2	2.58	0.012	MH
195	206	20˚38.8434'	72˚47.199'	2.32	50	50	81.16	42.16	12.7	0.31	0.001	MH
196	180	20˚45.738'	72˚35.7078'	2.66	30	70	67.87	32.12	93.2	2.69	0.005	MH
197	194	20˚19.554'	7241.9982'	2.45	17	83	68.16	33.35	3.37	0.68	0.003	MH

198	196	20˚32.4108'	72˚41.9898'	2.42	1	99	72.44	41.66	6.13	0.75	0.01	CH
199	199	20˚51.6918'	72˚42.0768'	2.38	1	99	55.62	30.11	448.71	3.23	0.006	CH
200	197	20˚38.8002'	72˚42.0696’	2.44	19	81	51.71	24.97	41.304	2.28	0.017	CH
201	28	20˚58.3338'	71˚43.6458'	2.38	48	52	80.4	35.14	32.48	0.11	0.001	MH
202	62	21˚11.2848'	72˚9.5382'	2.79	5	95	27.67	10.05	4.2	1.27	0.029	CL
203	161	21˚36.9816'	72˚28.9908'	2.67	2	98	33.19		3.12	0.92	0.036	ML
204	3	20˚32.3304'	71˚11.2404'	2.71	3	97	32.95	7.61	6.22	1.56	0.041	ML
205	200	20˚58.266'	72˚42.0186'	2.34	1	99	64.27	37.91	6.67	1.34	0.043	CH

4.7 Wave climate

The observed wave data were provided at two locations shown in Figure 4-30. The locations and wave parameters are presented in Table 4-7.

Figure 4-30 Observed wave data

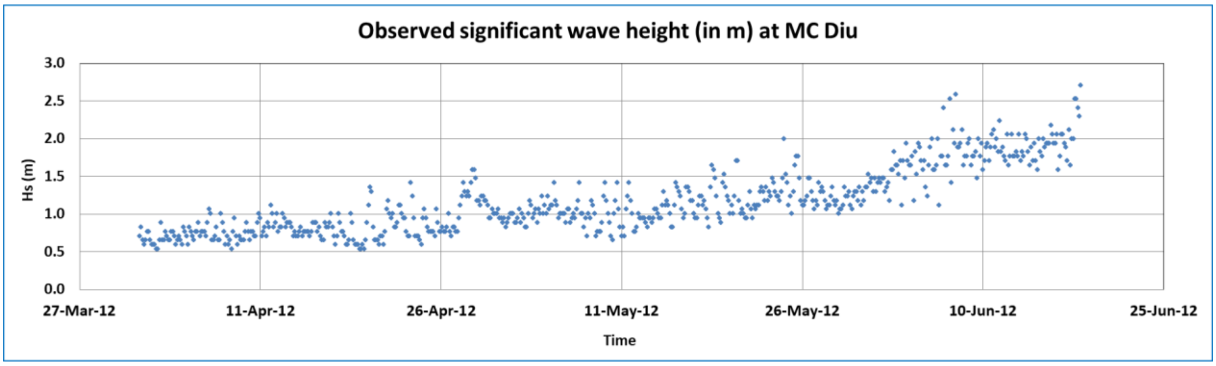

Figure 4-31 Observed significant wave height at MC Diu

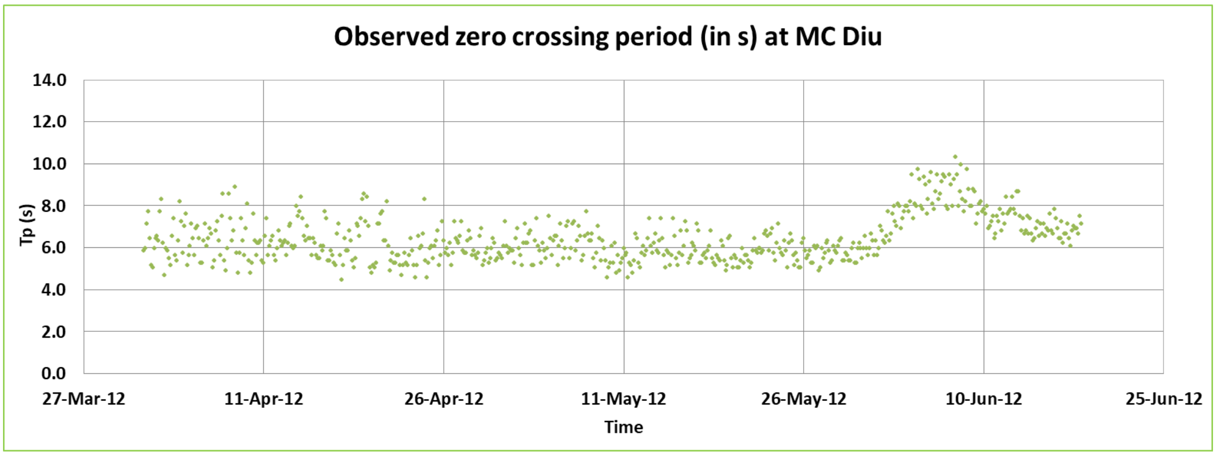

Figure 4-32 Observed zero crossing period at MC Diu

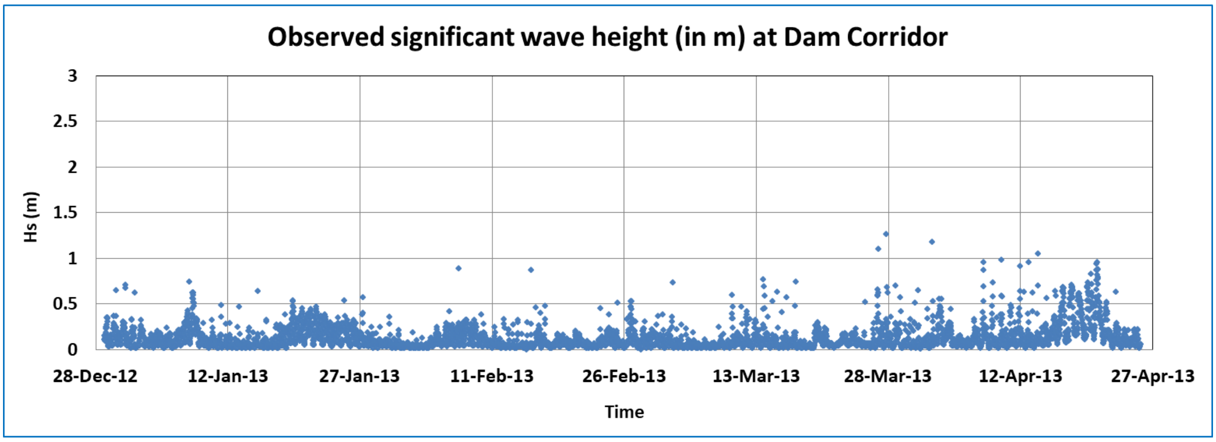

Figure 4-33 Observed significant wave height at Dam Corridor

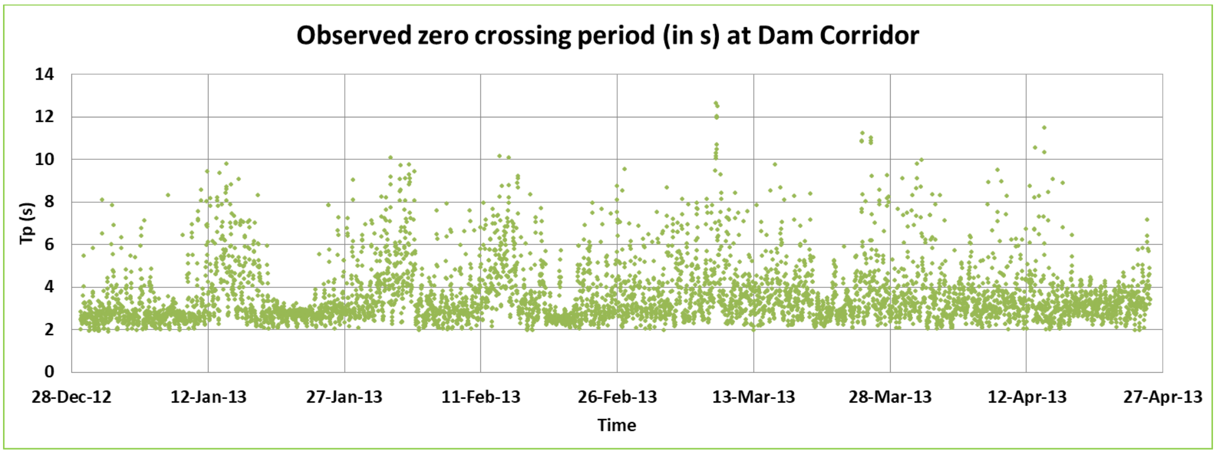

Figure 4-34 Observed zero crossing period at Dam Corridor

Table 4-7 Observed wave heights

Location	Longitude	Latitude	Observation Period	Wave height range(in m)
MC Diu	71.88	20.28	March 2012 to June 2012	0.5 - 2.5
Dam Corridor	72.28	21.78	December 2012 to April 2013	0.1 – 1.3

4.8 Cyclones

A storm surge is often associated with a tropical cyclone or similar weather system. The several factors that contribute to amount of a surge at a location are central pressure, storm intensity, size of the storm, storm forward speed, angle of approach to a coast, shape of coastline, width and slope of ocean bottom and local features.

Storm surge study was carried out using the cyclone data provided at Joint Typhoon Warning Centre's (JTWC) website for period 1945-2022. JTWC is a combined United States Air Force/Navy organization under the operational command of the Commanding Officer, Naval Maritime Forecast Centre/ Joint Typhoon Warning Centre (NMFC/JTWC), Pearl Harbour, Hawaii.

The data provided in the best track's formats are 6 hourly positions of the cyclone's eye, maximum wind speeds, radius of maximum wind speeds, the central pressure, and the neutral pressure. This information is necessary for various modelling studies involving cyclones such as storm surge modelling.

About 64 cyclones have passed within 300km radius of the study area from 1945-2022. However, only four cyclones have passed in close proximity to the Gulf of Khambhat. During May 2021, Tauktae, an Extremely Severe Cyclonic Storm made its landfall near the gulf with wind speeds close to 200 kmph.

The tracks of cyclones which passed within the domain chosen and possessed sufficient data to simulate water levels are presented in the Figure 4-35. A typical cyclone track in Saffir-Simpson Hurricane Scale is provided in Figure 4-36. All the factors that could affect the storm surge have been considered in the model.

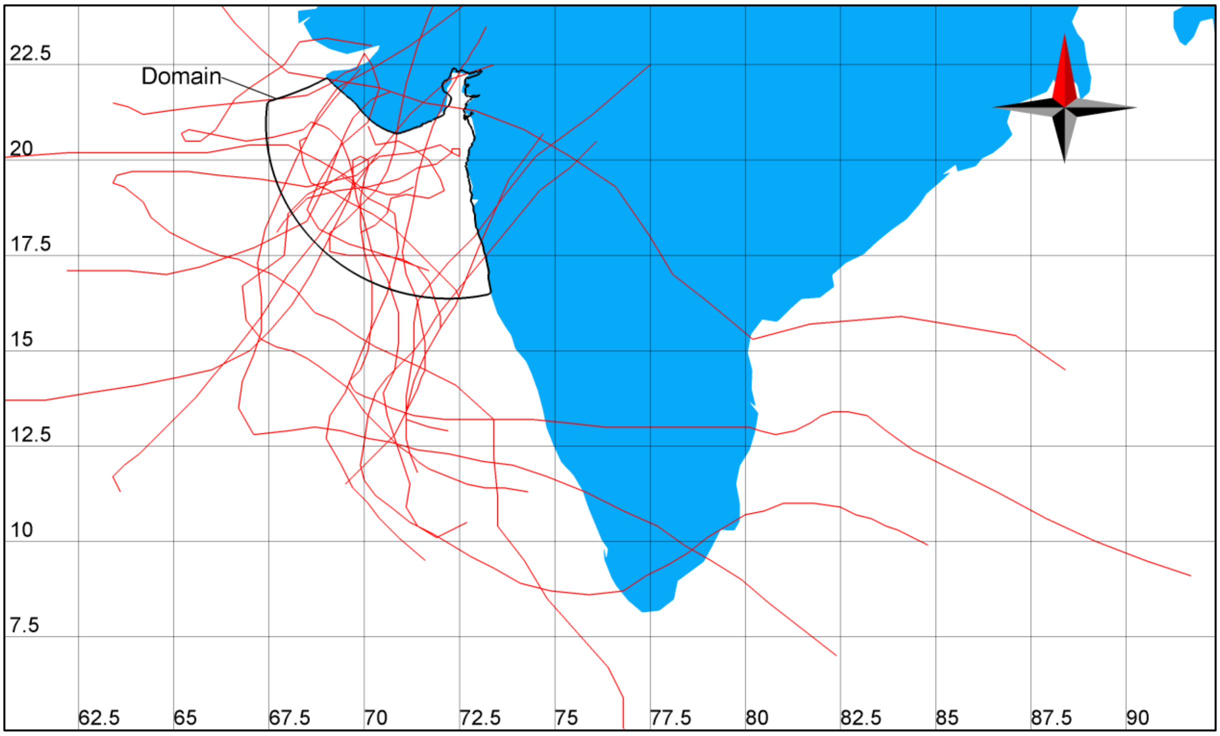

Figure 4-35 Tracks of cyclones that have passed close to the study area

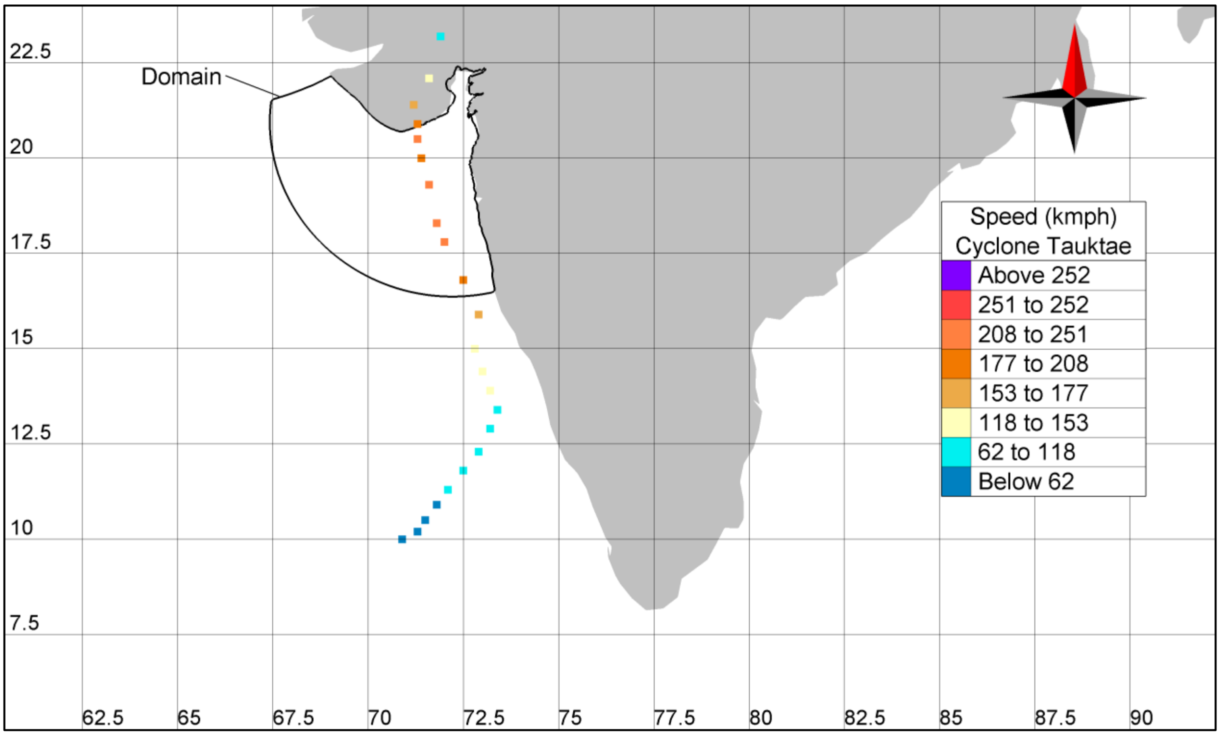

Figure 4-36 Track of Extremely Severe Cyclonic Storm Tauktae (IMD Scale) in Saffir-Simpson hurricane scale

The list of cyclones for which simulations were carried out is provided in Table 4-8.

Table 4-8 List of cyclones used for storm surge study

Serial no.	Cyclone Name/ No.	Year	Cyclone Type (IMD Scale)
1	Tauktae	2021	Extremely Severe Cyclonic Storm
2	Nisarga	2020	Severe cyclonic storm
3	Vayu	2019	Very Severe Cyclonic Storm
4	Maha	2019	Extremely Severe Cyclonic Storm
5	Hikaa	2019	Very Severe Cyclonic Storm
6	ARB 01	2011	Depression
7	Phyan	2009	Cyclonic Storm
8	Yemyin	2007	Cyclonic Storm
9	ARB 05	1998	Cyclonic Storm
10	ARB 01	1996	Severe Cyclonic Storm
11	ARB 02	1996	Severe Cyclonic Storm
12	ARB 01	1989	Depression

Serial no.	Cyclone Name/ No.	Year	Cyclone Type (IMD Scale)
13	Tropical Storm Seven	1987	Tropical Storm
14	ARB 03	1982	Extremely Severe Cyclonic Storm
15	Tropical Storm One	1981	Very severe cyclonic storm
16	Tropical Storm Three	1980	Depression
17	Tropical Storm Seven	1979	Cyclonic Storm
18	Cyclone Two	1976	Extremely severe cyclonic storm
19	Cyclone Sixteen	1975	Very Severe Cyclonic Storm

4.9 Sea Level Rise

Sea level rise (SLR) is caused primarily by two factors related to global warming: the added water from melting ice sheets and glaciers, and the expansion of seawater as it warms. Rising seas pose both a direct risk of flooding unprotected areas and indirect threats of higher storm surges, tides, and tsunamis.

In case of Kalpasar dyke, increase in mean sea level is expected to alter the hydrodynamics of the gulf and in turn change the extreme water levels. Therefore it is necessary to evaluate the sea level rise and its impact on the factors driving the extreme water levels. Also, increase in extreme sea water levels will impede reservoir outflow which increases the probability of floods upstream.

The Intergovernmental Panel on Climate Change (IPCC) is the United Nations body for assessing the mean sea level changes driven by climate change. IPCC's 6th Assessment Report (AR6) data was downloaded from NASA's Sea Level Projection Tool[2]. The projections are relative a 1995-2014 baseline and provided for 5 SSP (Shared Socio-economic Pathway) scenarios. The median/likely value of SSP3-7.0 scenario, near the entrance of the Gulf, is chosen for the present study and the projection is presented in the Figure 4-37. As per chosen scenario, the sea level rise by the end of 21st century is 0.57 m which is used for estimating the extreme water levels.

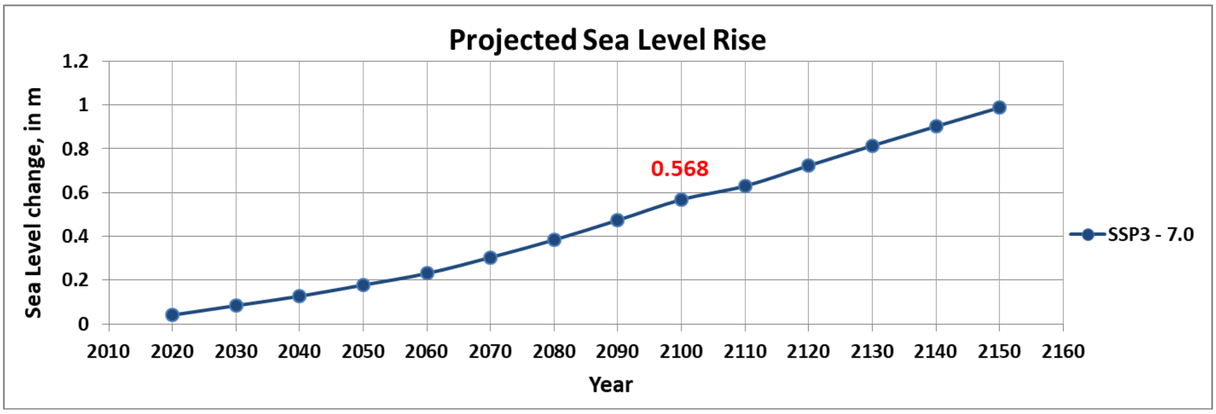

Figure 4-37 Projected sea level rise (SSP3-7.0)

2 sealevel.nasa.gov/ipcc-ar6-sea-level-projection-tool

5 Hydrodynamic model

Hydrodynamics deals with the dynamics of fluid and aims at studying the forces exerted by fluids in motion. For a large water body such as a sea, the study becomes very complex owing to vast number of processes going on simultaneously. Processes such as tides, waves and wind interactions cause motion of fluid which in turn has far reaching effects. The motion of fluid, otherwise called as currents can induce a number of phenomenon such as erosion and accretion along shoreline, morphological changes and forces on marine structures.

Study of hydrodynamics is a predecessor for other studies such as sediment transport study. The greater accuracy with which the hydrodynamic model replicates the actual conditions, the greater is the success of the subsequent studies.

The TELEMAC is a set of finite element programs developed by National Hydraulics and Environment Laboratory (Laboratoire National d'Hydraulique et Environnement - LNHE) of the Research and Development Directorate of the French Electricity Board (EDF-DRD). It uses a string of common processes (digitization and graphics) and contains two- and three-dimension modules for the study of currents, sedimentation, waves and water quality.

TELEMAC-2D is a program forming the core of TELEMAC Modeling System for the solution of the two-dimensional Saint-Venant equations. The water depth and the velocity averaged on the vertical are the main variables, but the transport of a passive tracer as well as turbulence can be taken into consideration. It uses triangular finite element discretization and can work with quadrilateral elements also. TELEMAC-2D can be used for numerous studies in fluvial and maritime hydraulic applications.

The appropriate governing equations for studying water environment in coastal and estuarine areas are the two-dimensional shallow water equations. These are obtained by vertically integrating the three-dimensional Navier-Stokes equations of motion making the following simplified assumptions,

- The flow is incompressible
- The flow is well mixed
- Vertical acceleration is negligible
- Bed stress can be modelled

Simulation of hydrodynamics is based on the following non-linear vertically integrated 2-D equations of conservation of mass and momentum.

Continuity Equation

$$\frac{\partial z}{\partial t} + \frac{\partial uh}{\partial x} + \frac{\partial vh}{\partial y} = 0$$

Equation of Motion in X-direction

$$\frac{\partial u}{\partial t} + u\frac{\partial u}{\partial x} + v\frac{\partial u}{\partial y} + g\frac{\partial z}{\partial x} + \tau_{hx} - C_f v - E_c\nabla^2 u = 0$$

Equation of Motion in Y-direction

$$\frac{\partial v}{\partial t} + u\frac{\partial v}{\partial x} + v\frac{\partial v}{\partial y} + g\frac{\partial z}{\partial y} + \tau_{hy} + C_f u - E_c\nabla^2 v = 0$$

Where,

z : Water surface elevation
h : Total water depth (z+d)
u,v : Velocity components in X & Y direction
C_f : Coriolis force
E_c : Eddy viscosity coefficient
d : Depth with respect to CD

These equations are numerically solved by finite element technique in TELEMAC.

A large domain was chosen for the model study such that it ensures proper propagation of tide and the geometric features of the region are resolved sufficiently. Mesh size was kept very less near the study area to resolve the proposed schemes and velocities properly. Mesh used for the model study is presented in Figure 5-1.

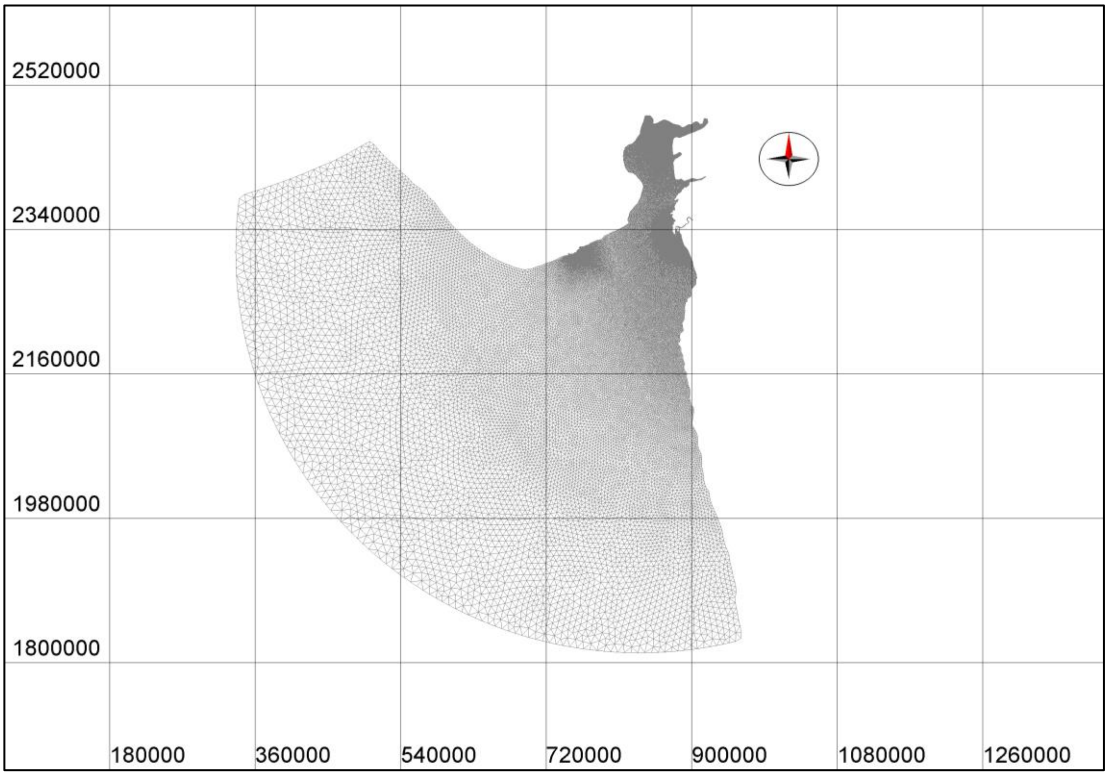

Figure 5-1 Mesh considered for Model Study

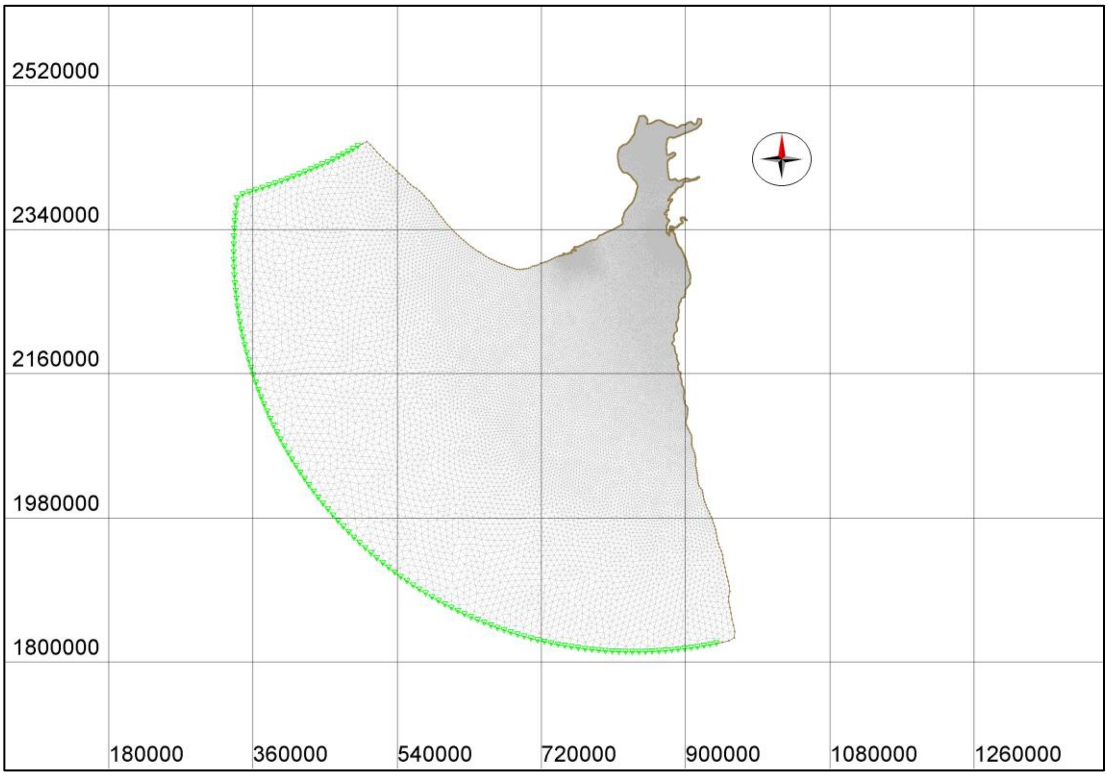

Figure 5-2 Boundary Condition

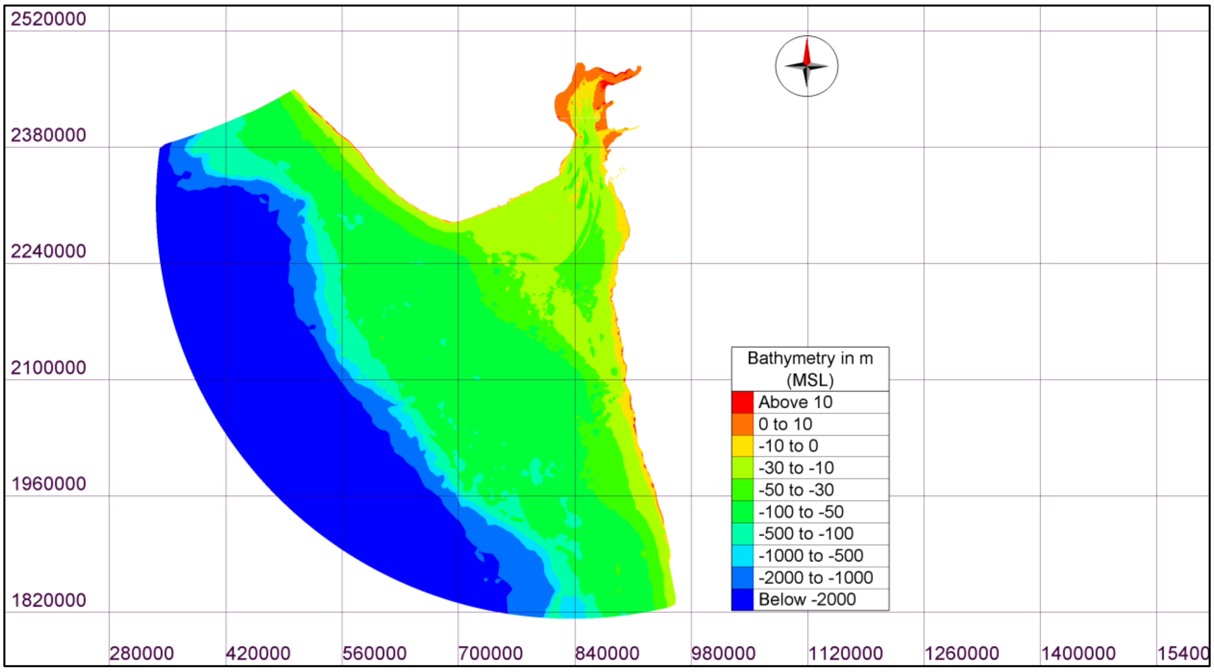

Figure 5-3 Model Domain (Existing scenario)

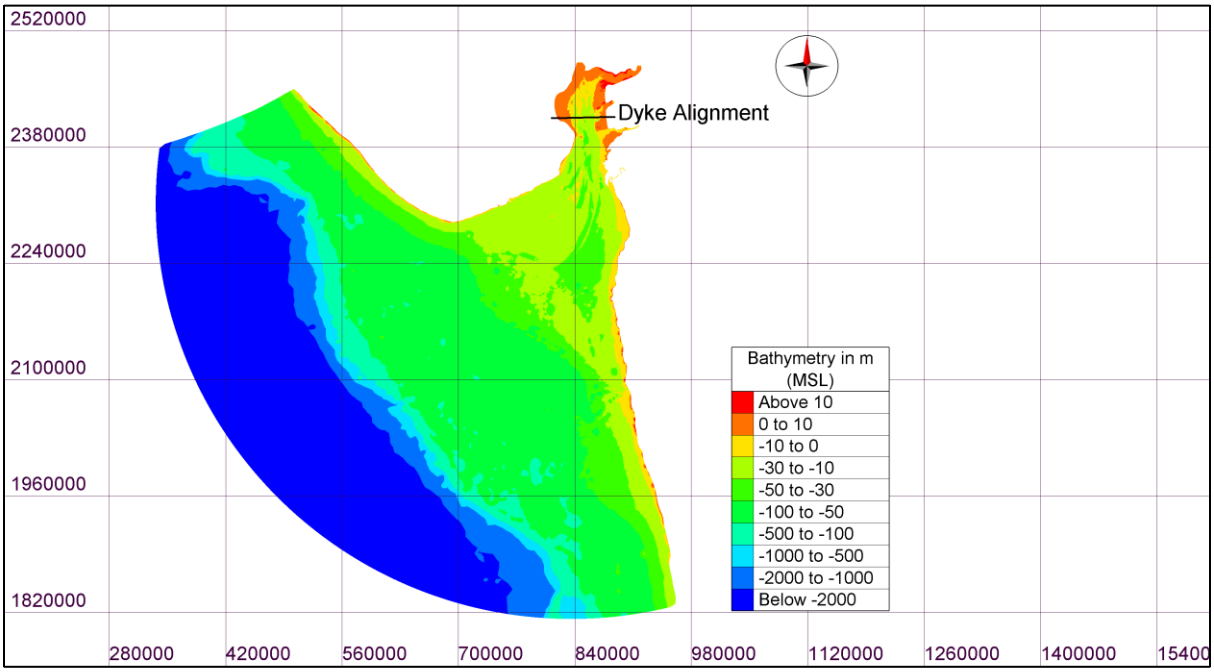

Figure 5-4 Model Domain (With dyke in place)

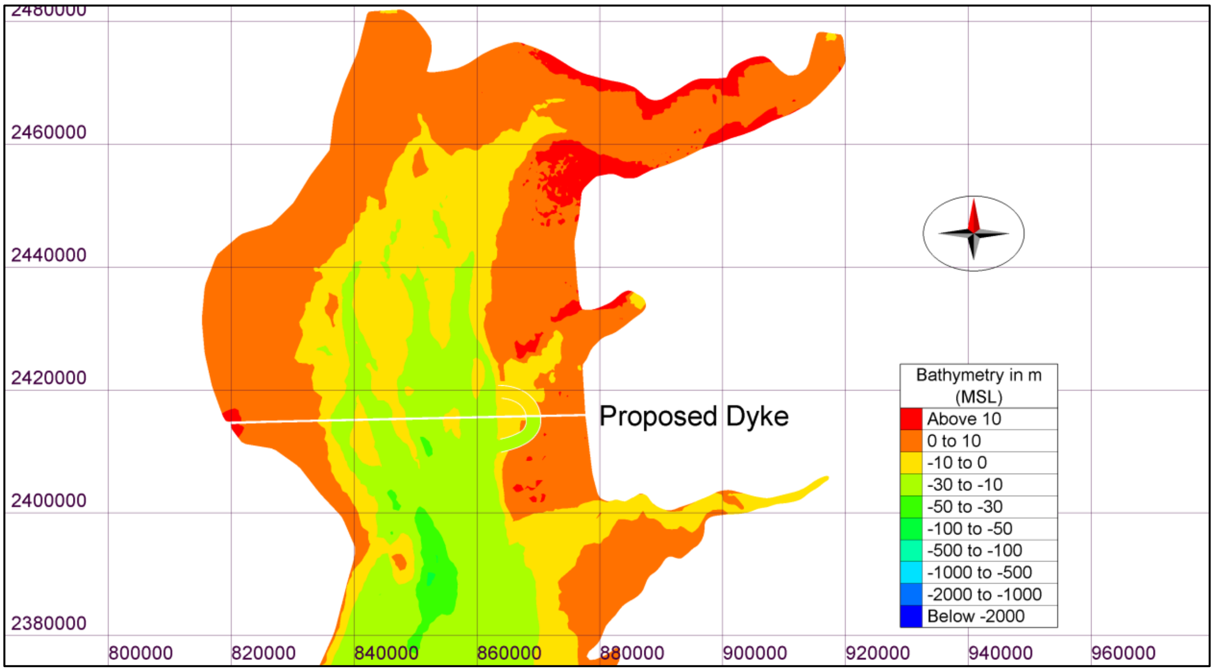

Figure 5-5 Model Domain (With dyke Close-up view)

The boundary condition is prescribed using tidal constituents provided by the global TPXO database and its regional and local variants from the OSU (Oregon State University) harmonic constants database. The TPXO models include complex amplitudes of MSL-relative sea-surface elevations and transports/currents for eight primary (M2, S2, N2, K2, K1, O1, P1, Q1), two long period (Mf, Mm) and 3 non-linear (M4, MS4, MN4) harmonic constituents

5.1 Calibration and Validation

A proper calibration of any numerical model is necessary for ensuring the authenticity of the model. A model can be said calibrated if the results are comparable with actual site observations during a sufficient period of time.

As the tide propagates, its levels are affected by bottom roughness. The effect of bottom roughness on tidal levels was studied by carrying out simulations with varying friction coefficient across the domain. The accuracy of results was checked by calculating Root Mean Sqaure Error (RMSE). Lower the RMSE values, the accuracy of the simulations are high. Based on the results, a friction map was prepared with varying friction for the Gulf of Khambhat. Further, the comparison between observed and simulated tide was carried out by applying vertical shift and time shift correction on the observed data in order to minimise the error.

The simulated water levels were compared with the observed tide levels at 16 locations within Gulf of Khambhat. The locations at which tide calibration were carried out are shown in Figure 5-6. Observed and simulated water levels (w.r.t MSL) are shown for each of the locations in the subsequent figures.

Observed and simulated water levels are in good agreement at all locations except the locations inside rivers. This may be because wind and river discharges are not considered for calibration study. It may be also due to error in survey bathymetry.

The root mean square value was found between observed and simulated tide levels. It provides an estimation of how well the model is able to predict the target value (accuracy).Lower the value of RMSE, better is the prediction. RMSE values generally ranges between 0.1 and 0.5.

The RMSE and R^2 values between simulated and observed bathymetry is presented in Table 5-1. The accuracy of the results mainly depends on the surveyed bathymetry and secondary bathymetry data.

The percentage variations (RMSE/Tidal range) at all the locations are below 5 percent, except at Kavi and Hazira.

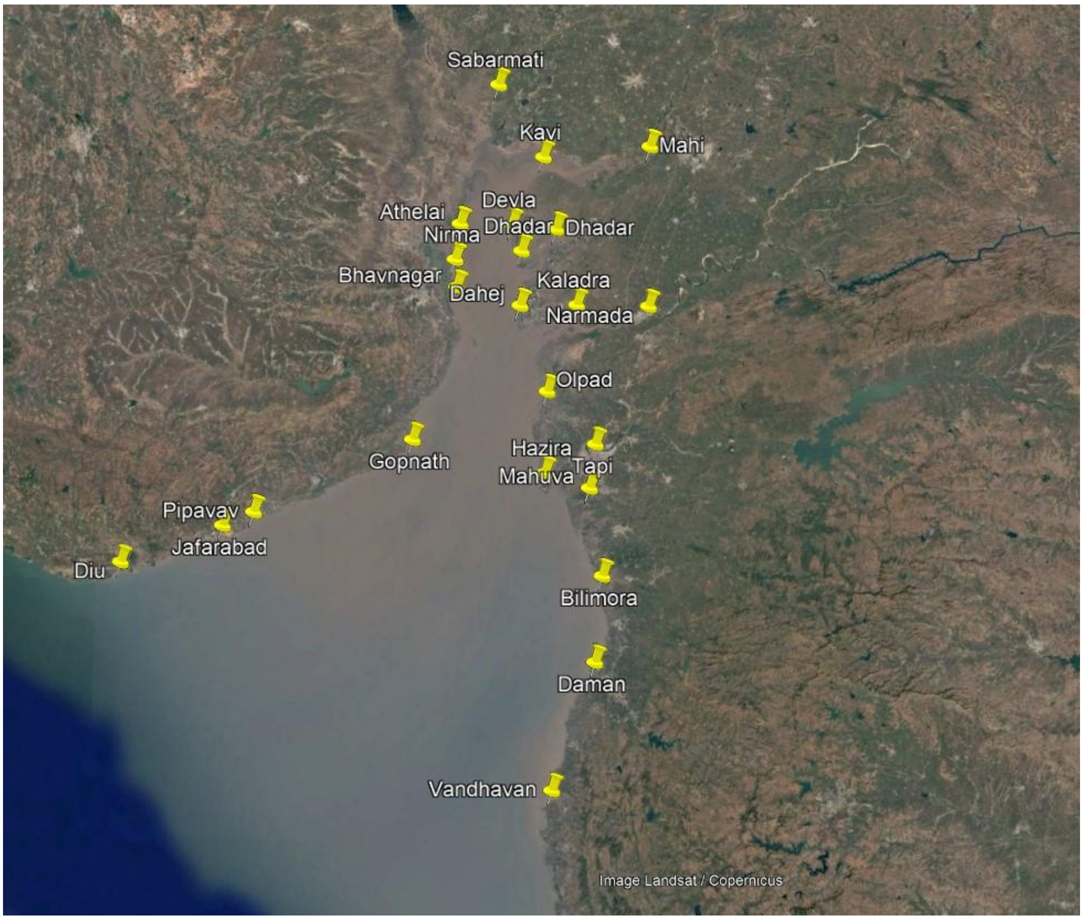

Figure 5-6 Locations at which tide calibration were carried out

5.1.1 Tide Calibration

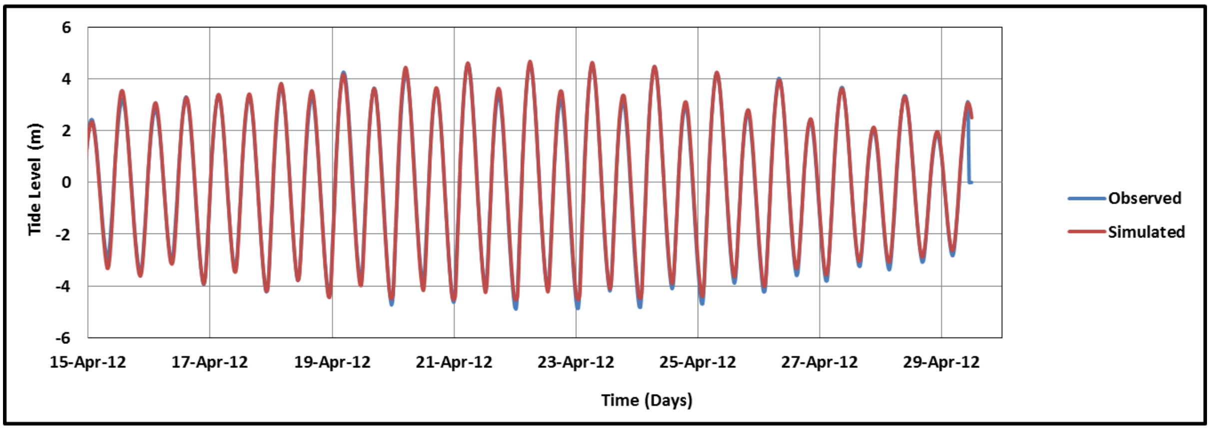

Figure 5-7 Comparison between observed and simulated tide at Athelai

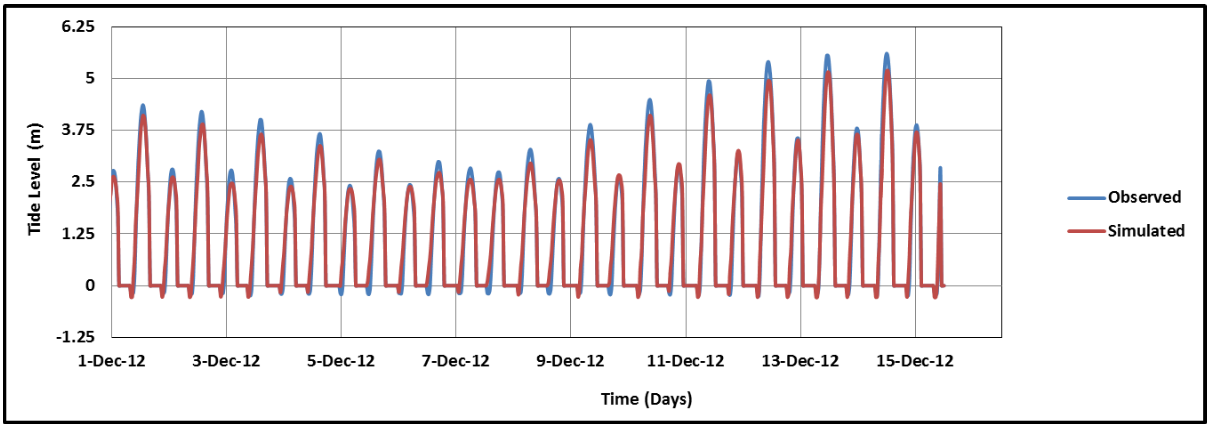

Figure 5-8 Comparison between observed and simulated tide at Bhavnagar

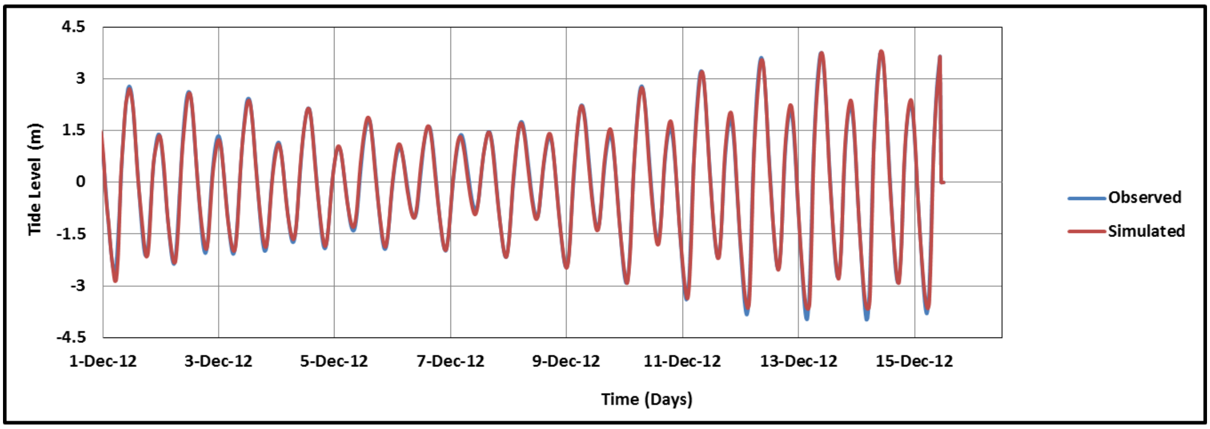

Figure 5-9 Comparison between observed and simulated tide at Billimora

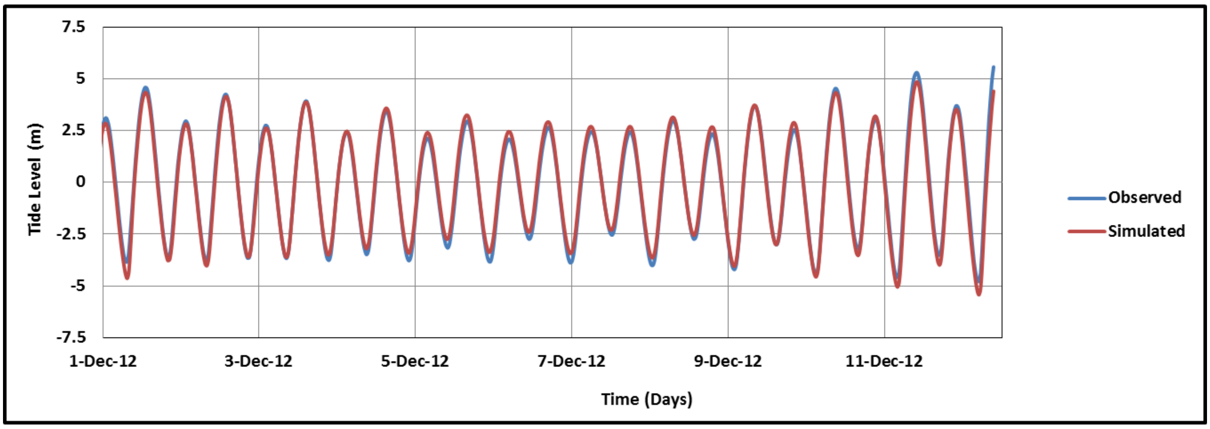

Figure 5-10 Comparison between observed and simulated tide at Dhadhar

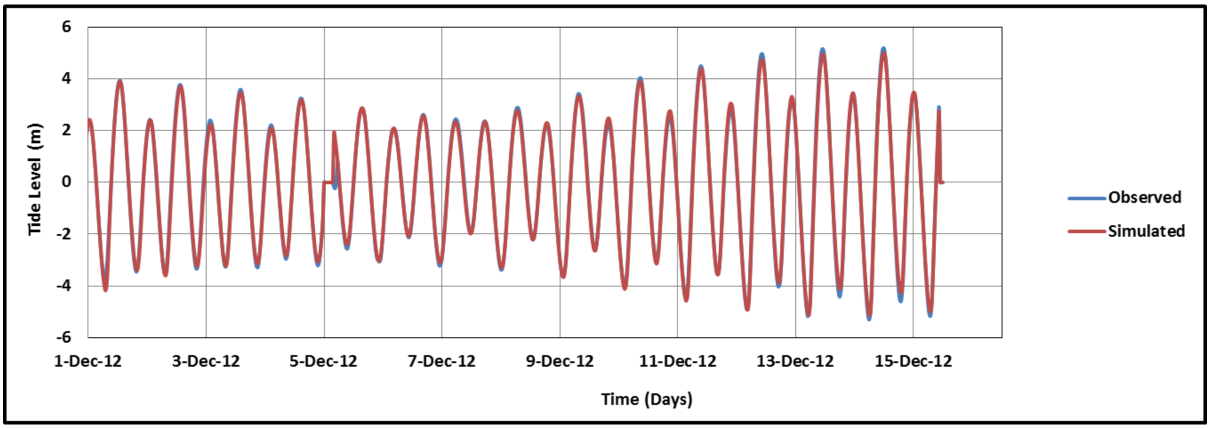

Figure 5-11 Comparison between observed and simulated tide at Dahej

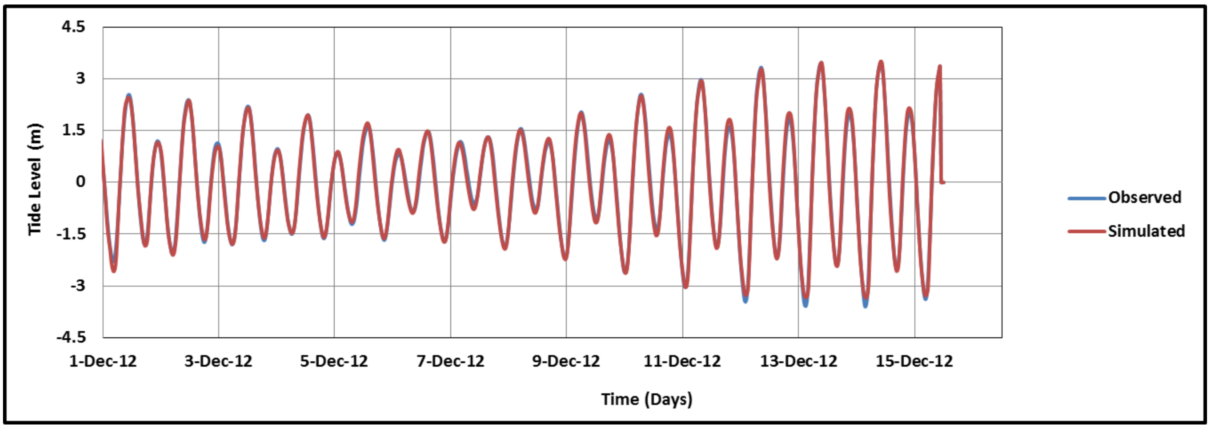

Figure 5-12 Comparison between observed and simulated tide at Daman

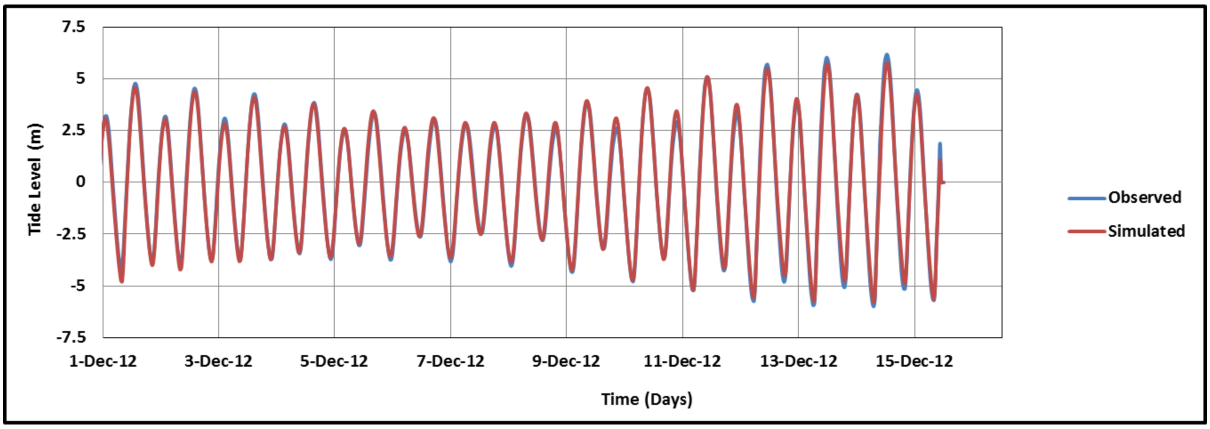

Figure 5-13 Comparison between observed and simulated tide at Devla

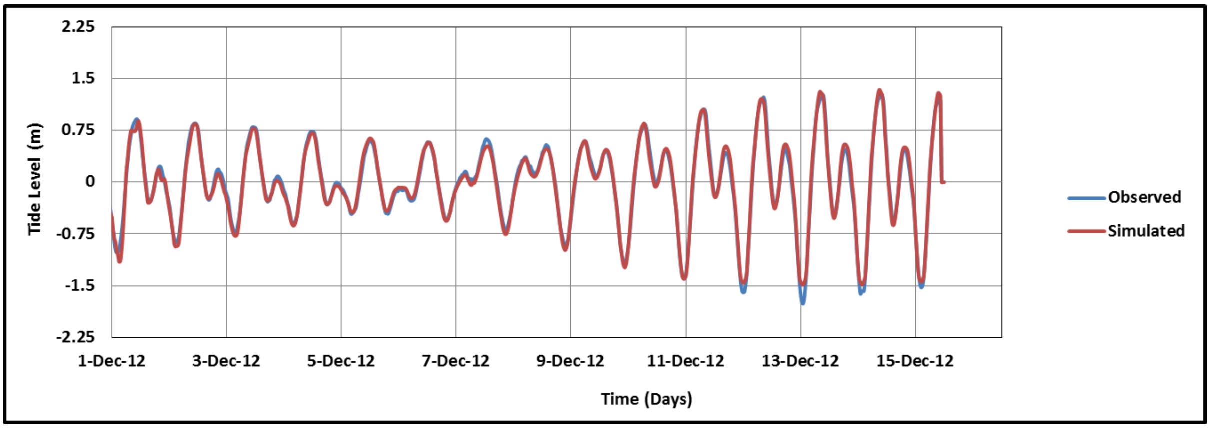

Figure 5-14 Comparison between observed and simulated tide at Diu

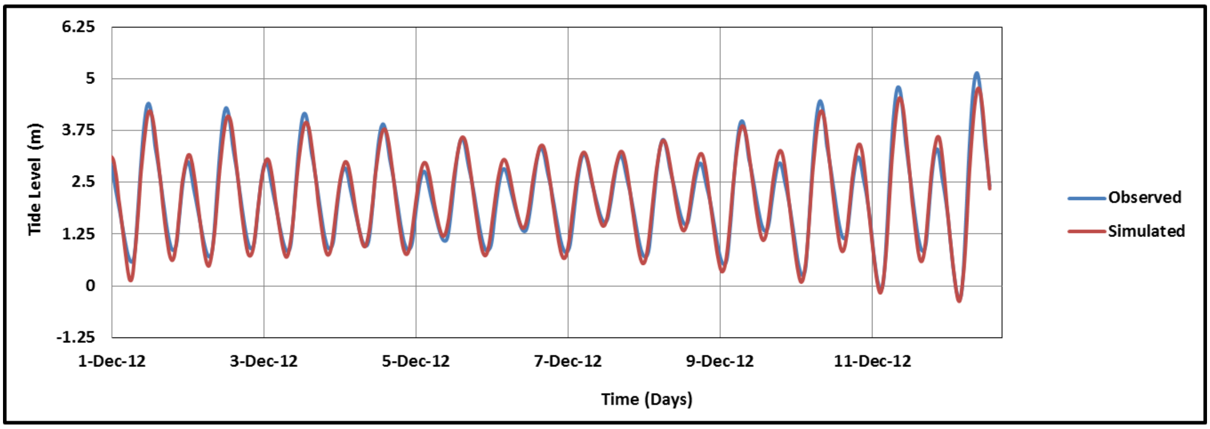

Figure 5-15 Comparison between observed and simulated tide at Gopnath

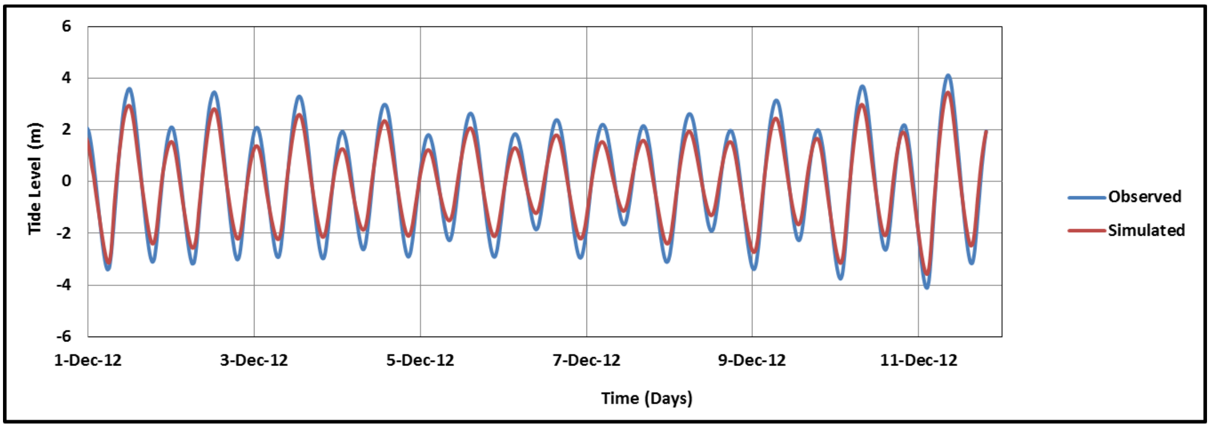

Figure 5-16 Comparison between observed and simulated tide at Hazira

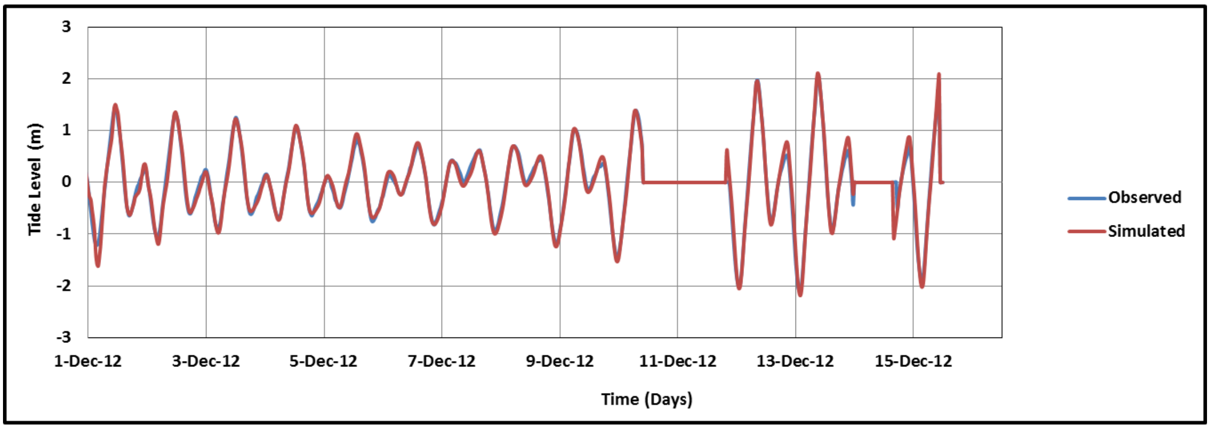

Figure 5-17 Comparison between observed and simulated tide at Jafarabad

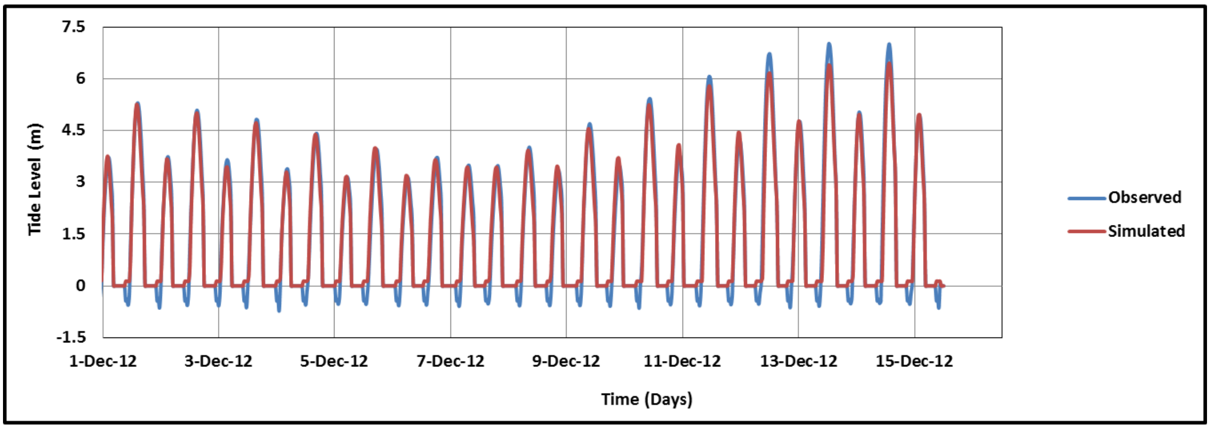

Figure 5-18 Comparison between observed and simulated tide at Kavi

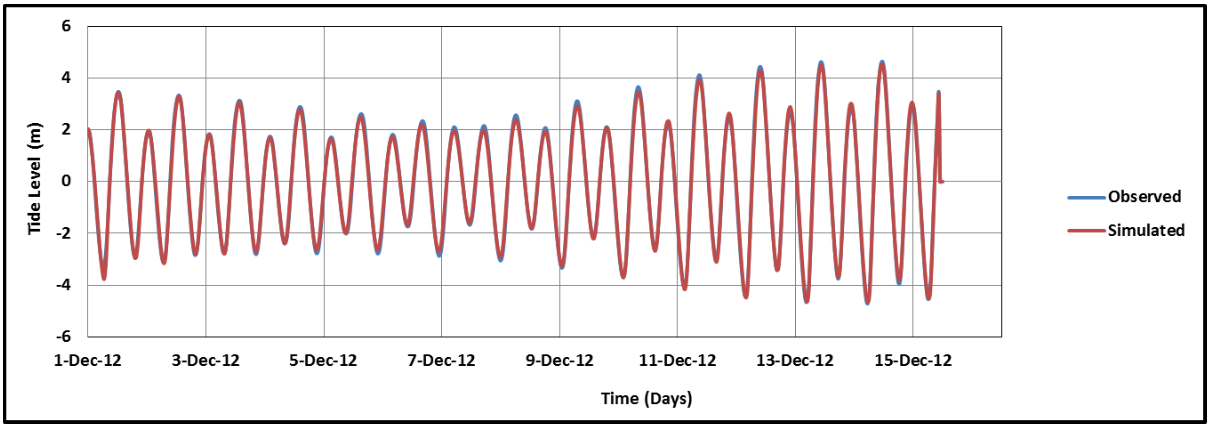

Figure 5-19 Comparison between observed and simulated tide at Olpad

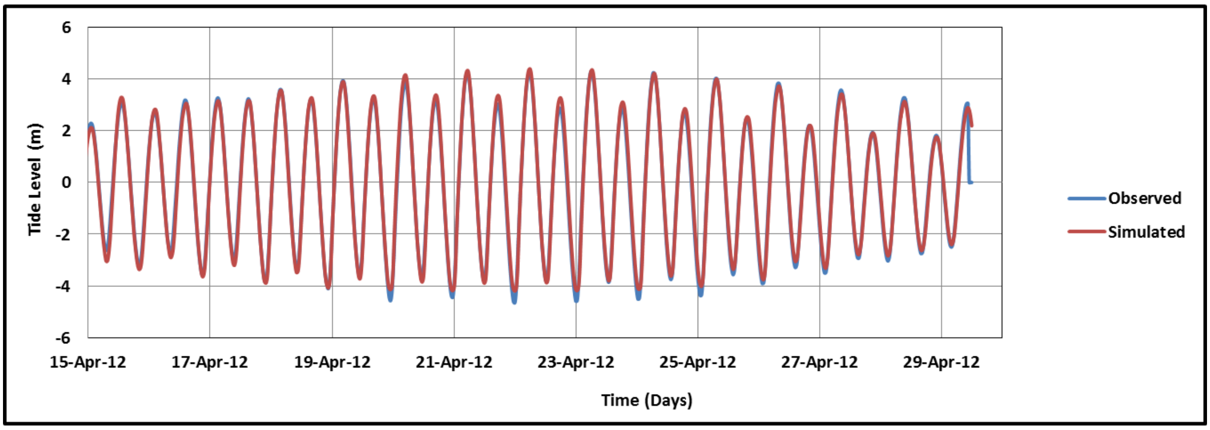

Figure 5-20 Comparison between observed and simulated tide at Nirma

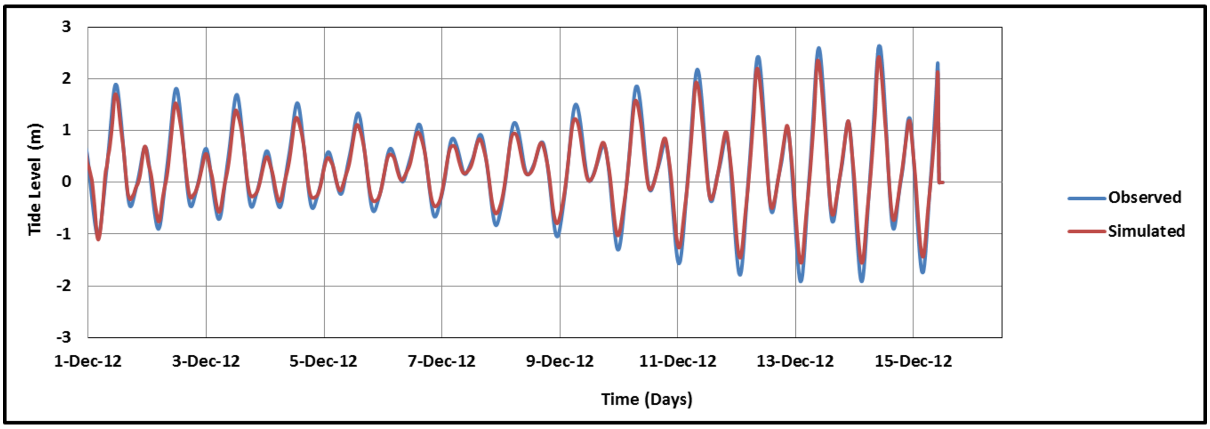

Figure 5-21 Comparison between observed and simulated tide at Pipavav

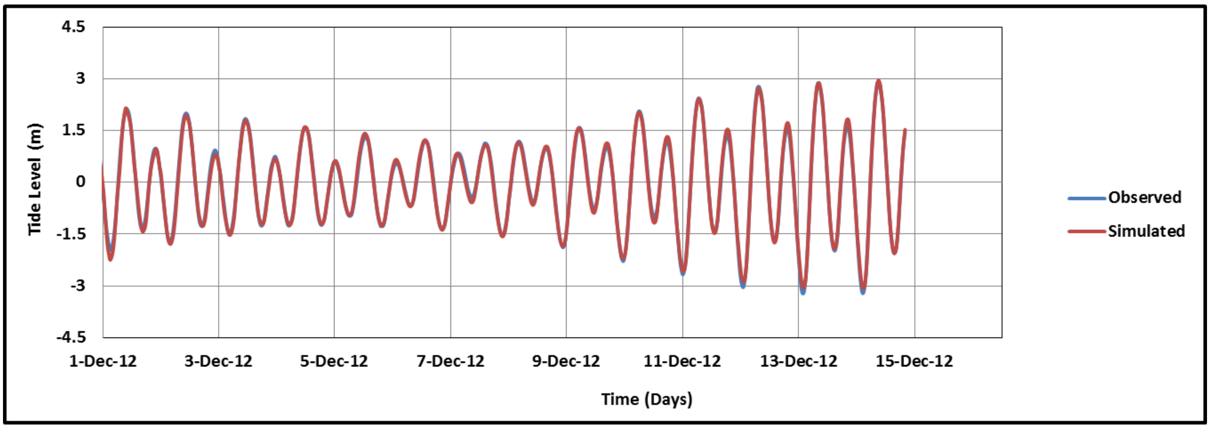

Figure 5-22 Comparison between observed and simulated tide at Vandhavan

Table 5-1 RMSE and R^2 correlation

Location	Tidal range in m (T)	RMSE(m)	Percentage Variation = (RMSE/T)*100	R^2
Athelai	12.53	0.28	2.2	0.986
Bhavnagar	6.18	0.30	4.9	0.979
Billimora	8.23	0.14	1.7	0.974
Dhadhar	12.18	0.30	2.5	0.983
Dahej	11.04	0.21	1.9	0.993
Daman	7.55	0.12	1.6	0.994

Location	Tidal range in m (T)	RMSE(m)	Percentage Variation = (RMSE/T)*100	R^2
Devla	13.24	0.30	2.3	0.993
Diu	3.12	0.07	2.2	0.990
Gobnath	7.33	0.22	3.0	0.987
Hazira	8.86	0.49	5.5	0.977
Jafarabad	4.23	0.12	2.8	0.985
Kavi	7.31	0.50	6.8	0.996
Nirma	11.91	0.20	1.7	0.954
Olpad	9.76	0.15	1.5	0.992
Pipavav	4.72	0.16	3.4	0.988
Vandhavan	6.27	0.09	1.4	0.994

5.1.2 Current calibration

Figure 5-23 Locations at which current calibration were carried out

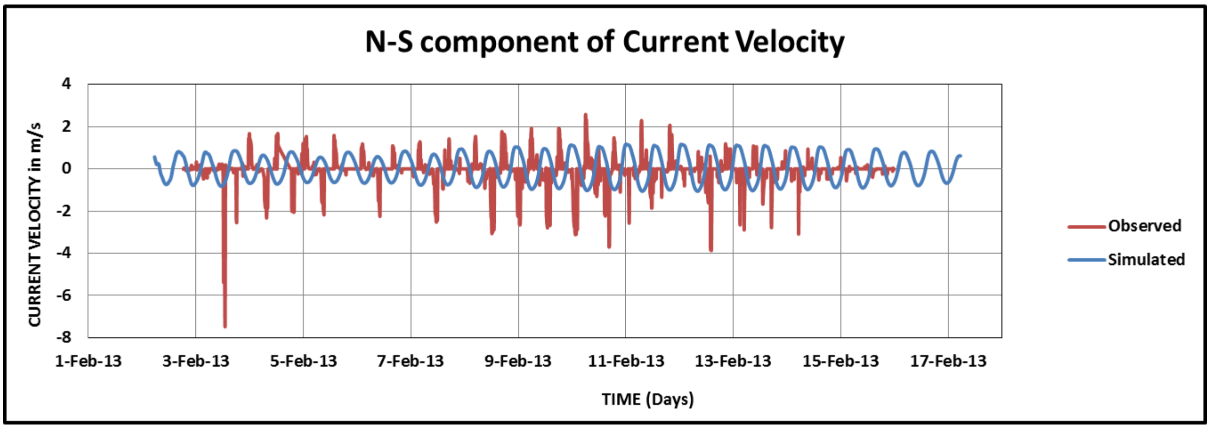

Figure 5-24 Comparison of N-S component of Current velocity at Dam-corridor (Season 1)

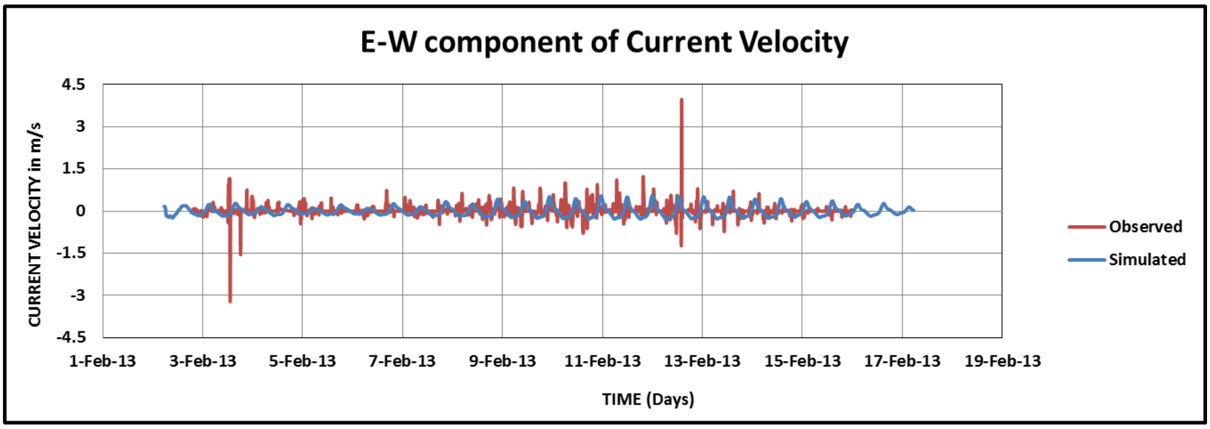

Figure 5-25 Comparison of N-S component of Current velocity at Dam-corridor (Season 1)

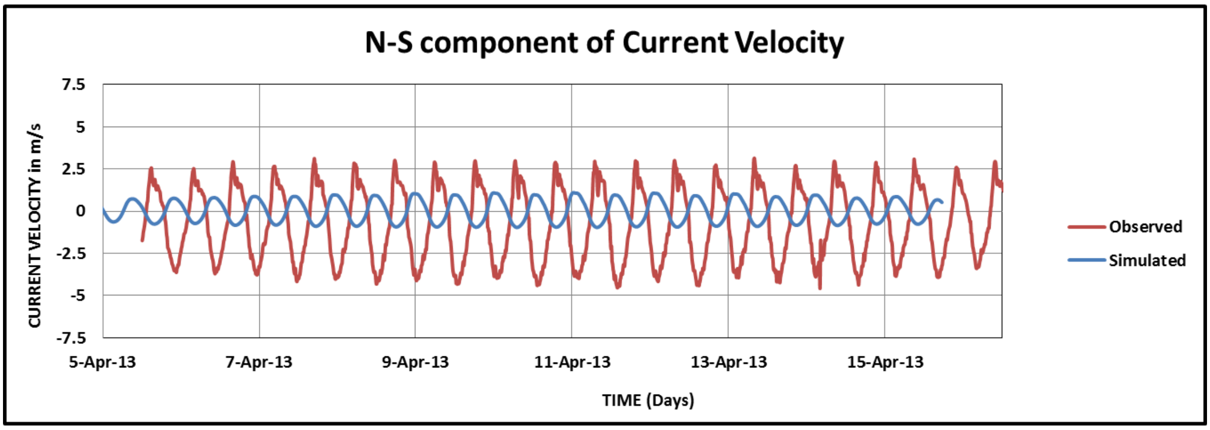

Figure 5-26 Comparison of N-S component of Current velocity at Dam-corridor (Season 2)

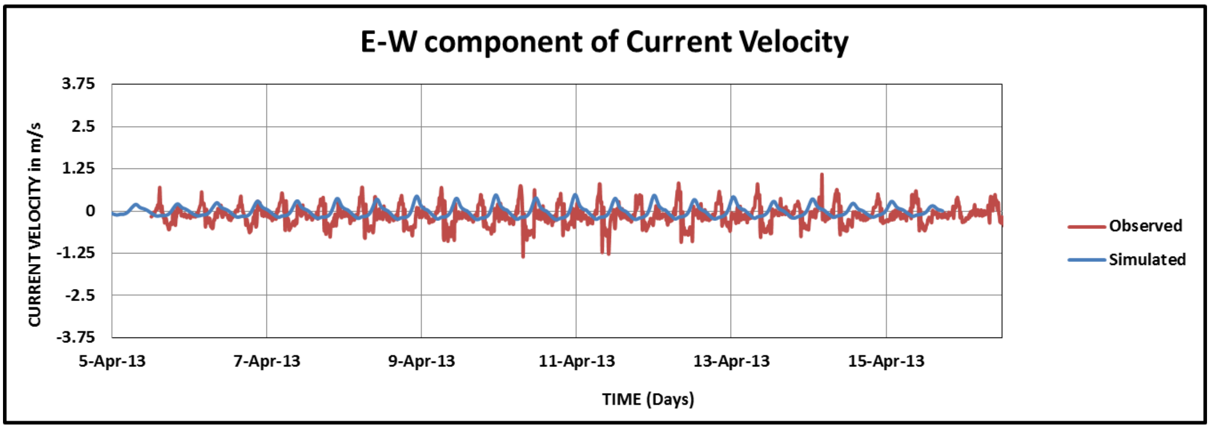

Figure 5-27 Comparison of E-W component of Current velocity at Dam-corridor (Season 2)

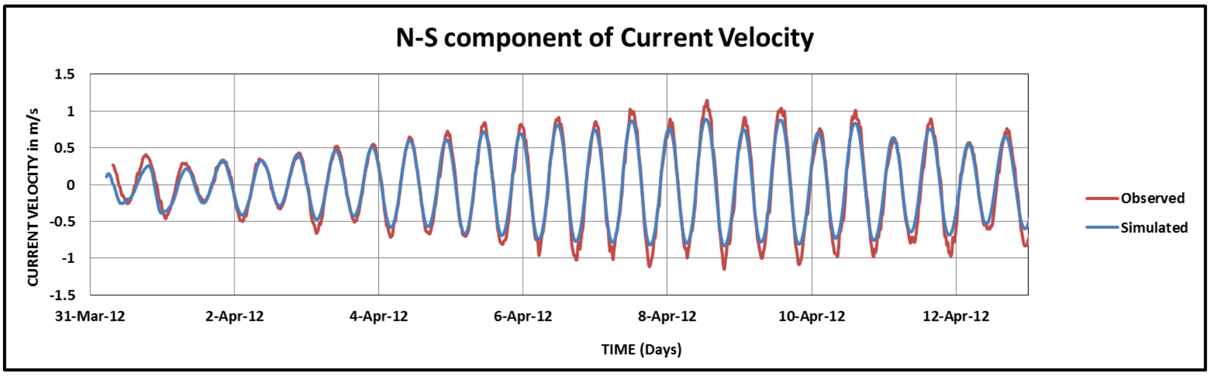

Figure 5-28 Comparison of N-S component of Current velocity at MC-DIU (Season 1)

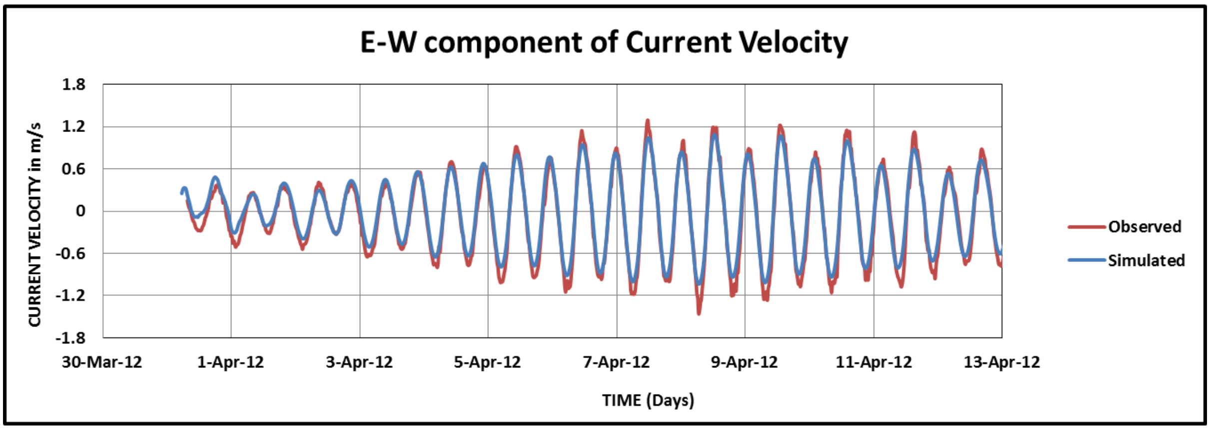

Figure 5-29 Comparison of E-W component of Current velocity at MC-DIU (Season 1)

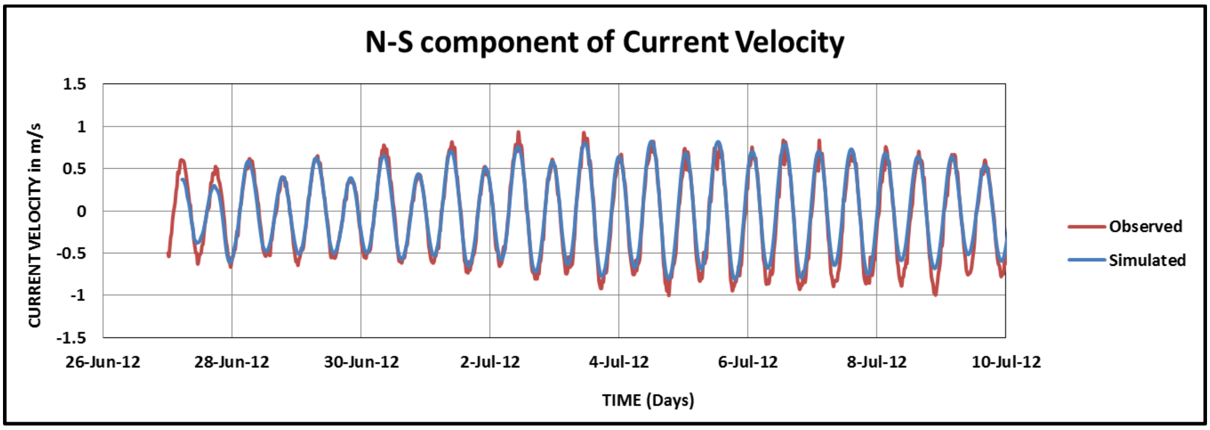

Figure 5-30 Comparison of N-S component of Current velocity at MC-DIU (Season 2)

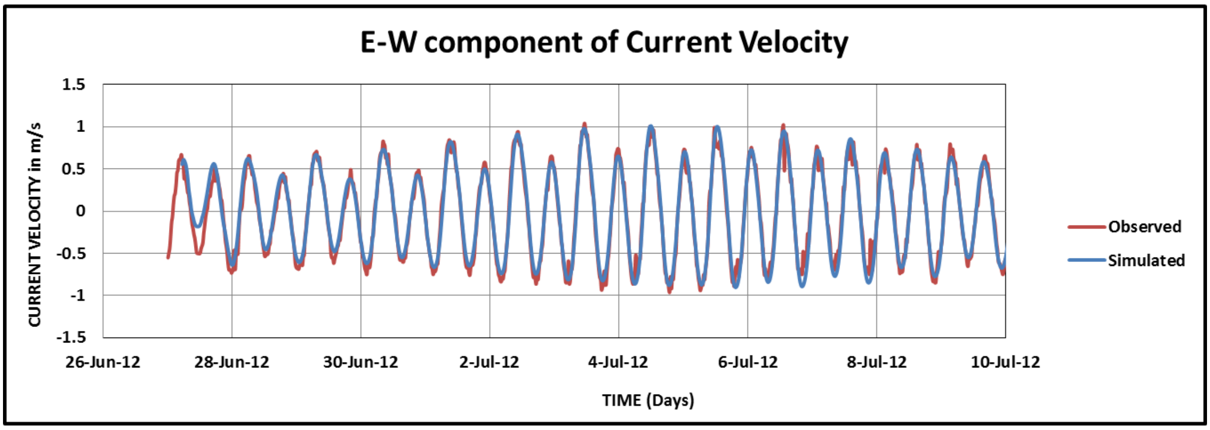

Figure 5-31 Comparison of E-W component of Current velocity at MC-DIU (Season 2)

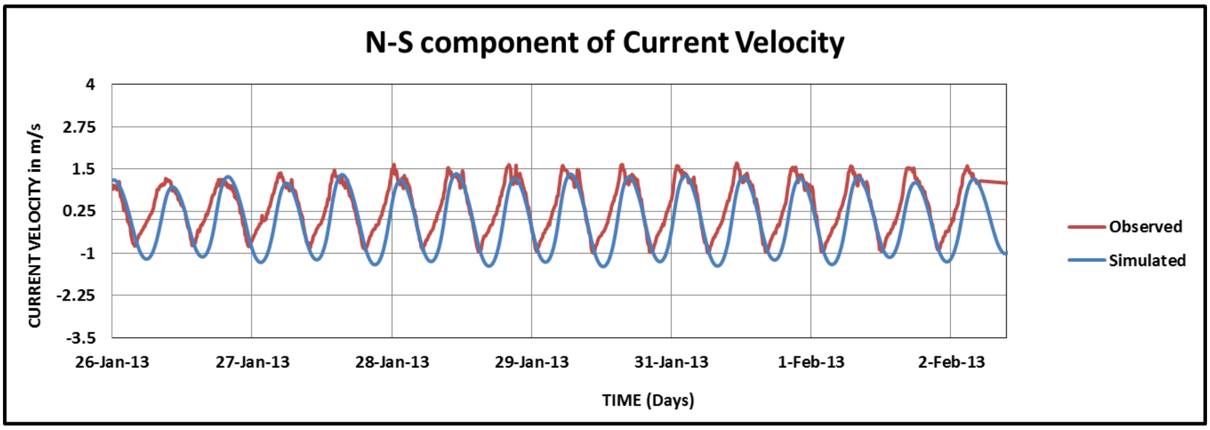

Figure 5-32 Comparison of N-S component of Current velocity at Midchannel-TSS5

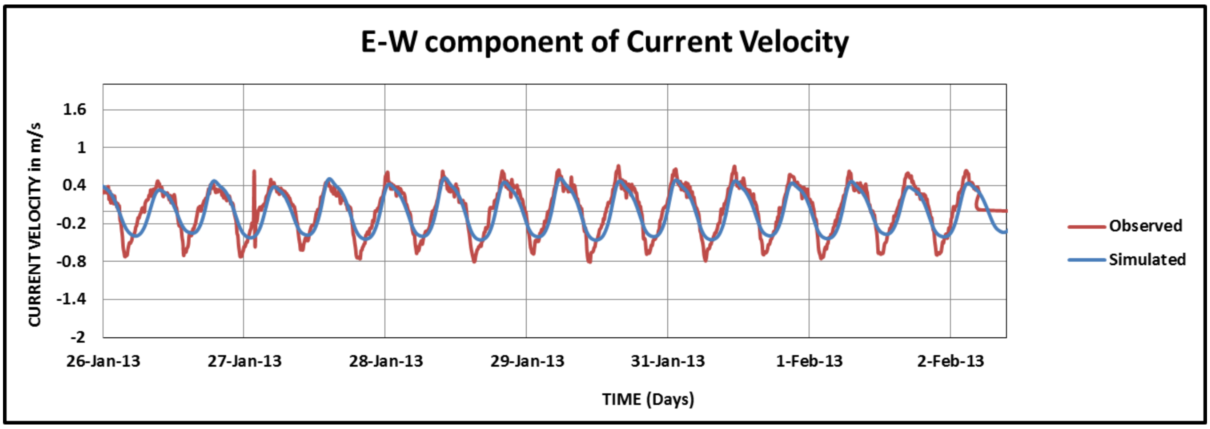

Figure 5-33 Comparison of E-W component of Current velocity at Midchannel-TSS5

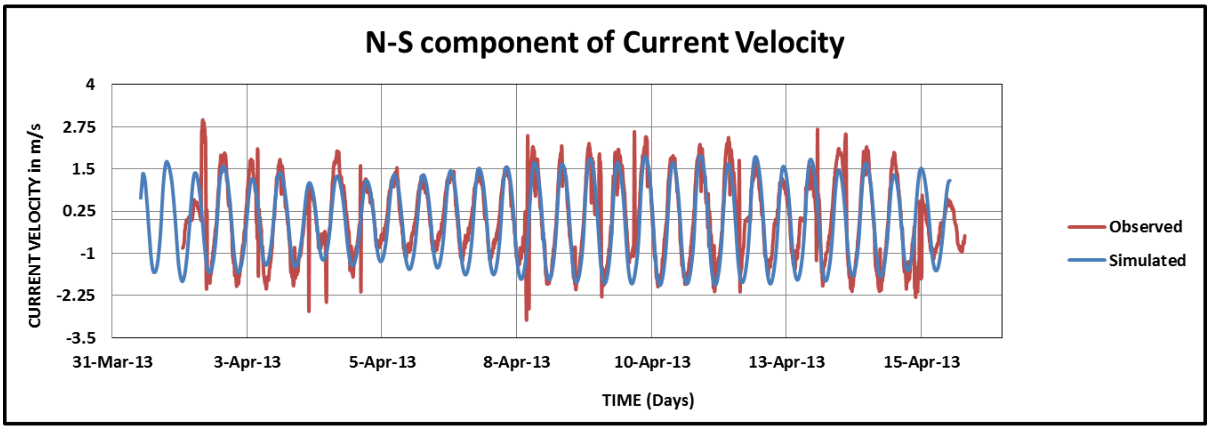

Figure 5-34 Comparison of N-S component of Current velocity at Midchannel-TSS8

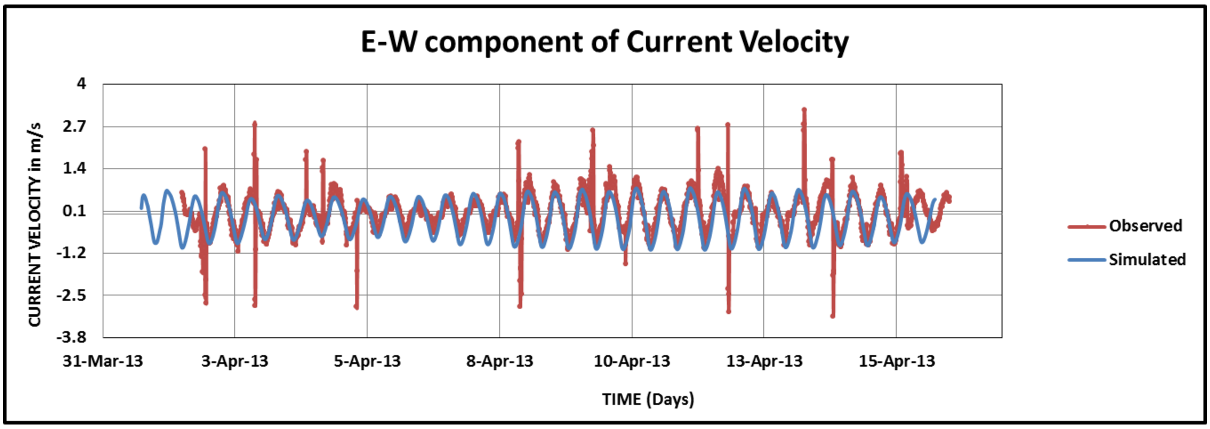

Figure 5-35 Comparison of E-W component of Current velocity at Midchannel-TSS8

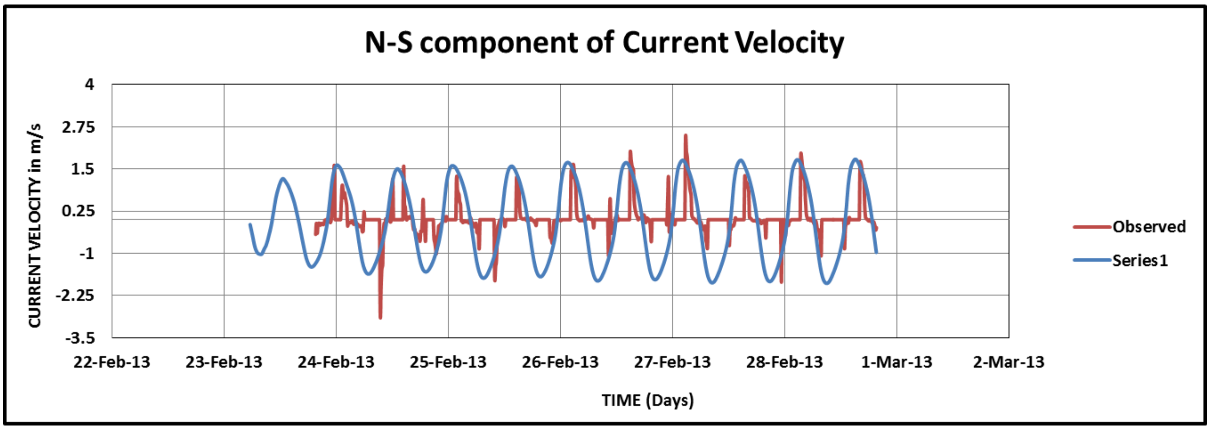

Figure 5-36 Comparison of N-S component of Current velocity at Narmada

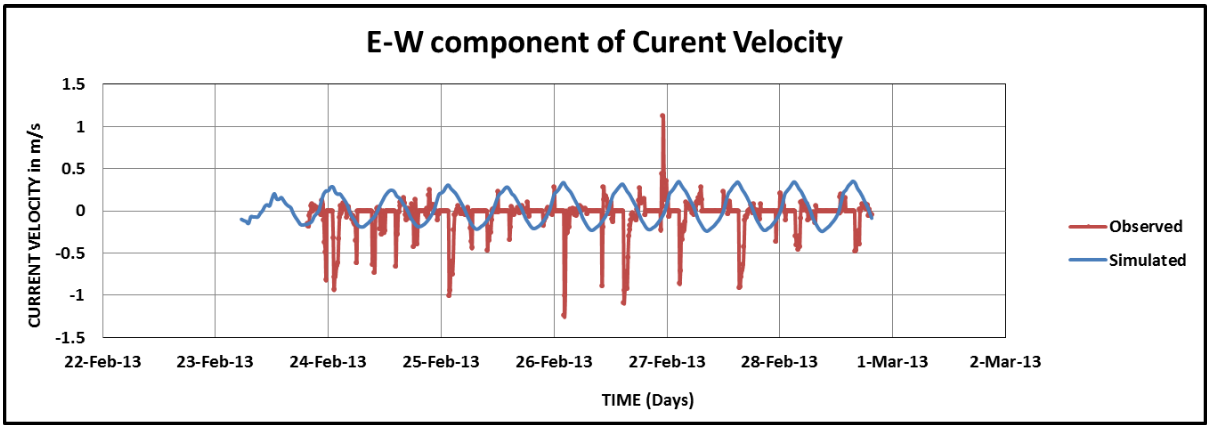

Figure 5-37 Comparison of E-W component of Current velocity at Narmada

6 Effects of the dyke on water levels downstream

Construction of Kalpasar Dyke is expected to make changes in the hydrodynamics of the Gulf which can cause changes in the expected high and low water levels in the Gulf. In order to study this impact, the calibrated HD model was used to simulate various situations with and without the proposed dyke in place. The maximum water level will mainly be affected by three major phenomena, namely, tide, storm surges and sea level rise (SLR).

To check if the sea level rise will cause any changes in the tide propagation pattern within the restricted area of the Gulf, the tidal simulations were carried out with the projected sea level rise of 0.57m for the year 2100. From the results, it was observed that there is no major changes in the water level pattern other than a shift by 0.57m, which is same as adding the sea level rise to the tide levels directly. Therefore, it was decided to add this affect arithmetically to the other results to account for possible sea level rise.

To get the maximum/minimum tide levels, it is pertinent to do the hydrodynamic simulations when the tidal range is maximum and the water levels will be close to HAT and LAT. To identify such period, tide levels at the project location were predicted for 20 years using the harmonic constituents obtained from the analysis of observed data. It is found from this analysis that the maximum tide levels were observed during January 2018.Therefore tide simulations were carried out during this period to obtain maximum and minimum tide levels, details of which are presented in the subsequent section.

As the number of cyclones which can cause storm surge passed over the Gulf in the past years are few, it is decided to do the storm surge simulation with the effect of only cyclone ignoring the tide. The maximum storm surge values obtained thus can be added to maximum tide levels to get a conservative estimate of maximum water levels. Details of storm surge simulations are presented in subsequent section.

6.1 Tide

Hydrodynamic simulations were carried out for January 2018 for two scenarios, ie., with and without the proposed Dyke in place. The water levels are extracted at 11 locations downstream of the proposed dyke. The locations where water levels are extracted are given in Figure 6-1.The time series plots of water level variations for these locations for the two scenarios are also presented. It is observed that the maximum water levels are increasing in the upper middle regions of the Gulf to the order of about 1.4 m. The difference in maximum water level for the entire Gulf is also plotted.

In addition to the maximum water levels, the changes in minimum water levels are also presented in a similar way. It is observed that the minimum water levels decrease at places in the order of 0.6m.

Figure 6-1 Locations of Maximum Free surface elevation extraction

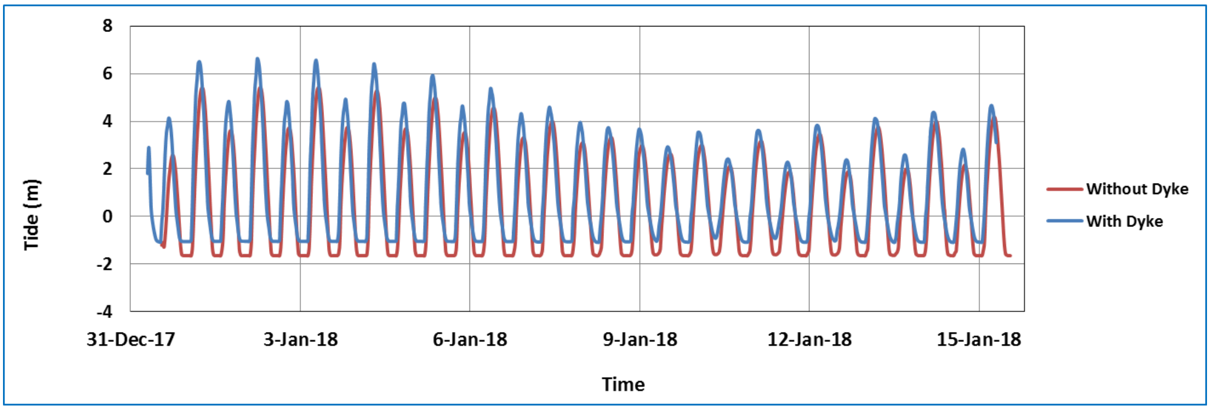

Figure 6-2 Comparison of water levels at Bhavnagar with and without dyke

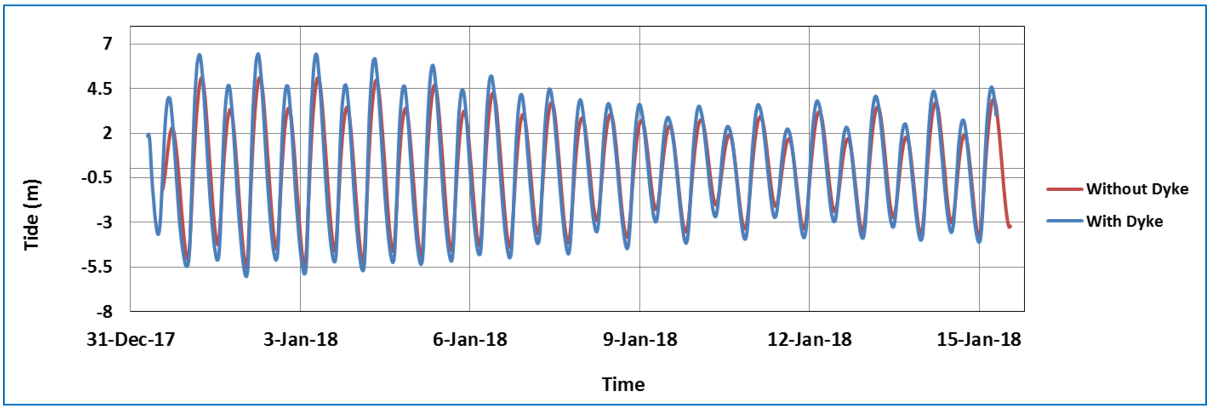

Figure 6-3 Comparison of water levels at Dahej with and without dyke

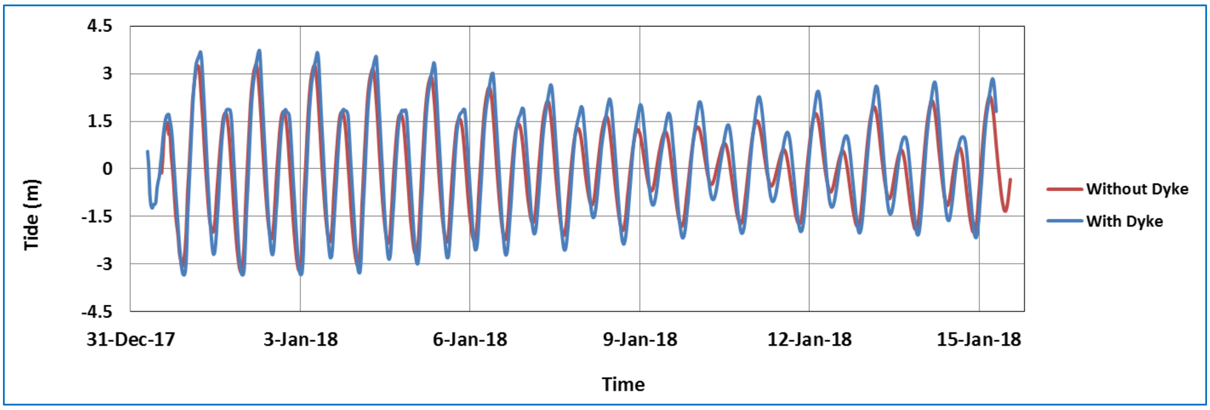

Figure 6-4 Comparison of water levels at Daman with and without dyke

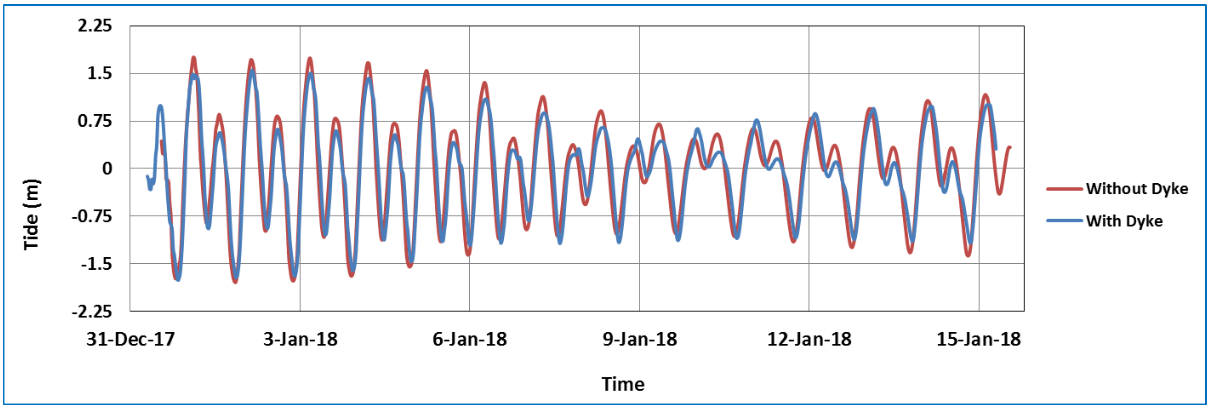

Figure 6-5 Comparison of water levels at Diu with and without dyke

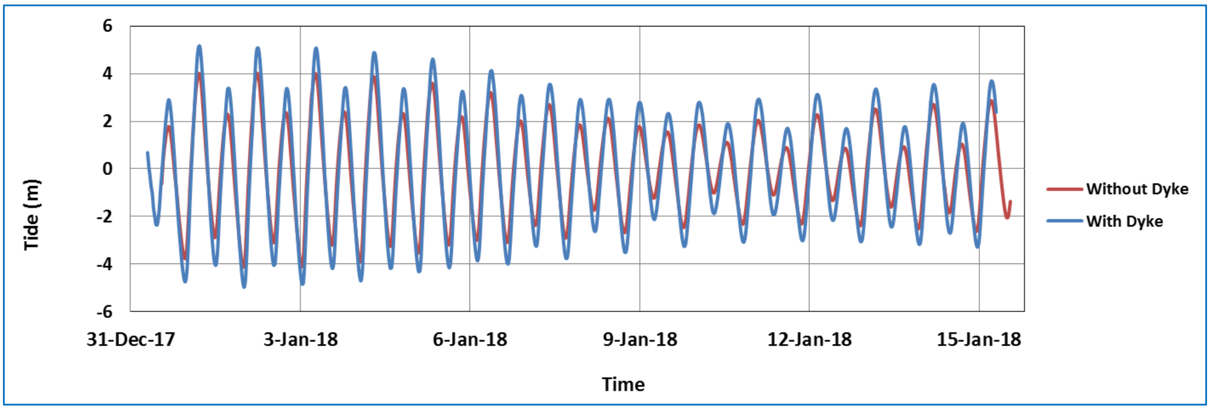

Figure 6-6 Comparison of water levels at Hazira with and without dyke

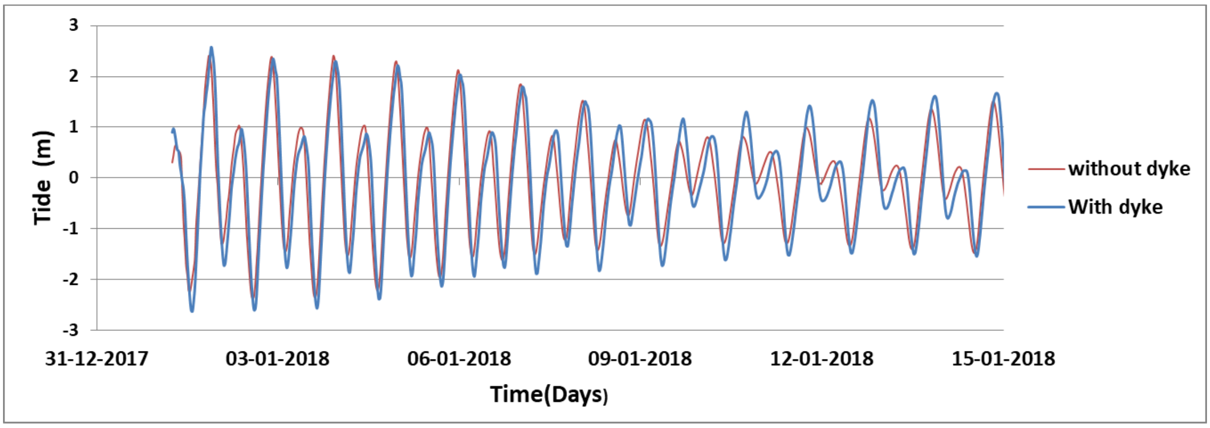

Figure 6-7 Comparison of water levels at Jafarabad with and without dyke

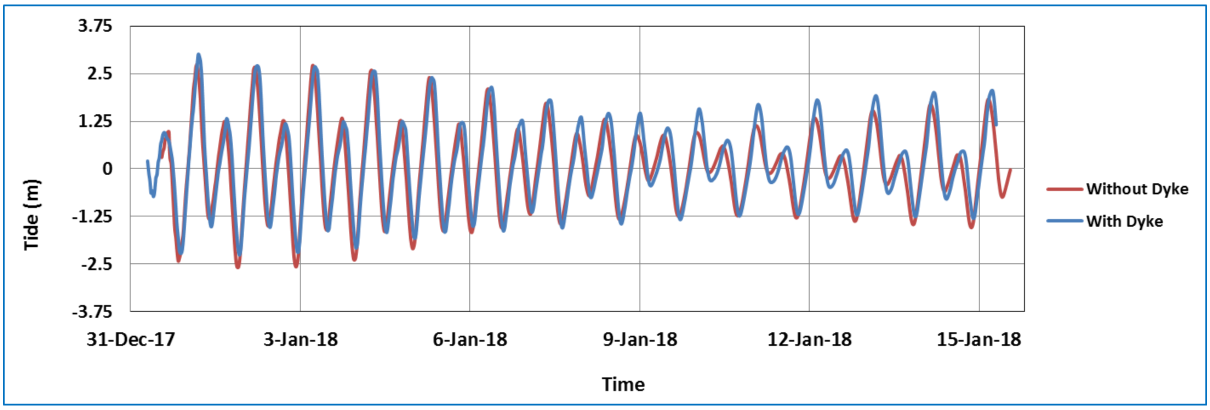

Figure 6-8 Comparison of water levels at Pipavav with and without dyke

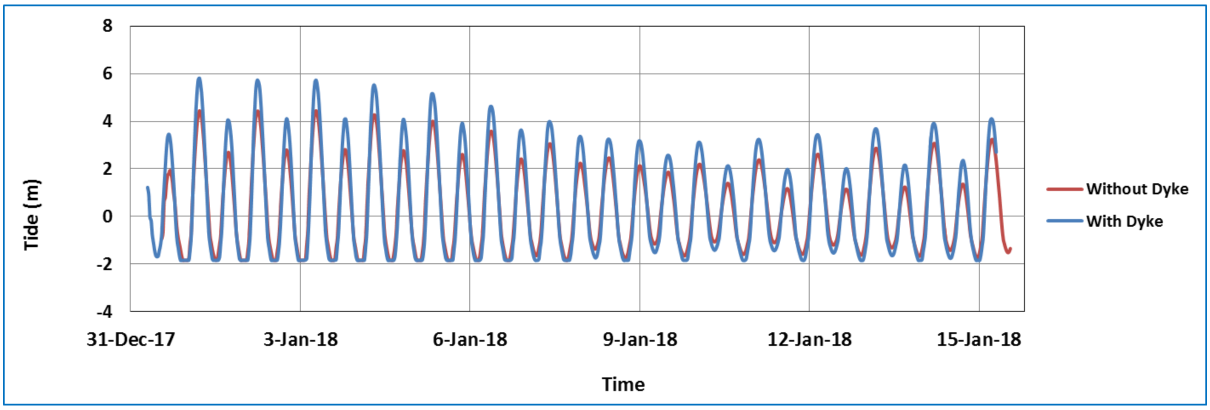

Figure 6-9 Comparison of water levels at Alang with and without dyke

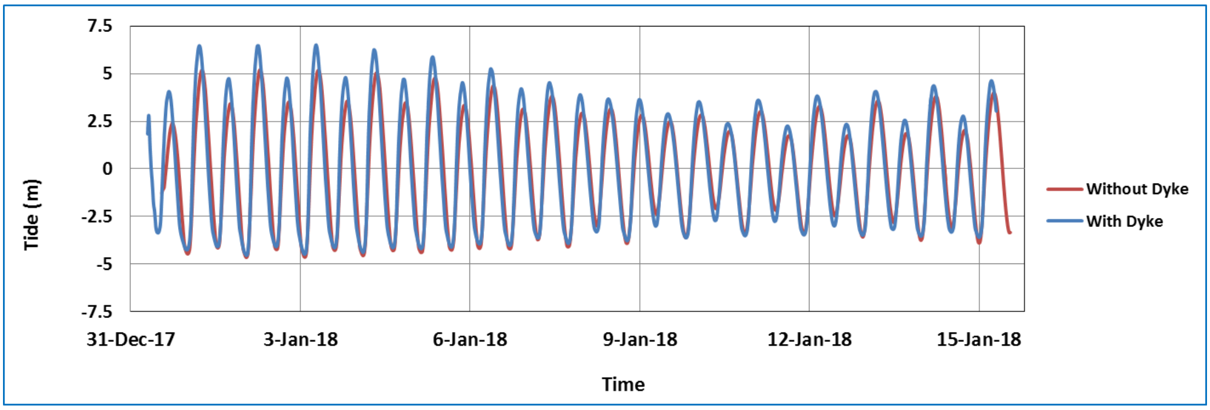

Figure 6-10 Comparison of water levels at Ghogha with and without dyke

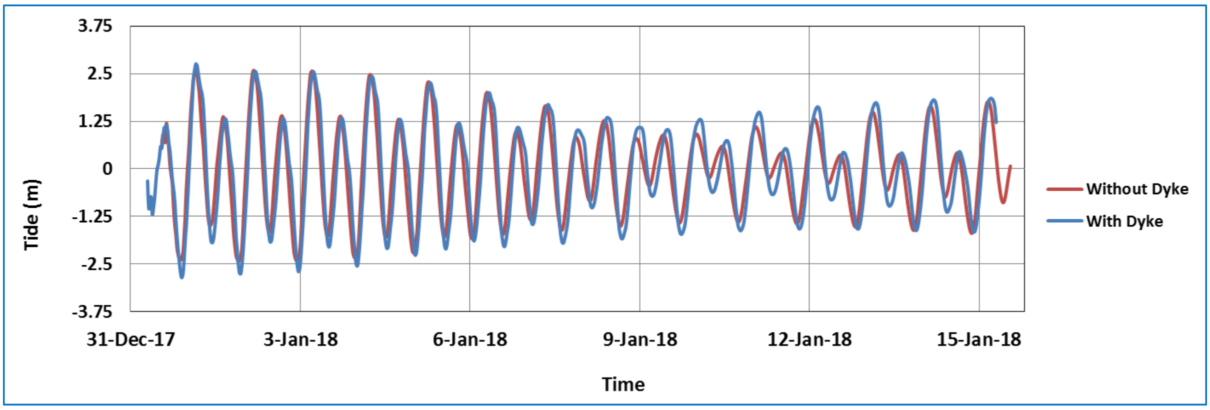

Figure 6-11 Comparison of water levels at vadhavan with and without dyke

6.2 Storm Surge

Simulations were carried out for the Cyclones which were passing over the Gulf as listed in Chapter 4 for both the scenarios i.e. existing condition and with the dyke in place. The results from each of these simulations were extracted at various locations marked in Figure 6-1 Locations of Maximum Free surface elevation extraction. The plot of free surface elevation for a typical cyclone, for existing scenario and with dyke scenario, is provided in Figure 6-12 and Figure 6-13 respectively.
Time series plots of free surface elevation for a typical cyclone, at eleven locations are provided in Figure 6-14 to Figure 6-24.

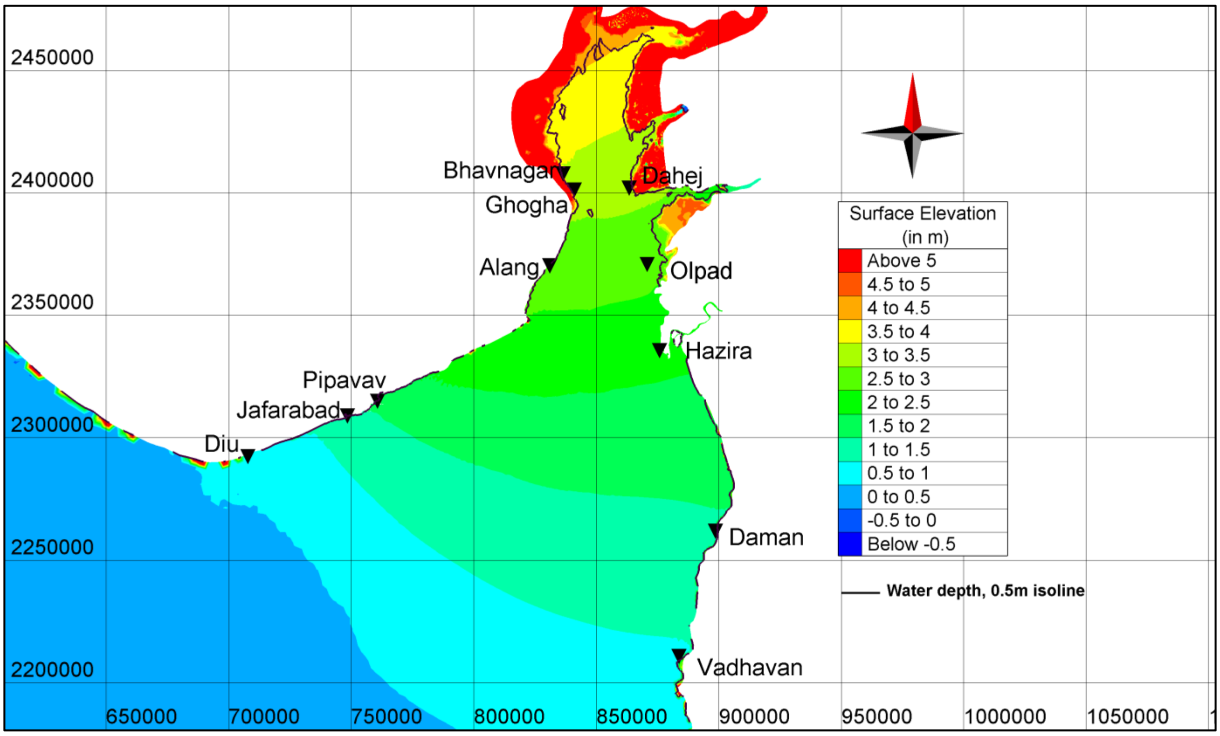

Figure 6-12 Surface elevation (with respect to MSL) for a typical time step for Cyclone Taukte (Without Dyke)

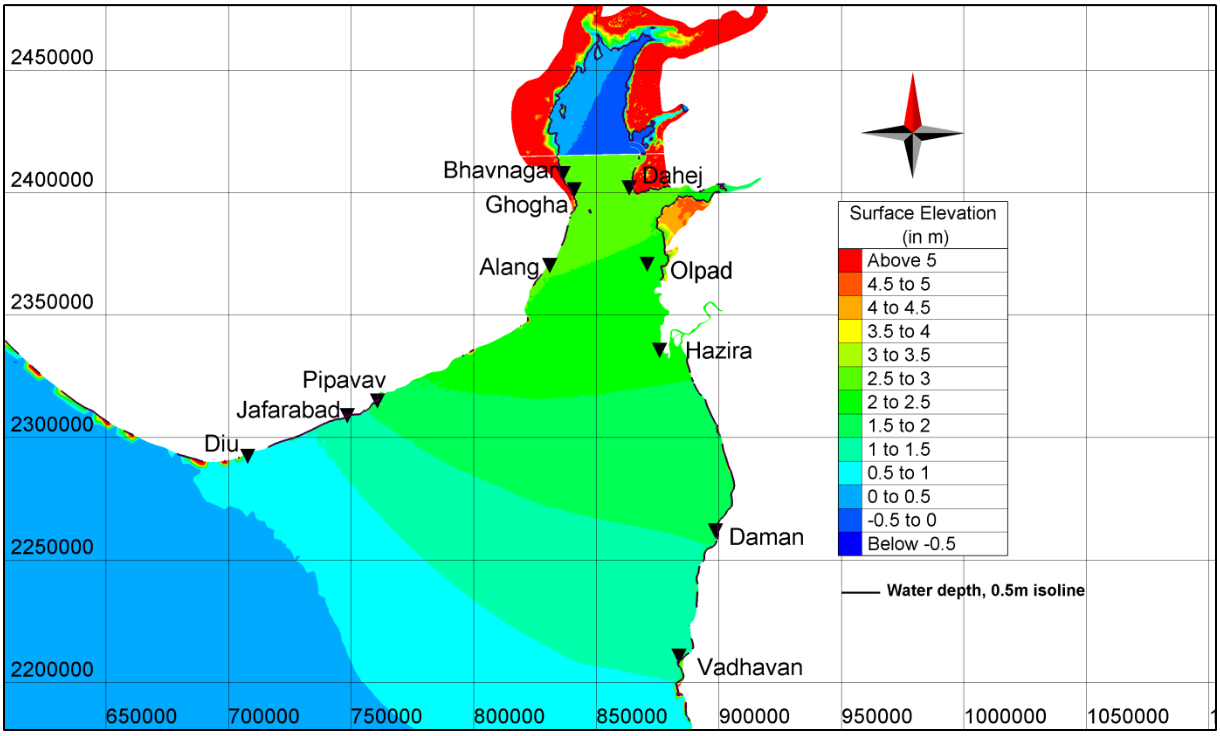

Figure 6-13 Surface elevation (with respect to MSL) for a typical time step for Cyclone Taukte (With Dyke)

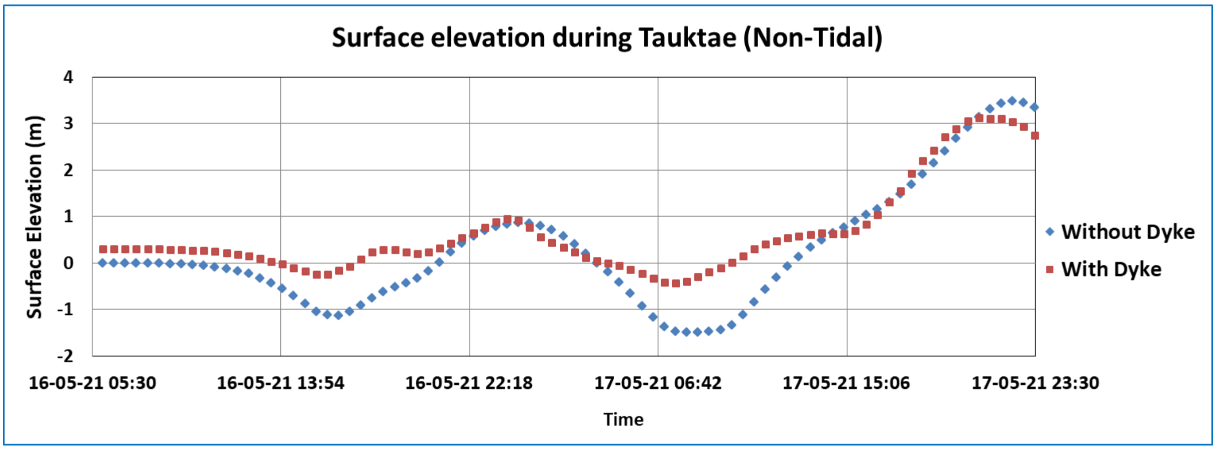

Figure 6-14 Typical graph of surface elevation variation off Bhavnagar during Tauktae

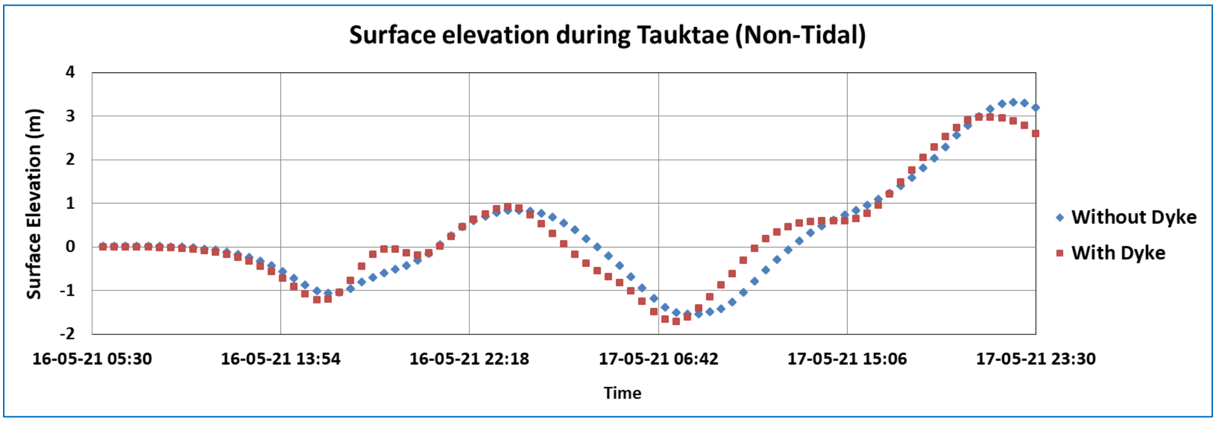

Figure 6-15 Typical graph of surface elevation variation off Ghogha during Tauktae

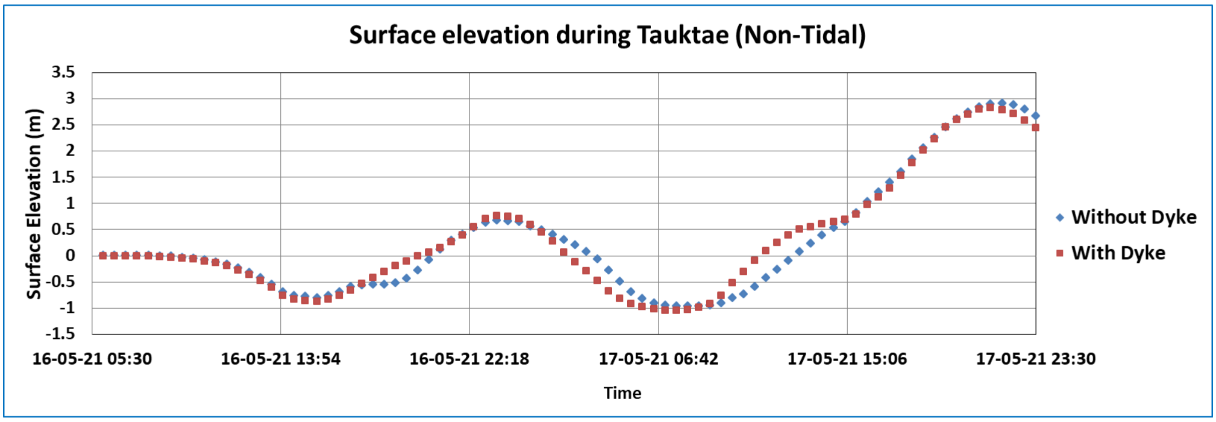

Figure 6-16 Typical graph of surface elevation variation off Alang during Tauktae

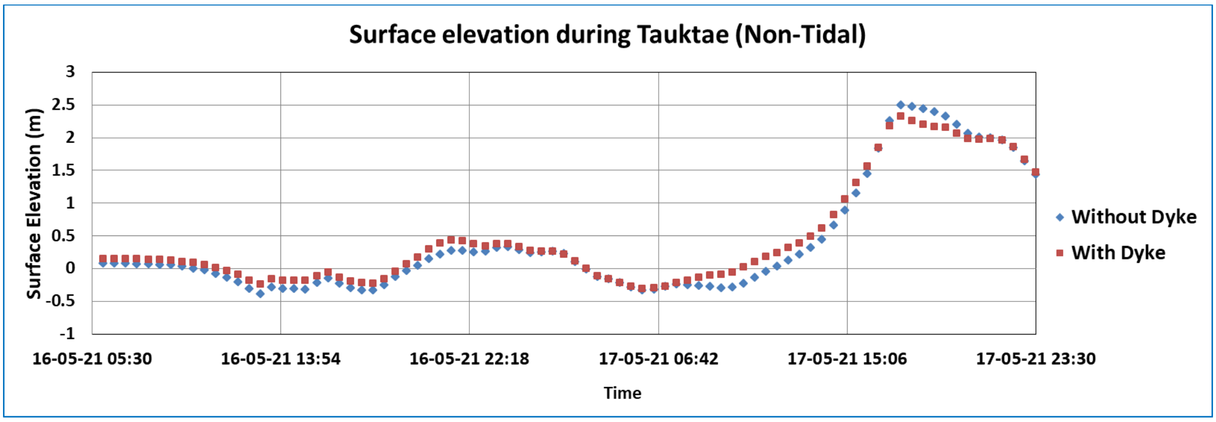

Figure 6-17 Typical graph of surface elevation variation off Pipavav during Tauktae

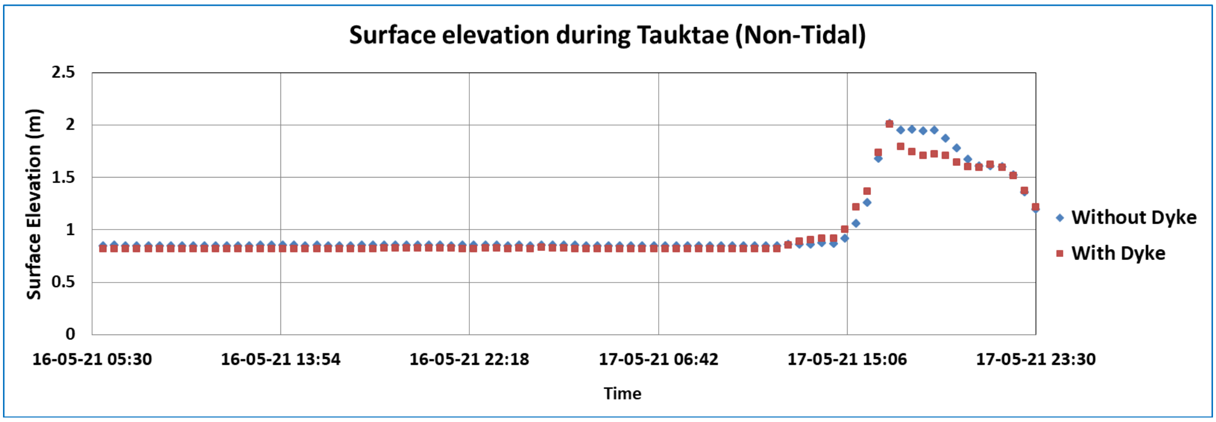

Figure 6-18 Typical graph of surface elevation variation off Jafarabad during Tauktae

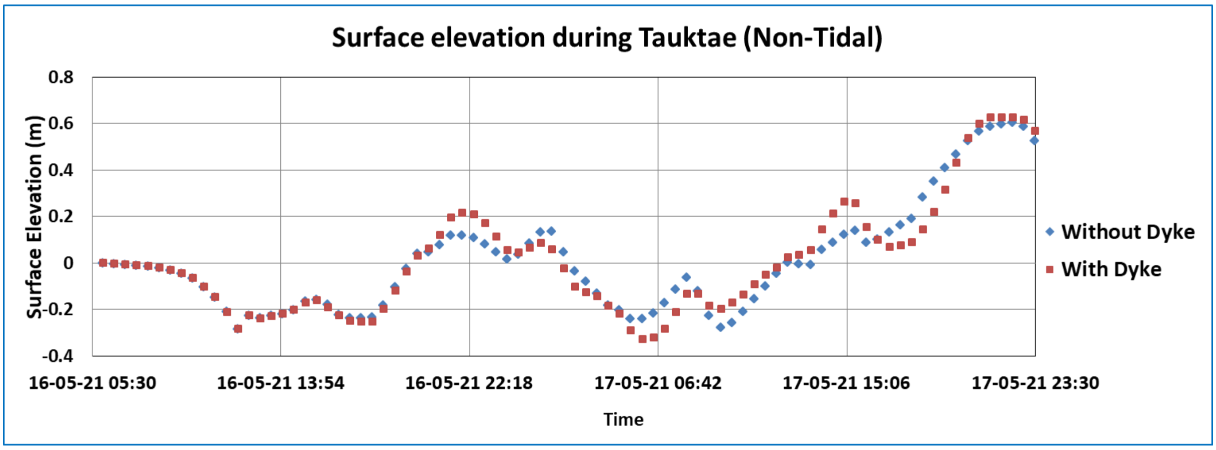

Figure 6-19 Typical graph of surface elevation variation off Diu during Tauktae

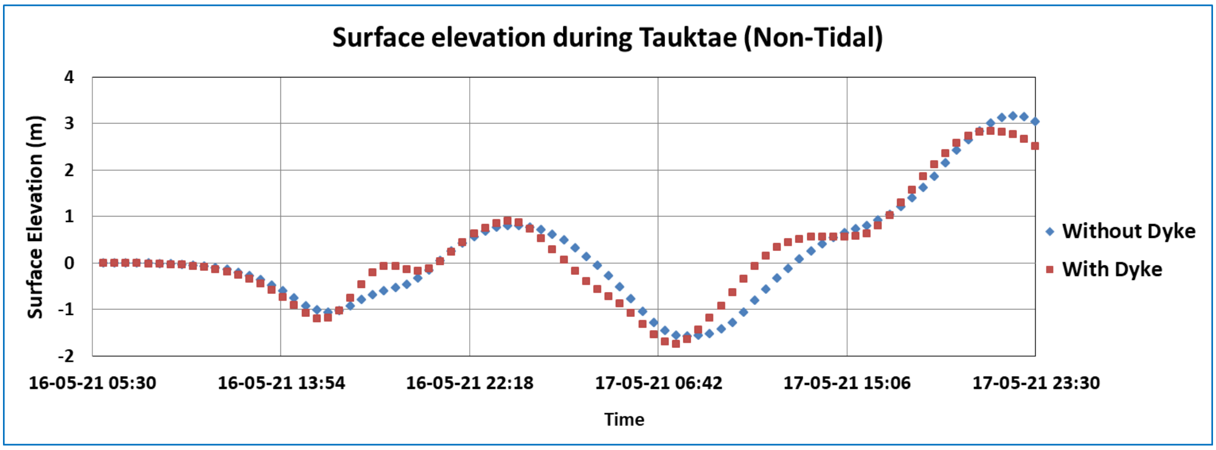

Figure 6-20 Typical graph of surface elevation variation off Dahej during Tauktae

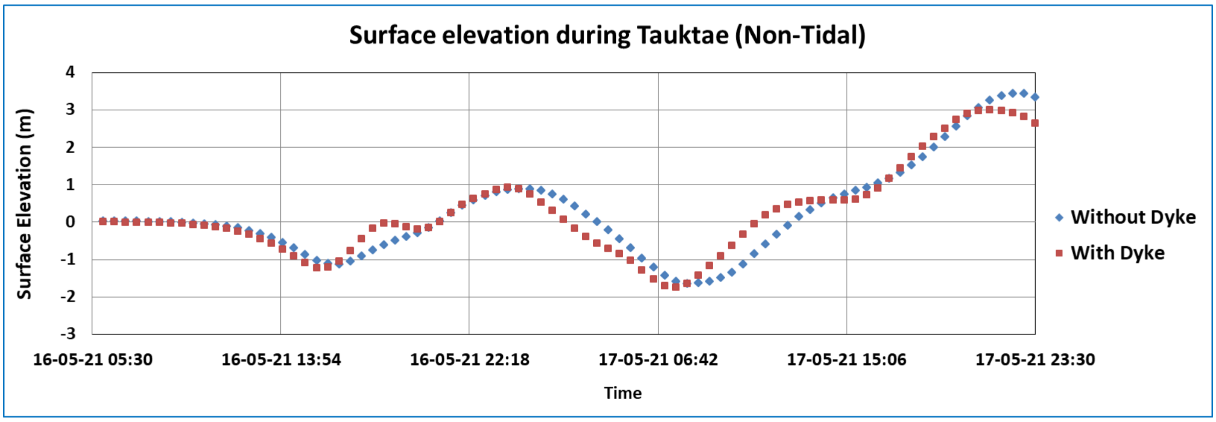

Figure 6-21 Typical graph of surface elevation variation off Olpad Tauktae

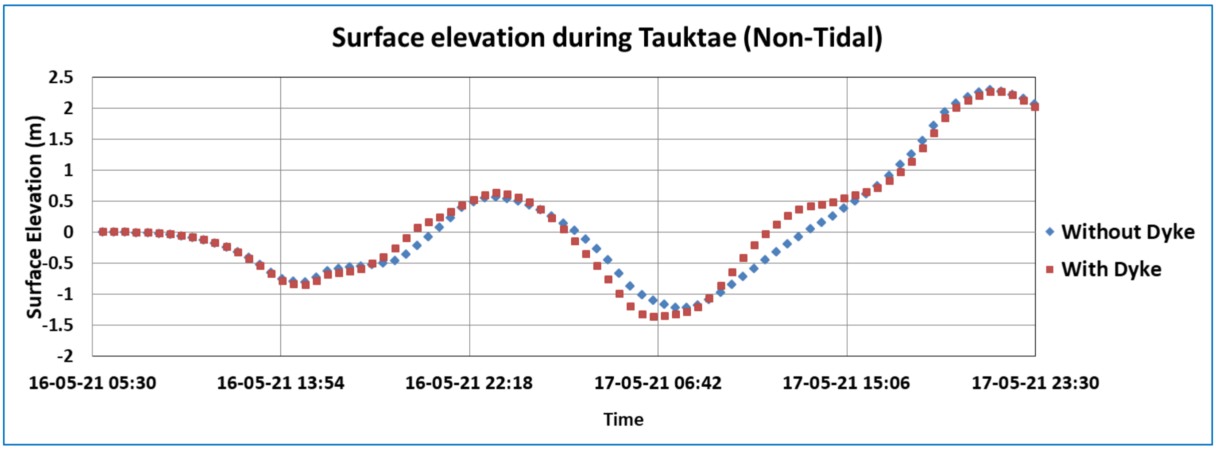

Figure 6-22 Typical graph of surface elevation variation off Hazira during Tauktae

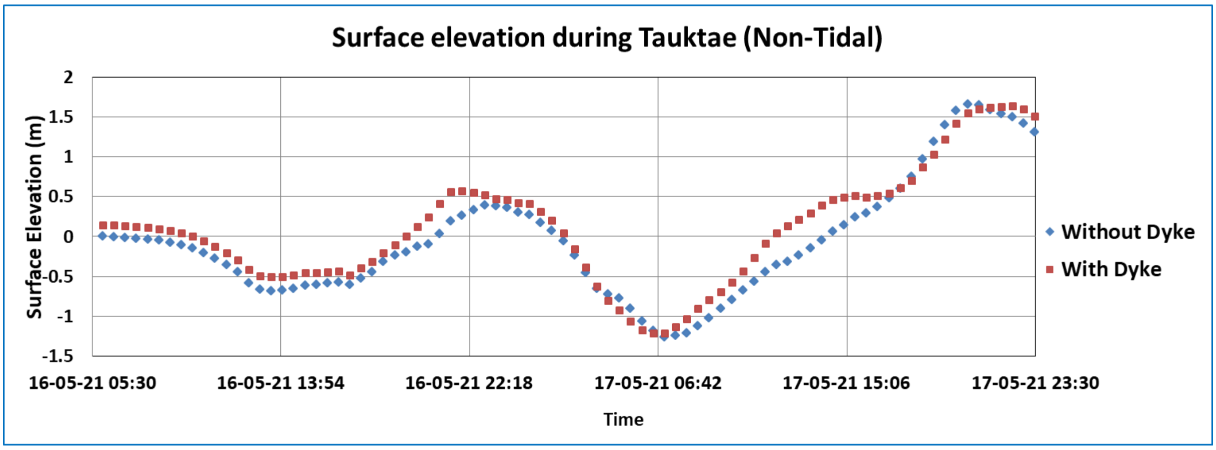

Figure 6-23 Typical graph of surface elevation variation off Daman during Tauktae

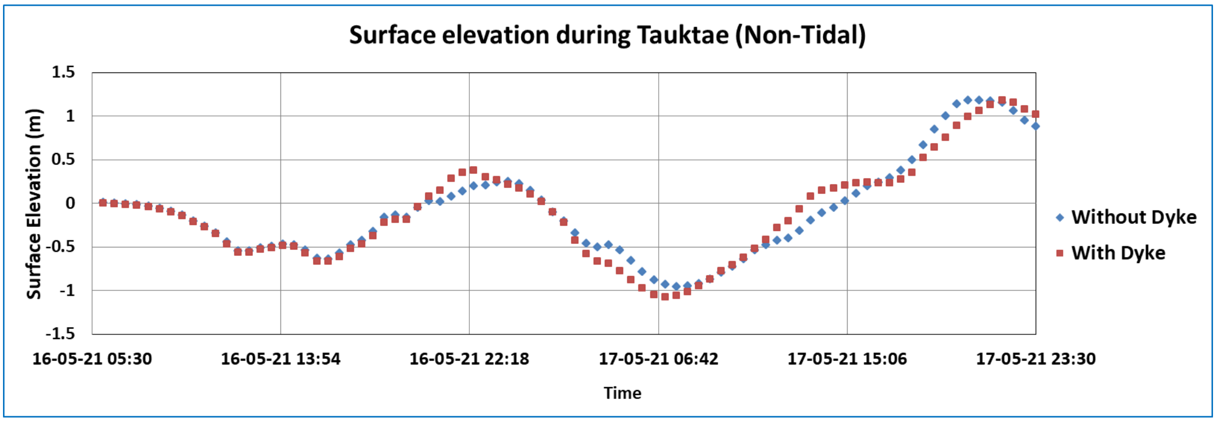

Figure 6-24 Typical graph of surface elevation variation off Vadhavan during Tauktae

The maximum and minimum water levels from all the storm surges at different locations were extracted and are presented in Figure 6-25 and Figure 6-26 respectively. The results are also presented in Table 6-1.

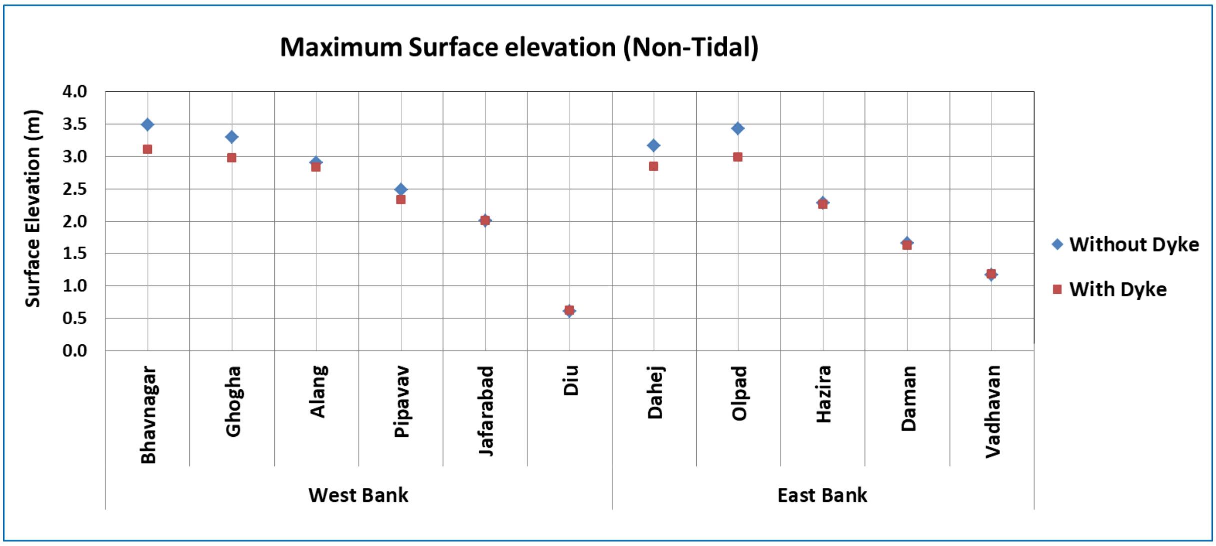

Figure 6-25 Maximum surface elevation with respect to MSL (Non-Tidal Component)

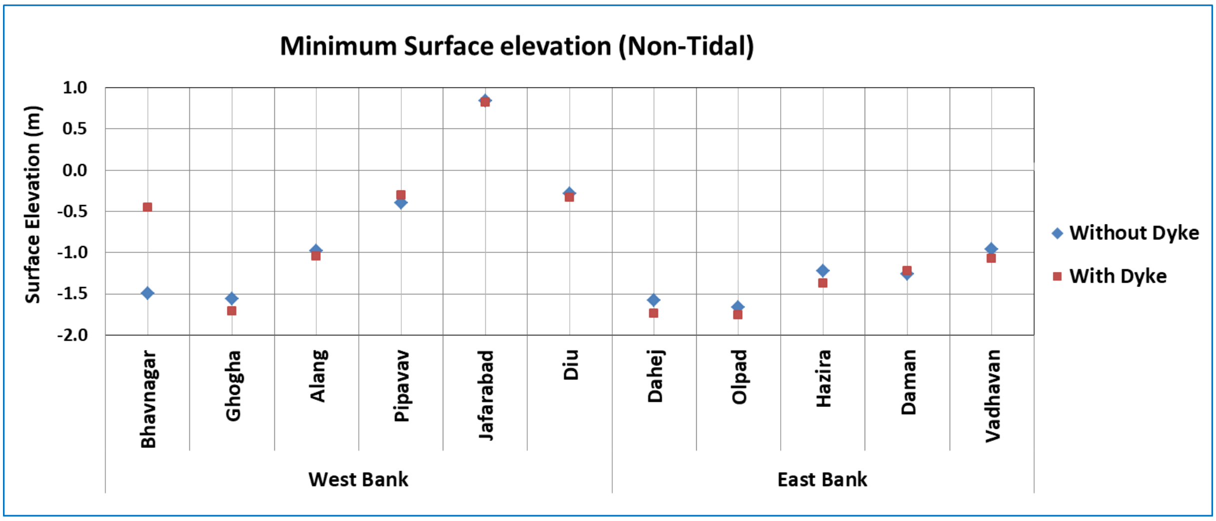

Figure 6-26 Minimum surface elevation with respect to MSL (Non-Tidal Component)

Table 6-1 Maximum and minimum free surface elevation

Bank	Location	Maximum Surface Elevation (m)		Minimum Surface Elevation (m)	
		Without Dyke	With Dyke	Without Dyke	With Dyke
West Bank	Bhavnagar	3.5	3.1	-1.5	-0.5
	Ghogha	3.3	3.0	-1.6	-1.7
	Alang	2.9	2.8	-1.0	-1.0
	Pipavav	2.5	2.3	-0.4	-0.3
	Jafarabad	2.0	2.0	0.8	0.8
	Diu	0.6	0.6	-0.3	-0.3
East Bank	Dahej	3.2	2.8	-1.6	-1.7
	Olpad	3.4	3.0	-1.7	-1.8
	Hazira	2.3	2.3	-1.2	-1.4
	Daman	1.7	1.6	-1.3	-1.2
	Vandhavan	1.2	1.2	-1.0	-1.1

6.3 Results

The results obtained are tabulated in the following tables in the form of Maximum Water levels for three cases given below (both existing and future scenarios.)

- Tide
- Tide + storm surge
- Tide + storm surge + sea level rise.

Table 6-2 Maximum Free surface elevation (w.r.t MSL) for various locations under existing conditions

S.no	Location	Long.	Lat.	Tide, in m	Tide + Storm surge, in m	Tide + Surge + sea level rise, in m
1	Bhavnagar	72.253	21.740	5.4	8.9	9.5
2	Ghogha	72.295	21.681	5.2	8.5	9.1
3	Alang	72.192	21.403	4.4	7.3	7.9
4	Pipavav	71.507	20.916	2.7	5.2	5.8
5	Jafarabad	71.388	20.864	2.4	4.4	5.0
6	Diu	70.995	20.719	1.8	2.4	3.0
7	Dahej	72.512	21.683	5.1	8.3	8.9
8	Olpad	72.576	21.401	4.6	8.0	8.6
9	Hazira	72.616	21.082	4.0	6.3	6.9
10	Daman	72.819	20.414	3.3	5.0	5.6
11	Vandhavan	72.665	19.955	2.6	3.8	4.4

Table 6-3 Maximum Free surface elevation (w.r.t MSL) for various locations with proposed dyke

S.no	Location	Long.	Lat.	Tide, in m	Tide + Storm surge, in m	Tide + Surge + sea level rise, in m
1	Bhavnagar	72.253	21.740	6.6	9.7	10.3
2	Ghogha	72.295	21.681	6.5	9.5	10.1
3	Alang	72.192	21.403	5.8	8.6	9.2
4	Pipavav	71.507	20.916	3.0	5.3	5.9
5	Jafarabad	71.388	20.864	2.6	4.6	5.2
6	Diu	70.995	20.719	1.6	2.2	2.8
7	Dahej	72.512	21.683	6.4	9.2	9.8
8	Olpad	72.576	21.401	6.0	9.0	9.6
9	Hazira	72.616	21.082	5.2	7.5	8.1
10	Daman	72.819	20.414	3.7	5.3	5.9

The increase in water level may cause inundations in the adjoining areas if it is flat and low lying. In addition, this can also affect the functionality of the existing port and other coastal structures. Similarly, a decrease in water level may affect the available depths in port basins and approach channels. It may be noted that the maximum storm surge values are directly added to the highest tides, which is conservative.

7 Effects of the dyke on water levels upstream

The major factors that drive the upstream water levels are intensity and duration of flood in the rivers, and outflow of the reservoir. The reservoir outflow is also governed by the reservoir level and the downstream sea water level as rise of sea level above the reservoir level will impede the outflow. The maximum sea water level will mainly be affected by three major phenomena, namely, tide, storm surges and sea level rise (SLR). The effect of storm surge is not considered since the concomitance of the PMF and Storm surge event happening is very less. Simulations were carried out to study the effect of dyke on upstream water levels with and without dyke. To simulate the maximum possible water level upstream, it was decided to do the simulations with an initial reservoir level as Full Reservoir Level and apply the PMF during spring tide.

The Full Reservoir level (FRL) and Maximum Reservoir level (MRL) of the proposed dyke is 3m and 5m as per the . Techno Economic Feasibility Report Kalpasar.

It is necessary to accurately model the spillway to correctly simulate the behaviour of upstream water level. A spillway of capacity 110,000 Cumecs with gross width of 2086 meters and net width of 1710 meters having 95 spans of 18 meters wide is recommended by IIT Roorkee. The crest level of the proposed ogee spillway is at -3.5m.

The discharge through an ogee spillway is given:

$$\mathbf{Q = cd \times L_e \times H_e^{(3/2)}}$$

Where cd= Coefficient of discharge, L_e= Clear width of spillway crest, H_e= Upstream energy head above the spillway crest.

As it is not practical to model the spillway with gate by modifying the bathymetry in Telemac2D, it was decided to implement this equation in the model to capture the spillway operation effectively. The coefficient of discharge (cd) factors and adjusted cd factors recommended by IIT Roorkee are considered for this study.. The spillway rating curve given by IIT Roorkee is compared with the rating curve from the model. The comparison is given in Figure 7-1. From the comparison, it can be inferred that model rating curve is following the same trend and is more conservative. The spillway discharge equation is also modified for partial gate operating conditions .The discharge through the spillway reduces when the water level in the downstream is above sill-level. When the sea water level exceeds the reservoir level, the gates of the spillways are expected to be closed. However, restricting entire backflow (flow form downstream towards upstream of dyke) may not be practically feasible. In view of this, simulations were carried out considering two aspects; with and without backflow.

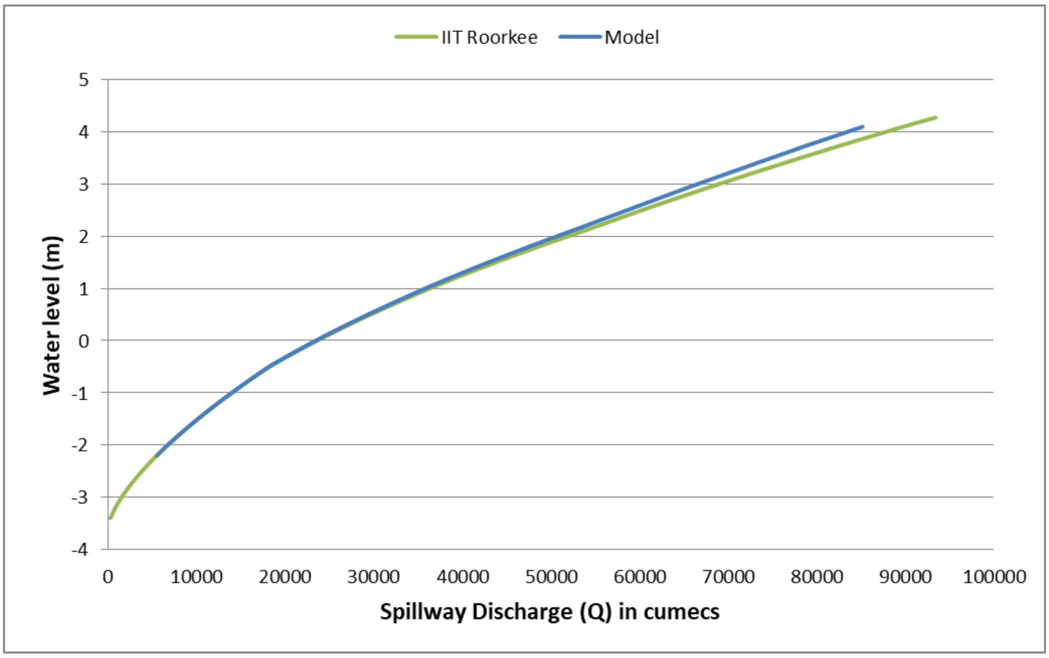

Figure 7-1 Comparison of Spillway rating curve

In the event of a high tide coinciding with maximum flood in the rivers, reservoir water levels will rise and in turn increases the probability of floods upstream of dyke. To get the maximum/minimum tide levels, it is pertinent to do the hydrodynamic simulations when the tidal range is maximum and the water levels will be close to HAT and LAT. To identify such period, tide levels at the project location were predicted for 20 years using the harmonic constituents obtained from the analysis of observed data. It is found from this analysis that the maximum tide levels were observed during January 2018. Simulations were carried out during this period by imposing the Probable maximum flood of different rivers at the respective boundaries. Studies were carried out by coinciding PMF with HAT and Neap tides. In addition, sensitivity studies were carried out by shifting the tide levels temporally to find the combination which provides maximum water levels. Simulations were carried out with and without the effect of sea level rise. The details of various scenarios simulated and their results are presented in subsequent section.

7.1 Results

The following cases were simulated with Tide and Probable Maximum Flood (PMF) as boundary conditions.

A) Existing Scenario

- The present condition without sea level rise
- The present condition with sea level rise

B) With dyke in place

- The proposed dyke without sea level rise and back flow allowed
- The proposed dyke without sea level rise and back flow restricted
- The proposed dyke with sea level rise and back flow allowed
- The proposed dyke with seal level rise and back flow restricted

The results obtained are tabulated in Table 7-1 & Table 7-2 in the form of Maximum Water levels. The locations at which water level were extracted in the upstream side of dyke is given in Figure 7-2. The time-series of water levels at upstream and downstream of the dyke are also presented in Figure 7-3 and Figure 7-4.

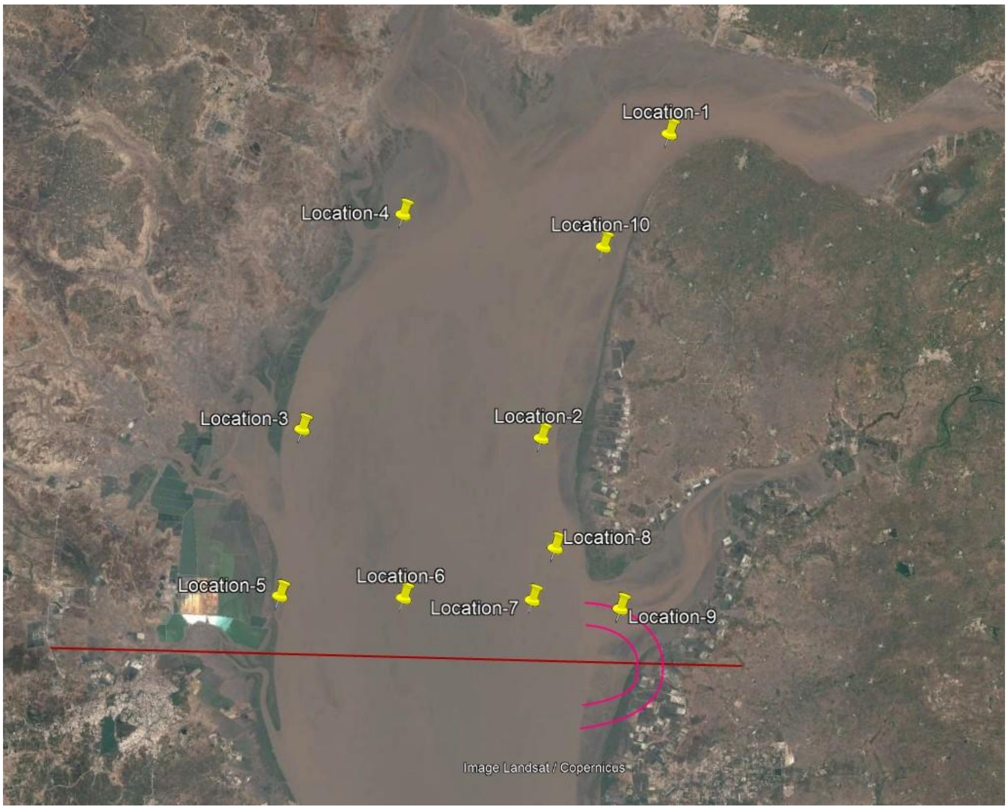

Figure 7-2 Locations of Maximum Free surface elevation extraction (upstream of the dyke)

Table 7-1 Maximum Free surface elevation (w.r.t MSL) for various locations under existing conditions

Location	Longitude	Latitude	Maximum Free surface, in m	
			No SLR	SLR
Location 1	72.572	22.209	7.1	7.7
Location 2	72.471	21.970	6.1	6.7
Location 3	72.270	21.972	6.1	6.7
Location 4	72.350	22.141	6.5	7.1
Location 5	72.255	21.842	5.7	6.3
Location 6	72.359	21.843	5.6	6.2
Location 7	72.467	21.844	5.7	6.3
Location 8	72.485	21.885	5.8	6.4
Location 9	72.541	21.839	5.7	6.3

Location 10	72.519	22.120	6.7	7.2

Table 7-2 Maximum Free surface elevation (w.r.t MSL) for various locations with proposed dyke

Location	Longitude	Latitude	Maximum Free surface, in m			
			No SLR		SLR	
			Backflow allowed	Backflow restricted	Backflow allowed	Backflow restricted
Location 1	72.572	22.209	6.2	5.5	6.4	5.6
Location 2	72.471	21.970	6.0	5.4	6.2	5.5
Location 3	72.270	21.972	6.0	5.4	6.2	5.5
Location 4	72.350	22.141	6.1	5.5	6.3	5.6
Location 5	72.255	21.842	6.0	5.4	6.2	5.5
Location 6	72.359	21.843	6.0	5.4	6.2	5.5
Location 7	72.467	21.844	6.0	5.4	6.1	5.5
Location 8	72.485	21.885	6.0	5.4	6.1	5.5
Location 9	72.541	21.839	6.0	5.5	6.2	5.6
Location 10	72.519	22.120	6.1	5.5	6.3	5.6

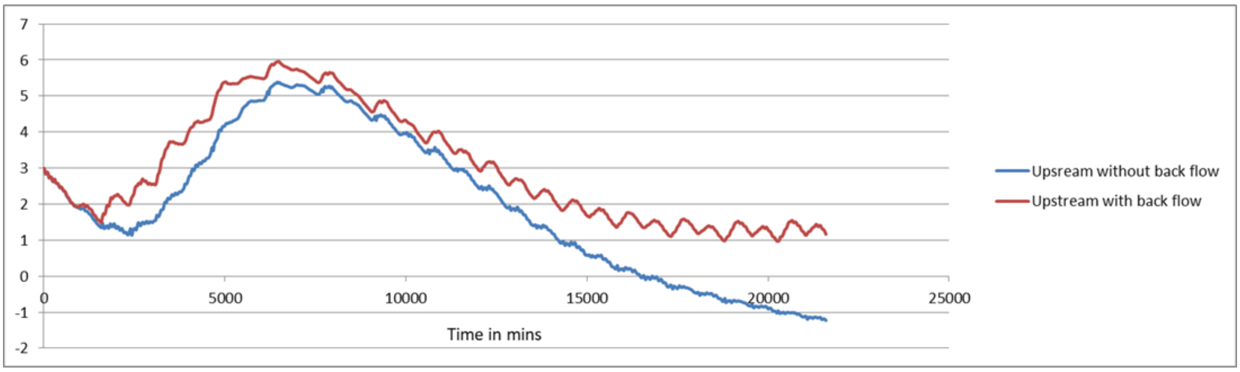

Figure 7-3 Water levels at upstream of dyke

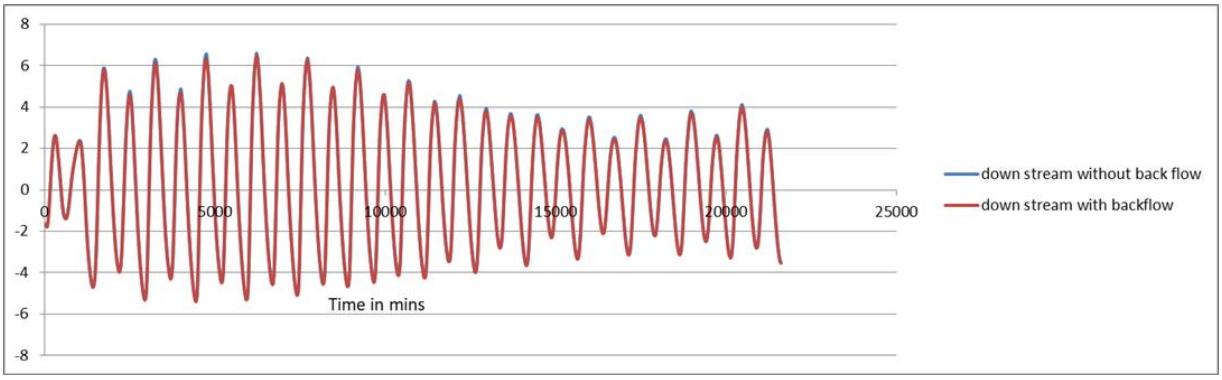

Figure 7-4 Water levels at downstream of dyke

The following are the observations from the study:

CASE A: When backflow is allowed

- With proposed dyke and when backflow is allowed through the spillway, the locations close to the dyke (5, 6, 7, 8 & 9) experiences an increase in water level of 0.3m compared with existing scenario (without dyke). In other locations water levels are lower than existing conditions.
- When effects of sea level rise are considered, there is no significant change in the water levels when compared with existing conditions. However when comparing with future scenario with no sea level rise, the water level within the dyke rises by 0.2m approximately.

CASE B: When backflow is restricted

- With proposed dyke and backflow is restricted through the spillway, the water levels obtained are lower than the ones obtained with existing conditions in all the locations.
- When effects of sea level rise are considered, there is no significant change in the water levels when compared with existing conditions. However when comparing with future scenario case with no sea level rise, the water level within the dyke increases by 0.1m approximately. This can be attributed to increased spillway discharge time. The spillway discharge is also governed by the downstream water level. Since the sea level rise increases the water level downstream, the spillway discharge time increases.

The maximum water levels obtained are above MRL (+5m) in all the scenarios simulated. Hence studies were carried out with reduced FRL levels, to analyse if an advance release of reservoir water will result in reduction of modelled maximum water levels. However, there was no significant change in maximum water levels. This is because rate of discharge reduces when the water level decreases in the upstream. It was found that there is no correlation between FRL and maximum water levels. Therefore FRL upto 4m is also feasible. The functional and operational conditions of the dyke shall be checked with maximum water levels. To limit the maximum water level upto 5m, the spillway capacity shall be increased.

8 Limitations and Assumptions

1. The resolution of bathymetry and topography data provided (approximately 1Km) was not adequate. Therefore data from secondary sources like GEBCO 2022 Grid (15 arc-second interval grid) and SRTM data were also considered for the model studies.
2. The storage of water on the upstream areas of the rivers is not considered for the present study.
3. The flow pattern and velocities near the spillway region do not replicate the real conditions.